Organization of gene expression within the 2-minute morphogenetic cluster of *Escherichia coli*

Daniel James Kenan

M. Phil.
University of Edinburgh
1985

Declaration of authorship

I declare that this thesis has been composed by myself, and that the work described within is my own, except as otherwise indicated, conducted in accordance with the requirements for the M. Phil. degree.

Contents

List of Figures

List of Tables

List of Abbreviations

Ap: ampicillin

bp: base pairs

CIP: Calf Intestinal Phosphatase

Cm: chloramphenicol

DPA: diaminopimelic acid

gal: galactose

kb: kilobase pairs

Kn: kanamycin

MW: molecular weight

NB: nutrient broth

PAGE: polyacrylamide gel electrophoresis

PBP: penicillin-binding protein

PSE: penicillin-sensitive enzyme

PSS: protein-synthesizing system

SDS: sodium-dodecyl-sulphate

Tc: tetracycline

wt: wild type, as in a lambda lysogen

Preface

Cell division is one of the most significant events in the bacterial life cycle, yet it remains poorly understood at every level. As is often the case with complex biological systems, mutational analysis has helped to define elements of the division system and their mechanisms of operation. However, we still know little about the biochemistry and physiology of cell division gene products. One approach to a better understanding is to attempt to define the molecular genetics of loci identified as being central to the division pathways.

Donachie's group has studied the organization of a large cluster of genes involved in cell division, envelope growth and morphogenesis, and this region remains the focus of our molecular genetics investigation. We would like to know how these gene products fit together to make up the division apparatus, what biochemical roles they play within the apparatus, how their expression and activities are controlled in keeping with cellular division requirements, and how expression is organized at the molecular level. My work has largely been within the realm of this last category, although it is impossible to consider one category in isolation from the others.

A discussion of division gene expression must consider how division is organized in the growing cell. We must consider the strategy of cellular organization, the physiology of division, the relationship between division and envelope growth, and the major role of division in morphogenesis. These topics are introduced in Chapter 1, but only salient points are considered for sake of brevity. In addition, the discussion in Chapter 1 considers two model systems for which the division biochemistry is beginning to be determined: the SOS response, which leads to inhibition of division under certain conditions, and the penicillin-binding proteins, which are responsible for important

aspects of envelope growth and morphogenesis. Chapter 2 introduces the organization of the morphogenetic cluster studied by Donachie et al. At the end of Chapter 2, I set out specific goals for my investigation into the organization of the murC-ddl-ftsQ-ftsA-ftsZ region. Chapter 4 discusses my subcloning, deletion analysis and complementation experiments; Chapter 5 discusses my use of a galK fusion system to identify transcriptional control signals; Chapter 6 describes a P_L fusion system used to express gene products from cloned inserts; Chapter 7 discusses effects of manipulating ftsQ and ftsA sequences; and Chapter 8 summarizes my conclusions and correlates them with the sequence data generated by A.C. Robinson. Both the sequence, extending from the beginning of ftsQ to the beginning of ftsZ, and some of my relevant results have been included in a recent publication (Robinson et al, 1984), which can be found in Appendix B of this thesis.

Acknowledgements

Synthesizing and assembling a thesis requires a formidable investment of energy, time, materials, and financial resources. The task would have been less bearable, or perhaps impossible, were it not for the contributions and support of my family, friends and colleagues, and I would like to thank everyone who has helped me along the way. I would especially like to thank the following people: Beth Dixon, for remembering me through my Edinburgh experience; Judy Kenan, for many a meal in hectic times; Pat Kenan, for sharing his office and his car; Susanne Wuchte, for sharing her word processor; Kim Walsh, for helping to keep it all part of the English language; Greg Wray, Todd Cowdery, Jim Schwarz, and Andy Wise, for proof-reading and criticisms; John Kenan, for help with the figures; Sarah Kenan, for help with the xeroxing; Richard Hayward, for valuable correspondence; and Tom Matthews and Ken Kreuzer, for helping me to bridge the 4,000 mile gap between Willie Donachie's lab and Durham, North Carolina. Very special thanks are in order for Keith and Vicky Derbyshire, for their lasting friendship and many helpful discussions along the way; Judy Pratt Rossitter, for years of enthusiasm and friendship; Kate Lakoski, for indispensable help with figures and many other details and for trying to keep me from getting lost in this project; Cliff Hern, for teaching me the gentle art of brewing; and Moira Allan, for making Edinburgh a particularly memorable experience. I am indebted to Neil Sullivan for showing me the ropes, Ken Begg for sharing strains and phage constructions, and Arthur Robinson for ongoing collaboration. Finally, I am deeply grateful to Willie Donachie, my supervisor, for making it all possible.

Abstract

The 2-minute region of the Escherichia coli chromosome contains a remarkable cluster of genes involved in cell division, cell envelope growth, and morphogenesis (Donachie et al., 1984). The absence of biochemical assays for most morphogenetic factors has hindered their characterization, however molecular genetic approaches are being used successfully to reveal the organization of morphogenetic pathways. A segment of the 2-minute cluster, spanning the genes murG, murC, ddl, ftsQ, ftsA, ftsZ, and envA, has been incorporated into a lambda transducing phage and was used in the preliminary characterization of this region (Lutkenhaus and Wu, 1980). I expanded upon their work by using subcloning techniques and deletion analysis to map the genetic boundaries of ddl, ftsQ, ftsA, and ftsZ. Moreover, functional promoter and terminator sequences were mapped through use of a gal-operon fusion system, and the gene products of ddl, ftsQ, and ftsA were identified by expression of cloned fragments from a P_L vector in a minicell system. My results complement the preliminary molecular genetic analysis by Lutkenhaus and Wu (1980) and the sequence data of Robinson et al. (1984). All loci between murC and ftsZ are transcribed in a clockwise sense; these loci are tightly linked without large intervening sequences; each of these loci has at least one independent promoter; a second promoter for ftsZ lies within the coding sequence of the adjacent locus, ftsA; no strong transcriptional terminators are found between murC and ftsZ; and expression of several adjacent loci within this cluster may be coordinated. The ddl product is identified as a 32,000 dalton protein, the ftsQ protein is 35,000 daltons, and the ftsA protein is 46,000 daltons. Over-expression of ftsQ and ftsA together is deleterious to the cell, and inactivation of ftsA reverses this effect. Transcription of ftsA in the absence of ftsQ translation disturbs cellular morphology, and ftsQ may be deleterious in high copy number unless its promoter is removed in the cloning process. A fortuitous galE-ftsQ fusion produces a hybrid protein that retains FtsQ function and is not deleterious in spite of high levels of transcription. These findings are correlated with the sequence data, and possibilities for future investigations are discussed.

Chapter 1 Introduction: organization of division in the growing *E. coli* cell

1.1 Perspective

Growth is the collection of processes employed by an organism to make more of itself. The speed at which a self-replicating system is able to accomplish this depends on how the system is organized and what materials are available in the environment. In the case of *Escherichia coli*, the best studied of the Gram-negative bacteria, the cells in a given population are able to double their number under ideal conditions in just over 20 minutes. Longer times are required with suboptimal conditions. We can expect the growth physiology of *E. coli* to be both efficient and adaptable in view of the two very different sorts of environments this organism inhabits. It colonizes the large bowel of humans and other animals, ensuring that some *E. coli* cells will regularly find their way to soil and water habitats. The ability to maintain a high growth rate under a wide range of conditions would help to promote survival through variable and hostile environments.

Growth rate can be expressed as the doubling time, that is, the time required for a given population of cells to double its number. Perhaps the most striking feature of how this doubling takes place is that the composition and morphology of cells in the population are uniform for cells of a given age class. Under conditions of balanced growth the newborn products of a dividing cell are essentially identical to each other, and to all newborn cells in that population, with respect to their chemical and macromolecular make-up, their dimensions, their physiological behavior, and their genetic complement (Marr et al., 1966, Ingraham et al., 1983). Such regularity implies a set of

constraints on the models we may propose to account for our experimental observations on growth of the E. coli cell.

In order for an E. coli cell to grow within the apparent limits of uniformity, mechanisms must exist to ensure that 1) the endowment of genetic (chromosome) and spatial (envelope) information is accurately duplicated; 2) the protein synthesizing system, or PSS, is duplicated; and 3) these duplicated components are evenly divided between daughter cells. In other words, a growing population must accomplish duplication processes and division processes. Duplication processes include uptake and synthesis of precursor metabolites, biosynthesis of building blocks, polymerization into macromolecules, assembly into cellular structures, energy supply, and regulation. These topics are summarized in an excellent text by Ingraham, Maaloe, and Neidhardt (1983). However, comparatively little is known about the processes that assure the equal and regular division of growing cells, which is the topic of this thesis.

1.2 Cellular organization

Both light and electron microscopy reveal that E. coli is rod-shaped, as is typical of the Enterobacteriaceae. One geometrical representation of a rod is a cylinder capped by hemispherical poles, and this representation is accurate for E. coli under most conditions (Donachie, 1981; Rosenberger et al., 1978). The size of the rod depends on growth conditions. Cells growing slowly have shorter lengths and diameters than cells growing at a higher rate, although the ratio of average length to diameter remains fairly constant over a range of growth rates (Donachie, 1981; Zaritsky, 1975). The growing cell accommodates its expanding volume almost entirely by an increase in length; diameter remains

constant for a particular growth rate (Marr et al., 1966, see Section 1.3).

Gross cellular structure appears relatively simple. The only obvious structures inside the cell are the chromosome and polysomes. The chromosome appears to be associated with the envelope through unknown means (Pettijohn et al., 1982; see Section 1.6). The envelope consists of 2 lipid bilayer membranes sandwiching a peptidoglycan layer.

The inner membrane, or cell membrane, defines the sharpest boundary between internal and external environments. It supports a variety of membrane-associated proteins involved in transport, metabolism, motility, and growth and division. The cell membrane and outer membrane are seen to fuse at approximately 200 sites randomly spaced over the cell surface (Bayer, 1974). Fusion sites (Bayer junctions) are postulated to serve essential roles in translocation and assembly of outer membrane components (discussed in section 1.5) and infection by certain bacteriophage.

The outer membrane is unusual in that only its inner face consists of phospholipids. Its outer face is made up of lipopolysaccharide, which is responsible for much of the pathogenicity of Gram-negative bacteria. The outer membrane acts as a selective permeability barrier, allowing primarily small hydrophilic molecules to pass, but excluding molecules larger than approximately 600 daltons. A variety of selective and nonselective transport proteins (porins) are responsible for the "molecular sieve" properties of the outer membrane and allow the cell to meet its nutritional needs in spite of the permeability barrier. The inner face supports the most numerically abundant protein in the cell, lipoprotein. The lipophilic end of this molecule dissolves into the outer membrane while the carboxy-terminus remains free or binds to the peptidoglycan sacculus. Sacculus-bound lipoprotein plays a structural role in support of the outer membrane (see section 1.5). Outer membrane physiology has

been considered in recent reviews by Nikaido and Vaara (1985), Osborn and Wu (1980) and Wright and Tipper, (1979).

E. coli cell envelopes must be capable of withstanding up to 5 atmospheres of internal osmotic pressure (Mitchell and Moyle, 1956). This is made possible in part by the peptidoglycan layer, a monomolecular network of repeating subunits (see section 1.4) forming a continuous "scaffolding" around the cell membrane. If the integrity of the peptidoglycan is destroyed by chemical or genetic means, then the cells will lyse (Ghuysen, 1977). Lysis may be prevented by culture in isotonic media, whereupon cells lose their rod-shape and grow poorly as spheres, termed "spheroplasts" (Daneo-Moore and Shockman, 1977). Peptidoglycan is also implicated in morphogenesis. Isolated sacculi retain the shape of the cells from which they were harvested (Henning, 1975). The combined functions of morphogenesis and osmotic stability make the peptidoglycan sacculus a major focus for growth and division studies.

The outer and cell membranes define a compartment called the periplasmic space. This compartment serves important functions in cell nutrition and defense as suggested by the transport and hydrolytic enzymes found there. We may also expect at least some cell division processes to be organized in the periplasmic space, for this is where the peptidoglycan layer is located. Because the intact sacculus offers no sites for new peptidoglycan to be added during growth, a mechanism must exist to "open up" growth zones in a controlled fashion. Indeed, a subclass of periplasmic hydrolytic enzymes, termed the autolysins, is capable of digesting the sacculus to a greater or lesser extent (Leduc et al., 1985, 1982, 1980), and seems to be essential for growth of the sacculus. How the activity of these enzymes is limited to prevent lysis in not known.

Finally, an analysis of cellular organization must consider the division septum. Here our conclusions must be guarded, because the division site as visualized by electron

microscopy appears different depending on the strain and the fixation procedure employed. Burdett and Murray (1974) examined a variety of strains with different fixation protocols and concluded that division in E. coli normally occurs by septation rather than constriction. Septa, however, are labile and the authors propose that they are destroyed by autolysins before fixation occurs with most protocols. The septum forms as an ingrowth of the cell membrane overlying a double layer of peptidoglycan. After the septum is completed, the closely apposed layers of peptidoglycan, which appear to be covalently linked, begin to separate. The separation process probably requires autolytic activity to split the double-peptidoglycan septum (see Section 1.6, Chapter 2; Wolf-Watz and Normark, 1976) and is accompanied by involution of the outer membrane. Although the outer membrane does not contribute to the primary septum, synthesis must continue in order to provide material to cover the new cell pole. In fact, extra outer membrane appears to accumulate as blebs at the septation site (Burdett and Murray, 1974) until it can be incorporated into the nascent pole. A cell-separation mutant designated envA, presumed deficient in the activity required to split the septum, continues to accumulate a large excess of outer membrane blebs at septation sites until cleavage of septa is completed (see Section 1.6).

1.3 The division cycle

Cell physiology experiments must be performed under conditions of balanced growth (constant growth rate), because bacteria vary in composition at different growth rates (Ingraham et al., 1983). Balanced growth is described as a state in which any one measurable property of a culture (cellular mass, for example) increases by the same factor as every other measurable property (Campbell, 1957). In such a

state, newborn cells in a culture would be identical in composition and organization to their parent cell and to other cells in the population.

A culture in balanced growth does not change its rate of volume or mass increase when cell division is inhibited by a variety of methods (see sections 1.4, 1.5). This implies that macromolecular synthesis and assembly of cellular structures is completely independent of division processes. Cells inhibited for division continue to replicate their chromosomes and elongate their surfaces (see Chapter 2), such that rod morphology distorts into a long filament. These and other observations are responsible for the model seen in Figure 1.1 (adapted from Donachie, personal communication).

The division cycle model shown in Figure 1.1 assumes that initiation of division and chromosome replication are sensitive to specific characteristics of cell growth, while cellular growth processes (other than DNA synthesis) are not directly affected by events specific to cell division or chromosome replication. Thus the growth time line continues much the same regardless of the division status of the cell. The elongation time line is shown separate from the growth time line because it represents a specialized aspect of growth.

The segregation functions that are accomplished by division probably occur passively for most cellular components, because their large number (of copies) assures roughly equal segregation upon binary fission. Segregation of spatial and genetic information must be more structured, however. Donachie (1981) summarizes the rules by which cell growth, segregation, and division appear to proceed. The following paragraphs discuss these rules of growth as they relate to replication and division.

Chromosome replication is constant at all growth rates, requiring about 40 minutes from initiation to termination of a round of synthesis (the C period of Cooper and

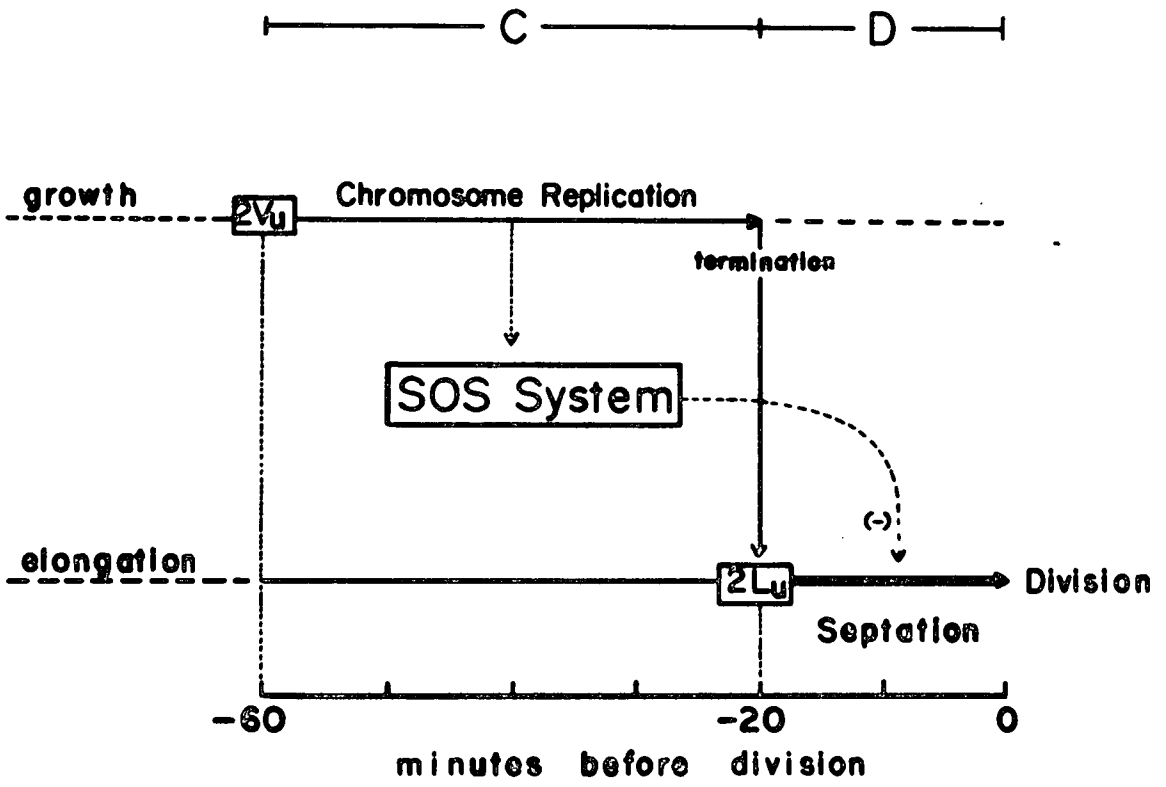
C
D
growth
2Vu
Chromosome Replication
termination
SOS System
(-)
elongation
2Lu
Division
Septation
-60
-20
0
minutes before division

FIGURE 1.1

Helmstetter, 1968). Some of the molecular events involved in initiation of replication have been described (see Kornberg, 1981 and 1982 for recent reviews), but control of the process remains largely unknown. What is known is that a growing cell initiates another round of replication when its volume reaches a critical size, $2V_u$ (or a multiple thereof, where V_u is the volume of a hypothetical newborn cell in a population at zero growth rate; Donachie, 1968). The initiation mass is independent of growth rate. Cells growing with doubling times faster than 40 minutes initiate new rounds of replication before the previous round has been completed (Helmstetter et al., 1968), as predicted by this model.

The nature of cell elongation is difficult to determine because of the small size of E. coli cells. Nevertheless, some guarded conclusions may be made. The rate of cell elongation increases sharply at a critical point in the division cycle (Donachie et al., 1976; Boyd and Holland, 1979; Rosenberger et al., 1978), represented in figure 1.1 by a thickening of the elongation line. Donachie et al. (1976) present evidence that this increase occurs at a critical cell length, $2L_u$ (where L_u is the length of a hypothetical newborn cell in a population at zero growth rate). One way this rate increase could come about is if the number of envelope elongation sites were to suddenly increase in response to a signal released when cells reached the length of $2L_u$. The nature of the signal is not known, and the threshold governing its release may be related to a process that parallels elongation. At the present time there is no obvious physiological significance to attribute to a cell length of $2\ L_u$.

The exact mode by which cells increase in length makes little difference for growth physiology models (only about 6 % predicted difference between exponential and linear models, Boyd and Holland, 1976), although it would be important for molecular models of envelope growth. While

elongation obviously depends on growth rate, Donachie (1981) also suggests that elongation is proportional to cell volume by the relationship:

$$dL/dt = (L_u/V_u)(V/T) \cdot 2^{(-40/T)}$$

where V is volume and T is the doubling time in minutes. This equation correlates well with observed patterns of E. coli elongation (Donachie, 1981), although other models cannot be excluded (see Helmstetter et al, 1979).

Whatever the exact mode of elongation, it seems unlikely that the rate of elongation, limited by synthesis of the envelope, should be always constrained to match the exponential increase in volume. If the pattern of elongation does not exactly match the surface area requirements for volume growth, then we should observe changes in cellular diameter over the division cycle. Treuba and Woldringh (1980) have confirmed this prediction, although the effect is small and becomes negligible at higher growth rates. Therefore, the common assumption that growing cells increase only in length at a fixed growth rate seems, to a first approximation, to be valid.

Figure 1.1 shows that a period of approximately 20 minutes is required between the termination of chromosome replication and cell division (the D period, Cooper and Helmstetter, 1968). It is in this segment of the division cycle that the final stages of assembly of the division machinery must be completed and the apparatus set into operation. We may expect, then, a requirement for synthesis of the gene products that make up the division apparatus, as well as regulatory or permissive factors, before septation begins. Most of this synthesis conceivably could take place at any point before division, but several lines of evidence suggest that at least one division factor must be expressed shortly before division commences (see Section 1.6, Chapter 2). This requirement is indicated in Figure 1.1 by an arrow

related to the termination event, although its characteristics are not known. Eventually a point is reached on the division time line after which cells are committed for division, with no further requirements for gene expression (Donachie et al., 1984).

At this point it is useful to consider the difference between critical periods for expression of a cell division gene and the pattern of expression that is normal for that gene. We can identify critical periods for expression of several genes (see Chapter 2), but we can infer nothing about actual patterns of expression. To investigate expression patterns, one needs to assay gene expression in the unperturbed division cycle. Lutkenhaus et al. (1979) examined total cellular proteins by 2-dimensional electrophoresis at different points in the division cycle, and found that none of the 750 polypeptides resolved by their system changed appreciably. They could not conclude that all genes are expressed continuously (for a given set of growth conditions) because of the limitations of their system, but they found no evidence that any particular polypeptide was synthesized only during a critical period. However, in the case of the chromosome replication cycle and the division cycle, discrete events take place that seem to require a trigger mechanism. If the trigger is not a relatively large burst of expression of an effector molecule, then what else could it be? Possibilities include 1) differential rates of specific protein synthesis with respect to cell growth, such that effector molecules either accumulate or become diluted (this could account for the critical mass for initiation of replication); 2) periodic synthesis of an effector polypeptide, in amounts too low to be detected by the 2-D system, that alters the activity of already-synthesized proteins; and 3) changes in activities of specific proteins due to development of critical spatial relationships of other factors, such as a cell wall elongation "clock" (Mendelson, 1982). Other theories could be

devised, but it must be remembered that periodic synthesis of regulatory factors has not been ruled out. All of these possibilities are consistent with the observation that timing of events in the division cycle correlates with the cell having attained specific critical dimensions.

Figure 1.1 summarizes the processes that normally occur before the cell division event at time zero. The timing of these processes is independent of growth rate. Therefore, initiation of predivision events begins at least 60 minutes before division, and the division cycle of a fast growing cell must have been set into action two or even three parent cells back. The fast growth rates achieved by E. coli would not be possible if division cycles could not overlap. The time line in figure 1.1 could be extended backwards to represent the "division history" of a particular cell line by superimposing each series of predivision events at intervals equal to the doubling time of the culture.

1.4 The SOS response

A growing cell in conditions of balanced growth expresses only the fraction of its genome needed to meet the specific catabolic and anabolic demands imposed by its culture medium. Expression of other genes is repressed unless they are induced by changing environmental stimuli. A system of genes that is induced in response to a specific stimulus is termed a stimulon. A set of stimulon genes that is induced by a single regulatory signal is termed a regulon. Expression of a regulon typically changes the physiological behavior of the cell in a manner that promotes survival. Balanced growth is disturbed, but the cell has heightened capacities to cope with an environmental challenge. One of the best characterized regulons is the SOS

response, induced when DNA metabolism is altered. Because one of the manifestations of the SOS response is inhibition of division, and some perturbations we may use to define the relationship between division and replication induce the SOS response, it is worthwhile to describe this system in some detail.

The SOS response includes induction of pathways active in DNA repair and mutagenesis, prophage induction, and inhibition of cell division. Inducing agents include nalidixic acid, thymine starvation, and ts-alleles at several loci (all treatments which alter progression of the replication forks) and UV-irradiation, alkylating agents, and cross-linking agents (all DNA-damaging treatments). Reviews have been published recently by Little and Mount (1982) and Walker (1984).

The SOS response is organized as follows: A variety of inducing signals (almost certainly related to DNA metabolism after a damaging event) trigger the inactivation of a single repressor, thereby inducing expression of at least 11 cistrons which make up the pathways of the SOS response. Development of a particular SOS phenotype, such as filamentation, depends on the behavior of unique molecular pathways operated by a subset of the derepressed cistrons.

The repressor-inducer circuits form the core of the SOS response. The repressor is the lexA gene product; it represses its own synthesis as well as that of the recA gene and several other genetic loci around the chromosome. However, recA repression is not complete, and it is normally expressed at levels sufficient to allow other RecA functions to continue. In the presence of an appropriate inducing signal, the RecA protein is altered such that it takes on a protease activity. One of the proteins recognized by the RecA protease is LexA. Upon LexA cleavage by RecA protease, the genetic functions of the SOS response are induced.

The arm of the SOS response leading to inhibition of cell division has recently been better characterized through

a molecular genetics approach. One of the loci induced by LexA cleavage is sulA (mapping at 22-minutes, Huisman and D'Ari, 1982, see figure 1.2). The sulA product is a polypeptide of approximately 18,000 daltons (Mizusawa and Gottesman, 1983), and acts to prevent cell division by blocking the action of the sulB product, which locus was recently shown by Lutkenhaus (1983) to be allelic with the essential cell division gene ftsZ (discussed in detail in Sections 1.6 and 2.4).

The SulA-FtsZ interaction must be in some way reversible, otherwise cells would not be able to recover from filamentation. In fact, another protease, the lon gene product, has been shown to degrade SulA, thereby relieving division inhibition. The Lon protease (also called CapR, molecular weight 94,000, Zehnbauer et al., 1981) plays an important role in degrading other cellular polypeptides (see Section 1.6), and lon mutants understandably have complex phenotypes (Schoemaker et al., 1982), including a hypersensitive cell division inhibition in response to even mild DNA damage.

The SOS response is invoked often these days in interpretations of division cycle experiments, especially those concerned with characterizing the relationship of division to chromosome replication (see Section 1.6). Many experiments have had to be reinterpreted in light of an improved understanding of SOS effects, and other experiments will need to be repeated with the SOS factor eliminated (by a sulA deletion, for example). Some of the questions addressed by these early experiments remain unanswered today, although we are approaching a level of understanding at which answers should be possible.

1.5 Envelope synthesis and assembly

The processes that incorporate new envelope material must overcome several physical and topological problems. How is new material added to the sacculus without permitting extrusion of the cell membrane and lysis? How are new phospholipids, proteins, lipopolysaccharides and peptidoglycan subunits synthesized in the cytoplasm or cell membrane and translocated to the periplasm and outer membrane? How is the synthesis of each of the three layers coordinated, and how is growth constrained to occur by elongation only? How is cell diameter increased by an increasing growth rate and how is it maintained essentially constant during growth at a fixed rate? The molecular mechanisms behind each of these questions are hardly known, yet ongoing investigations are bringing us closer to answers. Some of these will be reviewed here.

Growth of the cell membrane requires phospholipid and protein synthesis and assembly into a topologically correct structure. Biosynthetic enzyme systems for phospholipids are located in the membrane itself (see Cronan, 1978 for a review) and incorporation of new lipids takes place by self-assembly. Envelope protein synthesis requires the combined activities of the complex PSS and the secretory apparatus.

The secretory apparatus is just beginning to be understood (see Randall and Hardy, 1984 and Inouye and Halegova, 1980 for recent reviews). Assembly of envelope proteins occurs during the stages of polymerization mediated by the ribosome, and seems to combine mechanisms of self assembly and assembly directed by the ribosome, secretory apparatus, and cell membrane. Many envelope proteins are synthesized with NH_3-terminal signal sequences that interact with the secretory apparatus such that the nascent polypeptide is polymerized through special secretory sites in the envelope (signal peptide hypothesis, see Blobel and Dobberstein, 1975). Some envelope proteins do not appear to use this mechanism, but instead are composed of polypeptide

chains capable of conformational changes at the cytoplasmic-cell membrane interface that position the molecule into its stable membrane conformation (membrane trigger hypothesis, Wickner, 1979). Growth of the cell membrane probably in no way limits cell envelope growth, and this discussion will focus on the outer layers.

The outer membrane, not unexpectedly, also appears to be constructed by a self-assembly mechanism (Yamada and Mizushima, 1978). The problem lies in translocating outer membrane components across the cell membrane. The inner face of the outer membrane is probably continuous with the outer face of the cell membrane at fusion sites (Bayer, 1974), so phospholipid synthesis and assembly should be straightforward. Lipopolysaccharides complete their biosynthetic steps in the cell membrane, and translocation to the outer face of the outer membrane almost certainly occurs at fusion sites. Polypeptides are probably also translocated at fusion sites (Osborn and Wu, 1980), and lipopolysaccharide interactions may play a role in their final assembly into the outer membrane. Assembled products must then diffuse away from the assembly sites (in accord with the fluid mosaic model, Singer and Nicholson, 1972) to allow assembly of emerging polypeptides to proceed. Lipoprotein is also assembled at fusion sites (Osborn and Wu, 1980), but the mechanism by which it enters the periplasmic space is not known. Control of linkage to the peptidoglycan sacculus has not been well characterized, but newly added peptidoglycan begins linkage to lipoprotein soon after its addition to the sacculus, and the process is essentially complete one-half generation later (Burman and Park, 1983).

The outer membrane probably plays little role in maintaining cellular morphology, but it may function indirectly in some stages of morphogenesis (see Section 1.6). One likely possibility is that the outer membrane carries topological information essential to those growth processes that determine the shape of the sacculus.

Due to its obvious role in structural integrity and morphogenesis, the peptidoglycan layer has been the focus of many cell envelope growth studies. This discussion will review the mechanisms of peptidoglycan synthesis and assembly, some of the enzymes that direct this construction, and a recent molecular model describing how this construction might be organized.

Peptidoglycan synthesis begins with synthesis of the basic subunit, the muropeptide, consisting of an (N-acetyl-glucosamine-muramic acid) disaccharide backbone and a pentapeptide side chain. Construction of the muramic acid residue and addition of the five amino acids (L-alanine, D-glutamic acid, Meso-diaminopimelic acid, and D-alanyl-D-alanine) occurs in the cytoplasm (Mengin-Lecreulex et al., 1982). Addition of the N-acetyl-glucosamine residue and translocation to the outer face of the cell membrane takes place on a membrane-bound undecaprenol carrier (see Tipper and Wright, 1979, for review). In the presence of a suitable acceptor site in the pre-existing peptidoglycan sacculus, the muropeptide is released from the lipid carrier, transglycosylated into the growing glycan chain (polymerization), and cross-linked (transpeptidated) with adjacent peptide side chains. In the predominant mode of peptidoglycan assembly, the cross-linking reaction requires a pentapeptide "donor" side chain in suitable configuration with a tetrapeptide "acceptor" side chain. The penultimate donor D-alanine is linked to the acceptor Meso-DPA, with cleavage of the donor terminal D-alanine (see below). Uncross-linked side chains are rapidly converted to tetrapeptides by the action of a periplasmic D-alanine carboxypeptidase (dePedro and Schwarz, 1981), thereby limiting the transpeptidation reaction. Mature peptidoglycan is only about 25% cross-linked, on average (Waxman and Strominger, 1983; see below), and evidence is accumulating that the degree of cross-linking may influence the shape of the sacculus (Torti and Park, 1981; Markiewicz et al., 1982).

Glycan chain structure reveals much about sacculus organization and construction. Average chain length is 30 muropeptide residues (de Pedro and Schwarz, 1981), and they assume a spiral conformation, such that pentapeptides radiate in all directions from the longitudinal axis of the chain (Barnickel et al., 1983). EM and X-ray diffraction studies suggest that glycan chains are oriented perpendicular to the long axis of the cylindrical cell, and that chains lie roughly parallel to each other (Burge et al., 1977, Verwer et al., 1978).

At constant growth rate, and hence constant diameter, peptidoglycan growth processes must account primarily for intercalation of parallel glycan strands to achieve elongation of the cylindrical cell (Burman et al., 1983) and incorporation of polar caps to achieve septation and division. From a structural point of view, cylindrical peptidoglycan is different from polar peptidoglycan, and it appears that the growth mechanisms resulting in its formation are different too (see below).

Some of the enzymes that are responsible for peptidoglycan assembly are known. These are primarily the penicillin- binding proteins (PBPs), represented by at least seven distinct classes in E. coli (reviewed by Waxman and Strominger, 1983; Matsuhashi et al., 1982, 1981; Spratt, 1977). They are all membrane proteins, and some of them have been well characterized. Their properties will be briefly summarized here, followed by discussion of a molecular model for peptidoglycan synthesis that is based on the PBP functions.

The PBP1 group consists of PBP1A, encoded by the mrcA locus, and 3 PBPBs, probably all expressed by the mrcB locus (see Table 1.2, Figure 1.2). Why the mrcB product should appear as 3 different bands is not understood. The PBP1 proteins represent the major peptidoglycan synthetic activities in the cell. Genetic or pharmacological inhibition of PBP1 group functions causes cessation of peptidoglycan

synthesis and eventual lysis. The fact that individual mrcA and mrcB mutations are well tolerated suggests that their functions may be redundant, however loss of either one causes the cell to become exquisitely sensitive to penicillin. Both of these enzymes are bifunctional with transglycosylase and transpeptidase activities, thus they are well suited to construct new glycan chains and to cross-link them into the growing sacculus.

Another PBP with transpeptidase and possible transglycosylase activities, PBP2, is encoded by the pbpA locus. Mecillinam binds specifically to PBP2, and produces the characteristic phenotype of ovoids and spheres of various sizes. Mecillinam-resistant pbpA mutants grow slowly as small, round cells. These results suggest a role for PBP2 in maintaining regular cylindrical growth. Both the PBP1 group and PBP2 are thus essential for elongation, the former by providing net peptidoglycan synthesis, and the latter by determining cylindrical organization of new peptidoglycan. Possible mechanisms by which these proteins participate in orderly growth of the sacculus are presented later in this section.

Whereas the first two groups of enzymes presented appear to function primarily in elongation, PBP3, encoded by ftsI, appears to function specifically in septation. ftsI maps to the 2 minute cluster containing several genes specifically involved in cell division, and is the only one of these genes for which a biochemical assay is available. PBP3 has dual transglycosylase and transpeptidase activities, and its properties suggest that it functions to build the septal peptidoglycan required by the division process. Broome-Smith et al. (1985) have constructed a site-directed mutant based on active site serine predictions from the ftsI sequence (Nakamura et al, 1983) in which serine-307 has been replaced by cysteine. Expression of the $PBP3^{cys-307}$ allele produces a dominant inhibition of division, suggesting that the inactive enzyme is able to replace the wild

type enzyme stoichiometrically in an enzymatic complex that is part of the septation apparatus. PBP3 may not be the only PBP involved in septation, as the recently discovered PBP1c has also been implicated (Botta and Park, 1981).

PBPs 4, 5, and 6 all carry D-alanine-carboxypeptidase activity, and therefore could regulate peptidoglycan assembly by limiting the abundance of pentapeptide precursors for the cross-linking reaction. One of the cell's major carboxypeptidases is PBP5, encoded by dacA. Levels of PBP5 can be increased almost 4-fold by cloning dacA into a pSC101 vector, and cells with increased dacA expression grow as ovoids reminiscent of PBP2 inhibition. Markiewicz et al. (1980) found that both PBP2-inhibited and PBP5-induced ovoids have increased levels of peptidoglycan cross-linking, leading these authors to propose the following model for morphogenesis of the sacculus: PBP2, which organizes cylindrical assembly of peptidoglycan, preferentially requires a pentapeptide substrate. However, D-alanine-carboxypeptidase activity, including a large contribution from PBP5, competes for these substrates and converts them to the less favorable tetrapeptide substrate. If tetrapeptides are preferentially acted upon by PBP3, as suggested by Botta and Park (1981), then PBP5 could act as a switch from elongation to septation by changing the pentapeptide to tetrapeptide ratio. Mirelman et al. (1977, 1978) do in fact describe a cyclical variation in carboxypeptidase activity, finding low levels in cells that elongate without dividing and high levels in synchronous cultures prior to cell division. This model has not been extensively tested, but it will likely lead us to a more complete understanding of molecular interactions in peptidoglycan assembly.

The discussion thus far has featured activities of specific enzymes involved in synthetic and degradative peptidoglycan metabolism. Of course, the penicillin-binding assay reveals only a few of the processes underlying morphogenesis. We can expect to find important roles for non-

penicillin-sensitive factors as well, and only through better characterization of these proteins, along with the PBPs, can we hope to improve our understanding of the molecular mechanisms of elongation and septation. The fundamental question remains: How are these activities coordinated in a mechanism that directs sacculus growth and morphogenesis?

While cell surface growth models are numerous, a recent molecular model proposed by Burman and Park (1984) elegantly integrates a collection of observations at the molecular and cellular levels. Their model begins with the controversial question of sacculus growth sites. Are new glycan chains added at topologically defined growth zones or are they diffusely intercalated into the peptidoglycan network? (Reviewed by Verwer and Nanninga, 1980; Burman et al., 1982.) They approach this question through the kinetics of a [^{14}C]DAP label during incorporation as donor muropeptides through maturation as acceptor muropeptides (the acceptor and donor halves of a muropeptide cross-linked dimer are stereochemically distinct). Their results suggest approximately 100 separate sites of incorporation, dependent on endopeptidase, transglycosylase, and transpeptidase activity. Their molecular model relies on 3 assumptions, which have been discussed above: 1) glycan strands are arranged in parallel, perpendicular to the long axis of the cell; 2) incorporation of new muropeptide subunits occurs through simultaneous transglycosylation and transpeptidation (Burman and Park, 1983; although not every muropeptide becomes cross-linked at the incorporation phase, those that do are linked simultaneous with the polymerization reaction); and 3) only the new muropeptides possess the pentapeptide side chains required of donor substrates in the transpeptidation reaction. Note that this model only pertains to elongation, and has not been extended to septation processes.

The Burman-Park model holds that a group or complex of plasma membrane enzymes follow along pre-existing sacculus glycan strands destined to serve as crossbridging acceptors. An endopeptidase opens a groove between adjacent strands while transglycosylase and transpeptidase activities incorporate new muropeptide chains and perform the preliminary transpeptidation for cross-linking. These membrane enzymes follow along in the direction of glycan strand extension in an eternal helical path, with approximately eight minutes required to extend new glycan about the circumference. This is equivalent to about 2500 muropeptide subunits at a rate of five muropeptides/sec at 37°C in minimal glucose media. Approximately 90 enzyme complexes are required over the surface of the cell, and two strands are incorporated simultaneously at each site. The helical path of the enzyme complex causes new glycan strands to be incorporated adjacent to the strands that were freshly added on the previous round. Of the two strands that are simultaneously laid down, the trailing strand is given twice as many peptide cross-links as the leading strand, resulting in a heavily cross-linked, permanent groove and a lightly cross-linked, temporary groove. The enzyme complex preferentially follows the temporary groove, requiring a minimum of endopeptidase cleavages to separate strands at the growth site. Thus, the trailing strand should form "permanent" crossbridges with the pre-existing peptidoglycan network and "temporary" crossbridges with the leading strand. The leading strand should form temporary crossbridges with both the trailing strand and the pre-existing peptidoglycan network. There is no evidence that distinguishes between the possible pathways of maturation of lightly crossbridged grooves. Are all lightly crossbridged grooves destined to accommodate a new glycan strand, or do some mature through secondary transpeptidation? The enzyme complex would have to reinitiate new chains roughly every 30 muropeptides, the average length of a glycan chain.

Speculation as to the identity and organization of the growth site enzymes relies primarily on the PBPs. The major PBPs 1A and 1Bs are candidates for the major transglycosylase and transpeptidase activity at the growth site, while PBP4 could well serve as the major endopeptidase activity. Spratt (1977) estimates about 230 molecules of PBP1A and 1Bs (together) and 110 molecules of PBP4 per cell, consistent with 90 growth sites per cell. Because transpeptidations between a left-sided acceptor and right-sided donor are stereochemically different from those between a right-sided acceptor and left-sided donor, two different glycan synthetic species could reasonably be expected at each growth site. PBP2, with a level of 20 molecules per cell (Spratt, 1977), could not be found at every growth site, but those few molecules could determine the overlapping or end-to-end organization of separate glycan chains around the circumference, perhaps by controlling reinitiation of new chains. PBP2, of all the PBPs, is found preferentially in cylindrical regions of the growing sacculus (Buchanan, 1981). PBP5 and PBP6, by removing terminal alanine residues, could switch new glycan chains from a donor to an acceptor role in crossbridge formation.

A different model of sacculus growth that deserves mention is the helical growth model presented by Mendelson (1982). Although his model differs from the Burman-Park model in molecular detail, some general aspects of helical addition of new wall material are shared by the two. Mendleson's model goes beyond molecular interactions to offer a theoretical basis for 1) septation, by reversing the twist of newly inserted glycan chains; 2) a clock for timing of cell cycle events; and 3) a mechanical basis for chromosome segregation. Although both of these models offer exciting new explanations and predictions, their accuracy remains to be determined.

Finally, envelope growth models must account for the differential effects of surface tension on an expanding

network surrounding a hydrostatically pressurized interior. These factors play a major role in morphogenesis and have been described in a model by Koch and Burdett (1984), but they are not directly relevant to the focus of this thesis.

1.6 Morphogenesis

Division of the growing cell marks the beginning and end of what was termed the "division cycle" in Section 1.3. This event culminates the processes of envelope growth that produce progeny cells generally identical to the rest of the population. The fact that environmental or genetic perturbations yield cells of different shape suggests that ongoing morphogenetic determinants are active between division events. Donachie et al. (1984) coined the term "morphogenetic cycle", which includes division as well as the inter-division events that affect cell shape.

Why morphogenetic controls are important to cell growth may not at first seem obvious. The disadvantages of morphological changes in a filamenting cell serve as a useful example. Filamentation does not promote survival. The cellular investment of building blocks and energy is locked up into relatively few, vulnerable units, motility is impaired, and regulation of growth processes may be expected to become increasingly chaotic as an increasing number of semi-autonomous "unit cells" add their signals to a common space. As was discussed in Section 1.3, regulatory signals in the division cycle seem to be triggered as the cell reaches critical dimensions. Therefore, morphogenetic regulation helps to ensure that cells in growing populations remain maximally functional and viable.

Table 1.1 shows a classification scheme for phenotypes of mutants with morphological perturbations. Note that considerable overlap occurs between classes of mutations because many of them give pleiotropic phenotypes. Donachie et al. (1984) have discussed the "morphogenes" defined by these mutations, and the following discussion is adapted

Table 1.1

Classification scheme for the morphogenes of *E. coli*

Class	Function
1	genes involved in muropeptide biosynthesis
2	genes involved in cylindrical elongation of the sacculus
3	genes affecting outer membrane proteins that influence morphogenesis
4	genes linking division with DNA replication
5	genes involved in septation site-localization and nucleoid segregation
6	genes involved in initiation of septation
7	genes required for septation
8	genes involved in cell separation
9	genes influencing septation site inactivation

from their review. Note that my Classes 1,2, and 3 do not correspond exactly to those listed by Donachie et al. The morphogenetic loci are illustrated in Figure 1.2 and described in Table 1.2.

Class 1 morphogenes, responsible for muropeptide synthesis, give the characteristic mutant phenotype of lysis under restrictive conditions (see Section 1.2). Their significance lies in the fact that they provide the substrates used by enzymes that direct peptidoglycan assembly. Most of the amino acid-adding enzymes are produced by genes in a tightly linked cluster mapping at 2 minutes and will be discussed in Chapter 2.

Class 2 morphogenes, responsible for cylindrical peptidoglycan assembly, give a variety of mutant phenotypes. The loci previously described consist of the PBP genes mrcB for PBP1Bs, mrcA for PBP1A, pbpA for PBP2, dacB for PBP4, and dacA for PBP5. Two other types of genes also seem to affect cylindrical growth, and both types are recovered as mutations conferring mecillinam resistance. One is the rodA locus, which maps in the same 15 minute cluster as pbpA and dacA. The product of the rodA gene is a 31,000 dalton protein, which like PBP2 is associated with the plasma membrane (Stoker et al., 1983), but no enzymatic activity has been demonstrated for it. The other class of mutations all map near the cya and crp loci at 85 and 74 minutes, respectively. Both cya and crp strains grow as small, round cells, although they do become slightly more spherical in the presence of mecillinam. These strains are also unable to form filaments when division is inhibited, in contrast to rodA and pbpA strains, suggesting that cylindrical growth requires participation by the cAMP-CAP complex. Donachie et al. (1984) propose that the cAMP-CAP complex negatively regulates septal peptidoglycan assembly. This could account for the small, round cells that are produced by a cya$^-$ or

Figure 1.2

The morphogenes of *E. coli*

Fifty-four morphogenetic loci are shown from the genetic map of *E. coli* K-12, Edition 7 (Bachman, 1983) and other sources (see Section 1.6 for further details). Adapted from Donachie et al, 1984. *lexA* and *recA* are not primary morphogenes, but are included in parentheses because of their role in SOS-dependent inhibition of division.

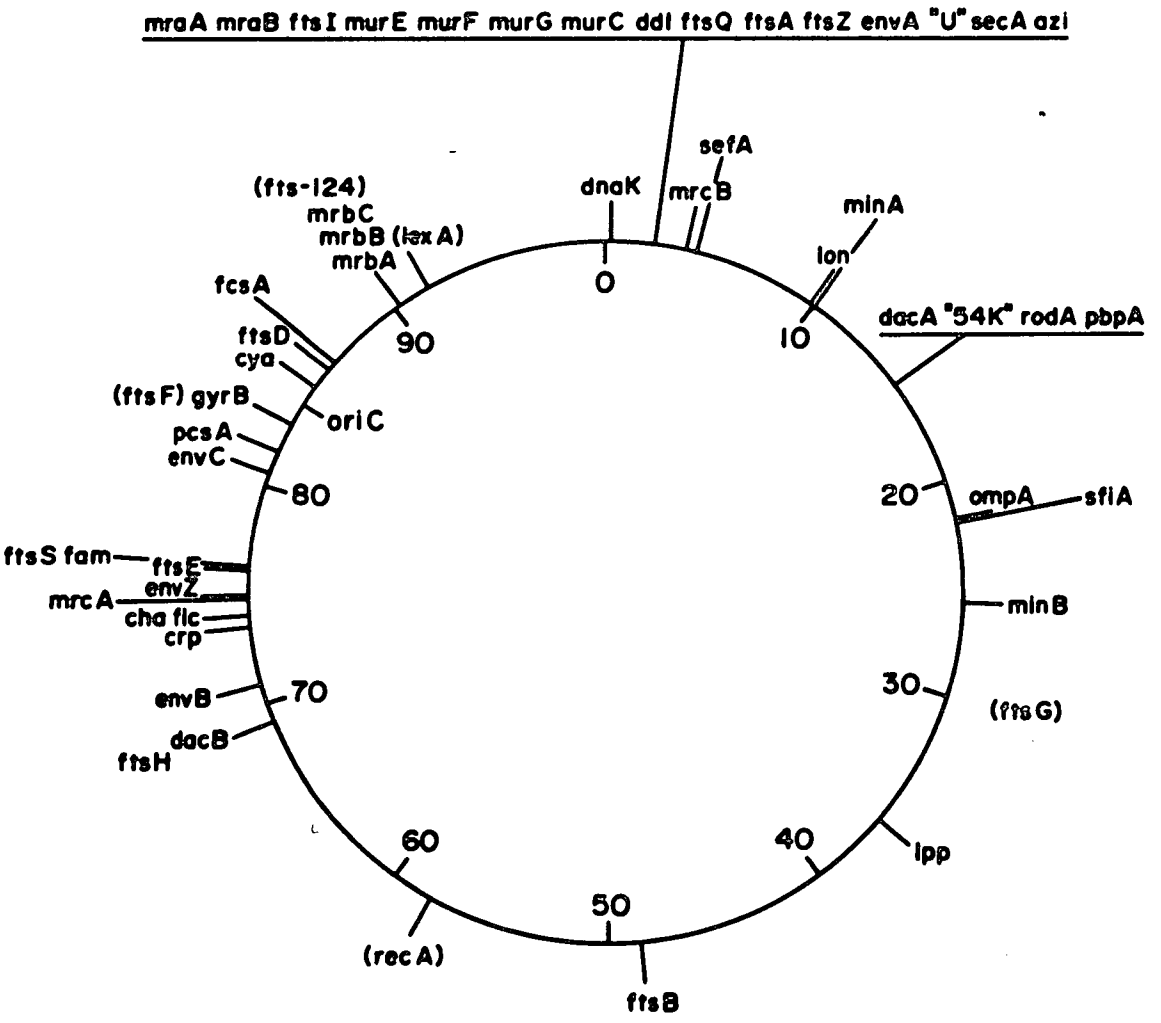
mraA mraB ftsI murE murF murG murC ddl ftsQ ftsA ftsZ envA "U" secA azi
dnaK
sefA
mrcB
minA
lon
dacA "54K" rodA pbpA
ompA
sfiA
minB
(ftsG)
lpp
ftsB
(recA)
ftsH
dacB
envB
ftsS fam
ftsE
envZ
mrcA
cha fic
crp
(ftsF) gyrB
oriC
pcsA
envC
ftsD
cya
fcsA
(fts-124)
mrbC
mrbB (lexA)
mrbA
0
10
20
30
40
50
60
70
80
90

FIGURE 1.2

crp⁻ strain. Supporting this argument are: 1) cAMP added to cya mutants restores rod shape and mecillinam sensitivity (Aono et al., 1979), and 2) another allele, designated fic (Utsumi et al., 1982) produces the phenotype of filamentation upon addition of cAMP. Septation resumes when cAMP is removed or cGMP added. Although fic maps very close to crp, the mutants exhibit different phenotypes, and Utsumi et al. (1982) feel that they are nonallelic. It remains possible that fic is a dominant allele of crp with properties of enhanced septation inhibition, but this has not been investigated.

The mechanism of the similar envB phenotype is poorly understood, but again it is possible that envB represents a different crp allele.

Whether the cAMP-CAP complex inhibits septation at the level of gene expression or enzymatic activity has not been shown conclusively. However Utsumi et al. (1983) report that an unknown 40,000 dalton protein is expressed upon induction of fic filamentation by cAMP. In at least some cases of division inhibition, then, the crp and cya products act at the level of gene expression. Evidence will be presented in Chapter 2 that the cAMP-CAP complex also affects expression of a cell division gene.

Class 3 morphogenes, responsible for outer membrane proteins involved in morphogenesis, consist mainly of ompA, coding for one of the major outer membrane proteins, OmpA, and a variety of loci that direct lipoprotein synthesis and incorporation into the outer membrane. lpp, the structural gene for lipoprotein, maps at 36 minutes. Deletion mutations are known (Hirota et al., 1977), but seem to give minor phenotypic abnormalities: The outer membrane appears less tightly bound to the sacculus, especially at septation sites, periplasmic proteins leak during growth, and cells are more sensitive to a variety of external toxins (Fung et al., 1978). An allele is also known that appears defective

Table 1.2 The morphogenes of *E. coli*
(as mapped by Bachman, 1983; other references in text)

Locus	Gene symbol	Function/Product	Class
0	*dnaK*	septation (heat shock protein)	6, 7
2	*mraA*	D-alanine carboxypeptidase	1, 2?
2	*mraB*	D-alanine requirement	1
2	*ftsI*	PBP3 (transpeptidase/ transglycosylase)	1, 6, 7
2	*murE*	*meso*-diaminopimelate adding enzyme	1
2	*murF*	D-alanyl-D-alanine adding enzyme	1
2	*murG*	murein biosynthesis	1
2	*murC*	L-alanine adding enzyme	1
2	*ddl*	D-alanine:D-alanine ligase	1
2	*ftsQ*	Septation	6, 7
2	*ftsA*	Septation	7
2	*ftsZ*	Septation	6, 7
2	*envA*	cell separation, control of N-acetylmuramyl-L-alanine amidase	8
2	"U"	unknown; septation effects at high copy number	?
2	*secA*	envelope protein secretion, effect on septation	8?
2	*azi*	septation (resistance to azide)	6, 7, 8?
4	*mrcB*	PBP1Bs	1, 2
4	*sefA*	septation	7
10	*lon*	protease La; inactivation of sfiA protein	4
10	*minA*	inactivation of septation sites	9
15	*dacA*	PBP5; D-alanine carboxypeptidase	2?
15	*rodA*	cylindrical growth	2

Locus	Gene symbol	Function	Class
15	pbpA	PBP2; transpeptidase/ transglycosylase	1, 2
22	ompA	outer membrane protein 3a	3
22	sfiA	inhibitor of ftsZ protein	4
26	minB	inactivation of septal sites	9
29-31	ftsG	septation/viability	6, 7?
36	lpp	murein lipoprotein	3
49	ftsB	septation/viability	6, 7?
69	dacB	PBP4; D-alanine carboxypeptidase	1, 2?
69	ftsH	septation	6
71	envB	cell shape	2
74	crp	cAMP-binding protein (CAP)	2
74	fic	cAMP-sensitive septation step	6, 7, 2?
74	cha	division/cell shape	6, 7, 2?
75	mrcA	PBP1A; transpeptidase/ transglycosylase	1, 2
75	envZ	regulation of outer membrane proteins	3?
76	ftsE	septation	6, 7
76	fam	murein lipoprotein control?	3, 6, 7
76	ftsS	septation	6, 7
81	envC	septation	7
82	pcsA	chromosome segregation	5?
83	gyrB	DNA gyrase B; chromosome segregation and septum placement	5
82-83	ftsF	septation/viability	6, 7?
85	cya	adenyl cyclase; cell shape	2
86	ftsD	septation	6, 7
86	fcsA	septation	6, 7
90	mrbA	UDF-N-acetylglucosaminyl-3-enolpyruvate reductase	1
90	mrbB	murein biosynthesis; D-alanine required	1
90	mrbC	murein biosynthesis	1
90(ca)	fts-124	septation	6, 7

in cross-linking to the sacculus, with a similar phenotype (Wu et al., 1977). Torti and Park (1980) report a mutation, fam (mapping at 76 minutes), temperature sensitive for division and low lipoprotein levels. They propose that this locus is somehow involved in regulating lipoprotein assembly as well as in processing one or more proteins involved in division. The close proximity and similar phenotypes of fam and ftsE (figure 1.2, see class 7 morphogenes), raises the possibility that they are allelic, although Salmond and Plakidou (1984) feel that they represent different elements in yet another morphogenetic cluster.

OmpA protein is unusual in that it appears to be preferentially incorporated and located at cell poles and nascent septa (Begg and Donachie, 1984). The role this protein plays is not clear, but it seems unlikely to be a porin (Nikaido and Varra, 1985). OmpA associates with lipoprotein (Palva, 1979), and possibly with the underlying sacculus (Endermann et al., 1978), although these associations have not been characterized. The protein appears divided into a large N-terminal membrane-associated domain and a C-terminal domain exposed in the periplasmic space. ompA mutants have relatively normal morphology, although, like lpp$^-$ strains, the outer membrane appears unstable.

ompA-lpp double mutants, however, grow as ovoid cells (Sonntag et al., 1978), reminiscent of pbpA and rodA strains. The question, then, is what role do these loci play in directing envelope growth? They are both probably involved in involution of the outer membrane as division septa split (Fung et al., 1978), although this is not likely to be the mechanism behind ovoid growth. The double-mutant phenotype may be related to an exaggerated separation between the outer membrane and the sacculus. Rodriguez-Tebar et al. (1985) report that most of the PBPs, including PBP2, are found approximately equally divided between the outer and cell membranes. Thus, PBP2 may be rendered topologically ineffective by outer membrane distortions in

cells with neither OmpA or lipoprotein to organize the outer membrane relative to the sacculus. Whatever the morphogenetic mechanisms of the lpp-ompA phenotype, it seems to be secondary to perturbations in outer membrane organization.

Class 4 morphogenes control the pathways that link division with chromosome replication. Normal cell division results in only 0.1% "DNA-less cells" (Howe and Mount, 1975), implying that the timing of division is somehow regulated relative to termination of replication. Attempts to dissociate division and replication generally lead to inhibition of division through the SOS response. The questions remain: Are there other mechanisms coupling division with replication, and does the SOS response play a role in unperturbed cell division?

Huisman et al. (1983) present strong evidence that the SOS response plays no role in normal division cycle control. They found that sulA$^+$ and sulA strains were quite similar in size and DNA content, and that sfiA expression could only be demonstrated in situations where the SOS system was induced. They account for the observed increased frequency of DNA-less cells in recA strains through higher levels of spontaneous DNA degradation (Capaldo and Barbour, 1975), and find lexA strains probably to behave similarly. sulA almost certainly represents the sole SOS division inhibition pathway, because sulA and sulB are able to completely suppress filamentation when the SOS system is induced in the absence of DNA damage (for example, by a lexA(ts) allele; George et al., 1975).

When DNA replication is inhibited, however, even sfiA$^-$, recA$^-$, and lex(Ind$^-$) strains begin to filament, albeit after a long delay (Inouye, 1969, 1971; Burton and Holland, 1983; Huisman et al., 1983), suggesting that a sul-independent, SOS-independent mechanism exists to prevent division before termination of replication. This filamentation follows different kinetics than SOS-induced

filamentation (Burton and Holland, 1983) such that D-period cells, already committed for division, are able to complete the process even if DNA replication is inhibited. The residual low levels of division that remain produce small cells of various lengths, and these cells contain no DNA (Inouye, 1969). In contrast to the sfiA-dependent pathway of division inhibition, the independent pathway is not sensitive to rifampicin (Burton and Holland, 1983), suggesting that expression of another division inhibitor protein is not a likely mechanism. Both sfiA-dependent and independent pathways require the recA locus (Burton and Holland, 1983), presumably through quite different mechanisms. Both pathways operate only in cells actively replicating their chromosomes. Schoemaker et al. (1982) report the identification of a RecA-independent, Lon-protease-sensitive polypeptide (11,000 dalton) induced by inhibition of cell division, confirming that more components of pathways regulating cell division await identification.

All of the above observations are consistent with a general mechanism of division in which replicating chromosomes are somehow bound to potential division sites, physically or chemically blocking septation at these sites until replication has terminated. (Note that such a model is also consistent with cellular organization as presented in section 1.2 and 1.3). The termination event presumably alters the association of the chromosome with the septation site, acting in a permissive capacity to allow septation to proceed. Certain mutants, such as a dnaAts strain, unable to initiate new rounds of chromosome replication do not elicit the SOS response or the alternative response, giving rise to cells that continue to elongate and divide to produce DNA-less cells (Donachie et al., 1984; Hirota et al., 1968). However, the cells that contain the chromosome are always longer (2 to 4 cell lengths) than DNA-less cells and wild type cells, as if the chromosome prevented septation at the central division sites.

Other models could be constructed to account for these observations, although they would probably have to contain the larger part of the interpretations presented above concerning SOS division inhibition, the alternative pathway, and the nucleoid block. One observation that has not been dealt with is the period of protein synthesis required early in the D period (Donachie et al., 1979). Whether this period of synthesis actually represents a control signal to the division apparatus that replication has terminated, such as the termination protein of Jones and Donachie (1973), or whether it represents some other requirement for organization and assembly of the division apparatus remains to be shown (Donachie et al., 1979; see Figure 1.1, events surrounding termination).

Class 5 morphogenes include those involved in positioning of the septation site and nucleoid segregation. It should come as no surprise that these properties should be related in view of the above discussion of the nucleoid block. Nucleoid segregation very likely depends on the association between the chromosome and the envelope (reviewed by Leibowitz and Schaecter, 1975), although the specific factors that perform the linkage, the chromosome domains involved, and the envelope sites involved are not known. Cell fractionation studies have repeatedly demonstrated that some envelope and chromosomal markers co-purify. Particular studies have found evidence implicating oriC, the terminus, the replication fork, and random sequences (Worcel and Burgi, 1974) in linkage with both cell membrane and outer membrane components (Kornberg, 1982). Chromosome replication does not depend on membrane-bound factors in vitro (Kornberg, 1982), thus the chromosome-envelope association may play no other role than segregation. Characterizing the elements of this linkage may reveal the nature of the septation site-localizing mechanism.

A priori, we could expect the septum site-determining mechanism to be somehow sensitive to cell elongation, such that septation is initiated at the proper location when cell length reaches $2L_u$. Whether the mechanism is actually sensitive to cellular dimensions, perhaps by counting the number of glycan chains intercalated, or whether it responds to a level of regulation underlying elongation is not known. In fact, only a few septum-localization mutants are known, indicating perhaps that the mechanism tolerates alterations poorly. As mentioned before, Inouye (1969) reported a recA allele that produced some small DNA-less cells of various sizes when DNA synthesis was perturbed. These cell sizes were not quantitatively analyzed, hence it is impossible to conclude that their lengths were truly random.

In contrast, deficiencies in the expression or activity of the gyrB gene product, the B subunit of DNA gyrase, leads to aberrant division localization, producing cells of random size distributions (Herrero et al., 1982; Fairweather et al., 1980; Orr et al., 1979). All other classes of division mutants are able to form septa at predicted locations related, not surprisingly, to L_u (Donachie et al., 1984).

The mechanism of the gyrB effect seems to be, in part, indirect. DNA gyrase B, carrying the ATPase activity of the holoenzyme, is essential for decatenating interlocked, newly replicated chromosomes (Steck and Drlica, 1984). Catenated chromosomes are not able to segregate, and in fact, dumbell-shaped nucleoids are seen in gyrA and gyrB mutants. A nucleoid block seems particularly likely in these strains. Also, gyrase deficiencies will interfere with maintenance of negative supercoiling needed for initiation and progression of replication and transcription, thereby affecting gene expression as well as chromosome structure (Wahle et al., 1984). Furthermore, as in the case of gyrase A-subunit inhibition, B-subunit inhibition does induce an SOS response, although at much lower levels (Smith, 1983).

Therefore, the mechanism behind altered placement of septation sites is likely to involve complex participation by adaptive cellular pathways.

The only other mutant known to give random localization of septa is described by Donachie et al. (1984). Although this mutation is unmapped, its general phenotype suggests that it is not allelic with gyrB. Like gyrB(ts), this mutant is unable to segregate its nucleoid. Details of the mechanism that directs sites of assembly for the septation apparatus are not clear, but it seems likely that nucleoid duplication and segregation are intimately associated with this mechanism.

Class 6 morphogenes are responsible for initiation of division. Septation cannot begin until all components of the septation apparatus are properly assembled, and it would not be unreasonable to predict that one or more of these components would function only in initiation. The mutations at ftsH (Santos and de Almeida, 1975) and an unmapped locus nonallelic to ftsH (Donachie et al., 1984) give the properties expected of an initiator mutation. After a shift to 42°C, these ts-mutants continue to divide at a normal rate for 20 minutes, the time required to complete septa initiated early in the D period, before division stops abruptly. Other possibilities that could account for this behavior include ts-expression or assembly of a gene product required in stoichiometric quantities for the septation apparatus or the slow inactivation of a septation gene product. Thus, while an initiation step in septation remains an intriguing possibility, it is by no means a certainty.

Class 7 morphogenes are involved in septation. A variety of genetic defects cause filamentation, but the mechanism by which filamentation occurs may be indirect. Hence, several loci are included in class 7 even though they probably play no direct role in septation. These include

the heat shock gene dnaK (0 min), the secretory apparatus gene secA (2 min, see Chapter 2), azi (2 min, see chapter 2), and the uncharacterized mutants ftsG (29-31 min) and ftsB (49 min; Ricard and Hirota, 1973).

In contrast, a variety of loci appear to be involved specifically in septation. These include the relatively well-characterized ftsI (2 min., coding for PBP3; see section 1.5 and Chapter 2), ftsQ, ftsA, and ftsZ (2 min., see Chapter 2), ftsD, ftsE, and ftsF (86, 76, and 82 min. respectively; Ricard and Hirota, 1973), and fts "ASH124" (90 min.; Holland and Darby, 1976). All of these fts-alleles (filamenting temperature sensitive) produce long, multinucleate filaments at the restrictive temperature. Resolving filaments produce septa at regular distances along the filaments, between segregated nucleoids, and all sites are generally equally capable of division (Tormo and Vicente, 1984; Donachie et al., 1976). ftsA is unique among all the other fts mutations in that its filaments have regular indentations at blocked septation sites. This phenotype suggests that ftsA is required at a stage after initiation of septation, and may not be a component of an organized septation complex. The fact that ftsA is the most commonly isolated class of fts-mutations (K.J. Begg, personal communication) supports this conclusion. ftsQ, ftsA, and ftsZ are discussed in detail in Chapter 2 and beyond.

Two other loci seem to influence septum completion after initiation: a cold sensitive allele of sefA (4 min.; Normark et al., 1976) and a nonconditional allele of envC (81 min.; Rodolakis et al., 1973). These loci are not well characterized.

Class 8 morphogenes are required for separation of newborn cells after septation has been completed. Separation is accomplished by cleavage of the double-layered peptidoglycan septum and involution of the outer membrane over the nascent pole (see Section 1.2). Although some

outer membrane mutants seem slightly altered in division site envelope structure (see Class 3 morphogenes), it is the peptidoglycan-splitting step that seems to limit cell separation.

Two mutants are known that grow as chains of cells, with longer chains at higher rates of growth: the noncondi-tional envA (2 min.; Normark et al., 1969) and cha (73 min.; Donachie et al., 1984). The envA phenotype was described in Section 1.2, and will be considered in detail in Chapter 2. In brief, this strain appears to have decreased levels of N-acetylmuramyl-L-alanine amidase (Wolf-Watz and Normark, 1976), which is important in cleaving the double-layered septum. The pleiotropic phenotype conferred by the envA mutation raises the possibility that this locus is involved primarily in envelope permeability, and that loss of amidase activity is secondary.

The cha allele has not been well characterized, but it does give rise to chains of cells that are similar to envA chains. The cha defect can be suppressed by a single extra copy of envA (as a envA$^+$ lysogen; Begg, unpublished results), suggesting that these loci might both be part of a tightly regulated envelope process. Overproduction of EnvA protein is deleterious to cells (Sullivan and Donachie, 1984b; see Chapter 2), perhaps by damaging secretory and permeability functions or by destroying the integrity of the sacculus.

Class 9 morphogenes are involved in inactivating division sites once a septum has been located there. A septation site-inactivation requirement might not have been anticipated were it not for the fact that mutations have been recovered in which cell poles (previously used septa-tion sites) appear equally likely to serve as a division site as a centrally located site (Adler et al., 1967; Teather et al., 1974). Polar divisions produce minicells,

while in the same population filaments of characteristic incremental lengths accumulate (Teather et al., 1974).

Two loci have been associated with the minicell phenotype: minA (10 min.; Frazer and Curtis. 1975) and minB (26 min.; Schaumberg and Keumpel, 1983). Originally it was believed that a double mutation including each of these loci was required to produce the minicell phenotype, but Davie, Sydnor, and Rothfield (1984) have shown that the minB allele is sufficient. Teather et al. (1974) suggest that each division cycle triggered by an L_u-doubling allows production of only enough septation materials to construct one septum. Cells with more than one potential division site can use these materials at only one site. If the site is polar, then a minicell is produced and the parent cell enlarges by approximately $2L_u$. All potential division sites can be used indefinitely and with equal probability.

Although minicell division behavior does suggest that a mechanism exists to inactivate used septation sites, an alternative model is that inactivation occurs as a normal consequence of constructing a septum, and that the minA and minB products interact to modify septum construction in such a way that some components of the potential division site remain exposed. Elucidation of the role of the minA and minB loci will no doubt reveal important characteristics of the division site.

Chapter 2 Organization and function of a cluster of cell surface and cell division genes mapping to the 2-minute region

2.1 Introduction

The distribution of genetic loci affecting E. coli morphogenesis is striking: figure 1.2 shows both general clustering about the origin of replication (oriC) and several smaller, regional clusters of morphogenes. The significance of the tendency for cell surface growth and cell division genes to map near oriC lies perhaps in the fact that these essential genetic functions are required by the cell within tightly regulated limits (Stoker et al., 1982) and position near oriC assures a more even gene dosage per volume over different growth rates (Donachie and Masters, 1969).

Several of the local clusters have been studied in detail. Mapping at approximately 76 minutes (see figure 1.2) is a cluster containing the essential cell division genes ftsE and ftsS, the lipoprotein gene fam, the cell lysis control gene dnaM, and the heat shock regulon gene htpR/hin (Salmond and Plakidou, 1984). Mapping at approximately 15 minutes is a cluster containing the structural genes for penicillin-binding proteins 2 and 5 (pbpA and dacA, respectively), an unidentified protein of 54,000 molecular weight, and the cell shape gene rodA, all of which appear to be involved in organizing cylindrical assembly of the sacculus. (Stoker et al., 1983a). The most impressive clustering occurs, however, at the 2-minute region where at least 14 genetic loci have been identified that play essential roles in cell surface growth, physiology, or division. Several of these genes were the target of my investigation, and the remainder of this paper will be concerned with their characterization.

2.2 Isolation and characterization of mutants with genetic defects mapping to the 2-minute region

A class of ts-mutants of E. coli K-12 was isolated by Rorsch (cited in Wijsman, 1972) that lyse when grown at the restrictive temperature. From this collection of mutants, several specific genetic loci were identified, and their biochemical activities were characterized through assays performed by Lugtenberg et al. (see below). All of these loci were concerned with the amino acid addition steps in the pathway of muropeptide biosynthesis (see Table 1.2; Figure 2.1). murC was identified to be the locus of L-alanine-adding enzyme, murE corresponded to meso-diaminopimelate-adding enzyme, and murF corresponded to D-alanyl-D-alanine-adding enzyme (Lugtenberg et al., 1972a and 1972b). ddl corresponded to D-alanine:D-alanine ligase (Lugtenberg et al., 1973). The order of these genes was determined to be murE murF murC ddl, and these loci mapped between leu and ftsA (Wijsman, 1972).

These biochemical assignments were reproduced by a different collection of ts-mutants isolated by Matsuzawa et al. (1969) and Miyakawa et al. (1972). They also identified 2 other loci mapping between leu and murE: mraA, corresponding to a D-alanine carboxypeptidase activity, and mraB, corresponding to an unknown peptide required for alanine usage. These loci obviously are involved in peptidoglycan metabolism, but at different levels than those of the mur cluster.

Another series of mutants have been constructed and described by the group of Lutkenhaus, Begg, and Donachie (see below), in which amber mutations of cell surface and division genes appear in the background of a ts-amber suppressor. One of their mutants lead to identification of a locus mapping between murF and murC, designated murG (Salmond et al., 1980). This mutant has a similar phenotype at the restrictive temperature to other mur(ts) mutants, but

no biochemical role has yet been assigned. All that can be said at the present time is that murG plays an essential role in peptidoglycan synthesis.

The other major class of ts-mutants mapping to the 2-minute region are those that are unable to complete cell division at the restrictive temperature, but continue growth to form long filaments. In several cases, the ts-inhibition of division appears as part of a pleiotropic response to a primary defect in permeability or secretory functions of the cell surface. Oliver and Beckwith (1981) describe a mutant that accumulates some, but not all, precursors of periplasmic and envelope proteins at the restrictive temperature. This strain also filaments under these conditions, but the filaments consist of cells that have completed septation without separation (see below for discussion). In subsequent analysis (1982) they have identified a genetic locus, designated secA, mapping to the right of envA (see figure 1.2). They determined that transcription was in a clockwise direction relative to the genetic map and that the gene product was a 92,000 dalton polypeptide. The mutant was complemented by a specialized lambda transducing phage carrying secA. This result strongly suggested that the primary defect is specifically in some part of the secretory apparatus of the cell, rather than the alternative hypothesis of an altered secA product jamming up the secretory machinery. The nature of the cell division effect is not known, but it is tempting to speculate that one or more envelope or periplasmic components of the division apparatus are prevented from reaching their proper destinations.

A series of ts-mutants determining azide resistance is described by Yura and Wada (1968), and their corresponding genetic locus is designated azi. Its biochemical defect is not known, but azi(ts) strains grow as filaments at the restrictive temperature. Unfortunately, there is little description in the literature of the physiology of azi strains, except in relation to effects of azide and

phenethyl alcohol. azi maps just to the right of secA, and its proximity suggests a possible primary role in secretion or envelope permeability.

A nonconditional mutant, envA, has been described by Normark (cf. Wolf-Watz and Normark, 1976). Like the secA(ts) mutant, envA strains grow as chains of septated, unseparated cells. The average length of the chains depends on growth rate, with an equilibrium length being established at each new rate, suggesting that these cells are in some way impaired in the separation phase of division. They are, however, competent for separation given the required amount of time. Wolf-Watz and Normark (1976) present evidence that envA strains have a drastic reduction in N-acetylmuramyl-L-alanine amidase activity. Fractionation studies suggest that this amidase is associated in large part with the outer membrane. They proposed a role for the amidase in cleaving the double layer of peptidoglycan found in nascent septa (see Chapter 1), thereby allowing cell separation. envA strains also show abnormalities in envelope permeability, possibly related to extensive blebbing of the outer membrane.

The primary biochemical defect leading to the pleiotropic phenotype of envA mutants is not clear, however envA does not appear to be the structural gene for the amidase. The envA gene product was determined to be 31,000 daltons (Lutkenhaus and Wu, 1980), while the amidase has a molecular weight reported at 39,000 (van Heijenoort et al., 1975). Thus, envA could code for a protein with a primary role in the secretory apparatus or regulation of permeability, both which could secondarily influence amidase activity in the envelope or periplasm. Only one mutation in envA has been isolated, and high levels of envA expression are deleterious to the cell through an unknown mechanism (Sullivan and Donachie, 1984b).

Within the envA-secA-azi region, most of the available coding capacity is filled except for a segment between envA

and secA, containing enough DNA to code for an average sized protein (Oliver and Beckwith, 1982). In fact, N.F. Sullivan discovered a promoter just to the right of envA, reading in a clockwise direction (as do all of the genes in this large cluster, see below) that apparently expresses a genetic function between envA and secA (Sullivan and Donachie, 1984b). This putative gene, designated "U" (for unknown) in figure 1.2, awaits further characterization through the techniques of molecular genetics.

Although many intriguing similarities exist between envA, secA, and azi, there have been no studies to date comparing their mutations for common properties such as azide resistance, amidase activities and envelope protein secretion. Elucidation of the mechanisms of action of the cell-surface, cell-separation, and secretory functions of the envA "U" secA azi cluster will likely reveal much about these essential cellular processes.

Whereas the chain-forming mutants just described appear blocked at a late stage of cell division, other filamenting mutants in the 2 minute region appear blocked in initiation and completion of septation. Allen et al. (1974) report the isolation of several filament-forming ts-mutants. Fletcher et al. (1978) subsequently showed that one of these strains had a mutation at a locus mapping between leu and murE, designated ftsI. Spratt (1977a,b) showed that ftsI corresponds to the structural gene for penicillin-binding protein 3, involved in septal peptidoglycan synthesis. Like other fts strains, ftsI grows well at 30°C, but septation is blocked at the restrictive temperature so that continued growth produces long, smooth-walled filaments.

By the late 1970s many groups had isolated mutants of the fts phenotype, and some of these mapped to the 2-minute region. Each group had introduced their own nomenclature, resulting in considerable confusion about which mutations corresponded to which genetic loci. A study of several of these mutants by Lutkenhaus et al. (1980) revealed that they

corresponded to two distinct loci, designated ftsA and ftsZ, mapping between ddl and envA. ftsZ mutants had a phenotype identical to other fts alleles, such as ftsI. In constrast, ftsA mutants form filaments with indentations at the locations of potential septation sites (described in Section 1.6). Presumably, these represent nascent septa that have been blocked in completion by defective ftsA product. This is the behavior that would be expected of a cell division gene that was required for progression of septation, but not for initiation of the process.

In a related study, temperature sensitive cell division mutants were selected by a filtration method (Begg et al., 1980, see below). These were screened for complementation with a series of specialized transducing phage carrying segments of the genome between murG and envA. One mutation was identified by the complementation results to correspond to a previously unknown fts locus, designated ftsQ. As is typical of other fts loci, ftsQ strains cease division immediately upon shifting to the restrictive temperature and form smooth filaments.

In summary, the 2-minute region consists of a remarkable series of genetic clusters concerned with muropeptide biosynthesis, peptidoglycan assembly, septation and division, and the secretory/ permeability apparatus. Genetic and biochemical analysis has revealed some aspects of the function of these genetic elements, but our general understanding remains poor. Of the 4 fts loci that map to this cluster, only ftsI has been somewhat characterized biochemically. The remainder of this chapter discusses the preliminary work that has been done on the molecular genetics of some of the loci between ftsI and envA, with special emphasis on ddl, ftsQ, ftsA, and ftsZ.

2.3 The role of ftsA in cell division

A series of nonsense mutations were constructed in a temperature sensitive amber suppressor strain, and one amber mutation was mapped to *ftsA* (Lutkenhaus and Donachie, 1979). A specialized transducing phage was constructed to complement this mutation by extension of a λ *envA* transducing phage (constructed by *in vitro* recombination of HindIII genomic fragments with a plaque forming, integration proficient λ*imm*^{21}) in an *attB*-deleted strain of *E. coli* K-12. A plaque forming transducing phage, designated λ16-2 was selected and subsequently found to carry a genomic insert extending from *murG* through *envA* (see figure 2.1). This recombinant phage has formed the core of our molecular genetics approach to the 2-minute region (see below).

Lutkenhaus and Donachie (1979) were able to identify the *ftsA* gene product using a λ16-2 derivative with the *ftsA*-amber allele transferred onto the phage. This derivative was used to infect uv-irradiated cells and the gene products produced by the transducing phage were labeled with [^{35}S]-methionine. A protein of 50,000 molecular weight was assigned to *ftsA*. In addition, 2-dimensional electrophoresis of an *ftsA*(ts) allele showed no change in charge or mobility of the active *ftsA* product, suggesting that this allele carried a missense mutation. They also estimated *ftsA* expression in a homoimmune lysogen (in which expression of inserted sequences is under genomic control) and found a level of approximately 400 molecules of the *ftsA* protein per cell. This method of measuring levels of gene products is, unfortunately, unsatisfactory because 1) uv-irradiated, multiply-infected bacterial cells cannot be expected to express a cell division gene as they would under less perturbed conditions and 2) these levels give no indication of the activity of the product; this would require a biochemical assay, which remains lacking. At present, no further measurements of *ftsA* levels and activity have been reported, but we can conclude that it probably is not expressed at high levels.

Figure 2.1

λ16-2 and its deletion derivatives

The top line represents the 15 loci that have been identified in the 2-minute region.

The chromosomal insert of 16-2, shown on the next line as an extended rectangle, carries intact sequences from murG to beyond envA. Relevant restriction sites are indicated: H=HindIII; E=EcoRI.

The entire insert is approximately 10 kb in size, as indicated by the scale bar on the next line.

Deletion derivatives are shown below. Constructions are described in Lutkenhaus et al. (1979) and Lutkenhaus and Wu (1980). See text for discussion.

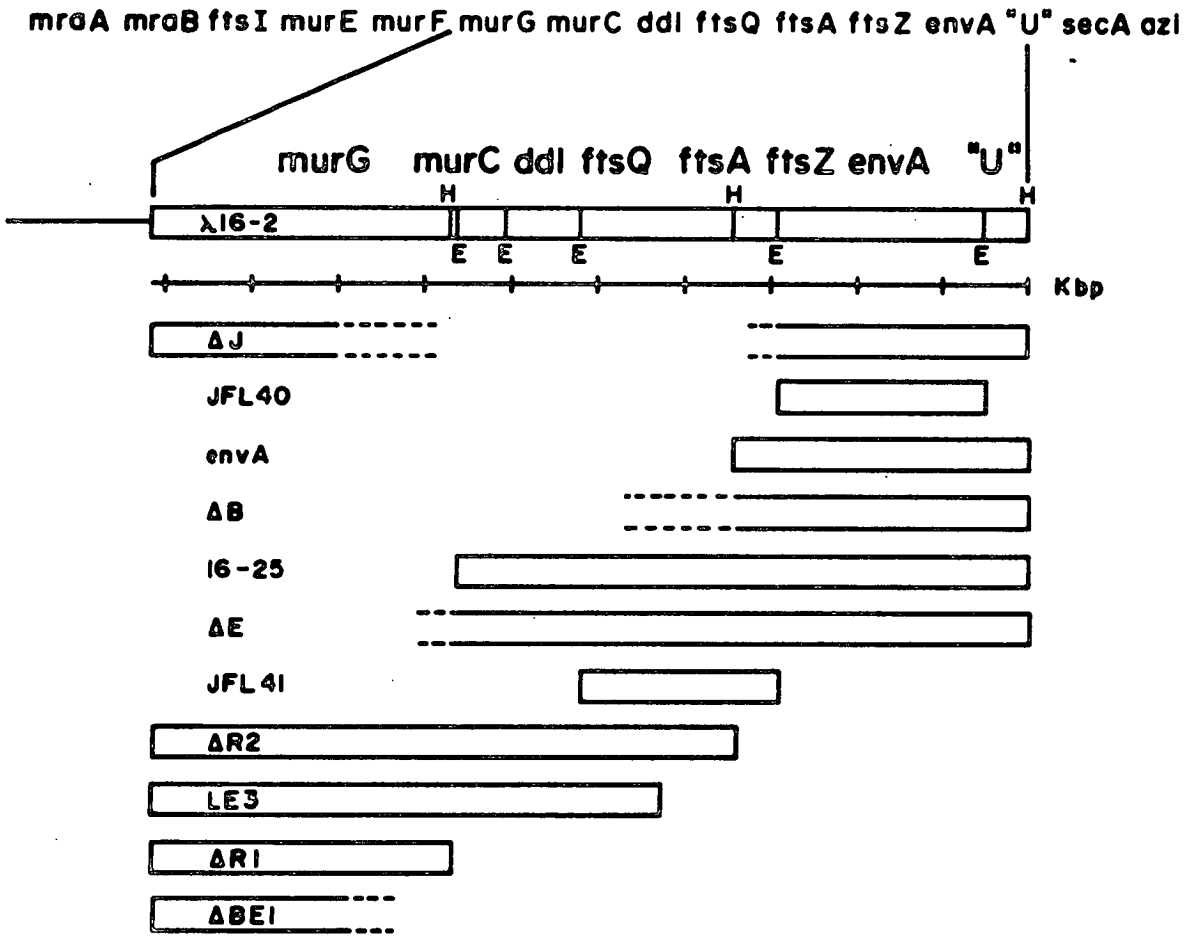
mraA mraB ftsI murE murF murG murC ddl ftsQ ftsA ftsZ envA "U" secA azi
murG murC ddl ftsQ ftsA ftsZ envA "U"
H
H
H
λ16-2
E
E
E
E
E
Kbp
ΔJ
JFL40
envA
ΔB
16-25
ΔE
JFL41
ΔR2
LE3
ΔR1
ΔBE1

FIGURE 2.1

Walker et al. (1975) reported that cultures of an ftsA(ts) strain ceased division immediately upon shifting to the restrictive temperature. They interpreted this to mean that the functional ftsA product was required throughout the process of septation. In an effort to further define the kinetics of ftsA utilization, Donachie et al. (1979) made use of their ftsA amber strain. The ftsA product produced by this allele is temperature stable, but expression depends on a suppressor allele, which was made temperature sensitive. Thus, their system allowed ftsA expression to be turned off and on by changing the temperature.

Growth kinetics of the ftsA(Am)-supF(ts) strain showed that division continued normally for 10 to 20 minutes after temperature-repression of ftsA expression. Thus, FtsA activity is limited to a period less than 20 minutes after its synthesis, implying that it is inactivated or somehow used up in the septation process. Because FtsA activity is required until completion of the final stages of division (Tormo et al., 1985; Donachie et al., 1979; Fletcher et al., 1978), septation stalls as FtsA is used up 20 minutes after expression is inhibited. Possible roles for ftsA, on the basis of these results, are structural (incorporated into the septum) or regulatory (as a division activator or permissive factor).

Donachie et al. (1979) carried out temperature pulse experiments with synchronous cultures (small cells selected from an asynchronous log-phase culture by sucrose-gradient centrifugation) to determine requirements for ftsA expression. They found that if conditions were made permissive for ftsA expression only at early stages of the division cycle, up to about 15 minutes before division should occur, then division remained inhibited. However, nonpermissive conditions early in the cycle, up to 15-20 minutes before division should occur, did not inhibit division. Therefore, ftsA expression is not required nor is it effective if expressed until about 20 minutes before division,

and a burst of ftsA synthesis at this time allows cells to become committed to division. The kinetics of turning off ftsA expression suggest that either ftsA is normally expressed only during a brief period before cells become committed for division or that cells are only competent to respond to ftsA expression during this period.

Figure 1.1 reminds us that the time period required for ftsA expression may coincide with the termination of chromosome replication, final synthesis of activation or permissive factors for septation, and final assembly and activation of the septation apparatus. Therefore, determining the role of the ftsA product in this complex organizational network will probably require deeper understanding of each of these related processes. The next few paragraphs discuss some preliminary steps that have been taken.

Tormo and Vicente (1984) compared septation in a thermo-irreversible allele of ftsA (ftsA3) with that in a thermo-reversible allele (ftsA2) and an amber allele (used by Donachie et al., above). They found that septation sites exposed to irreversibly-inactivated FtsA divided poorly when returned to permissive conditions. Thus, it appears that inactive FtsA was incorporated into the septal structure and blocked septation in the presence of active FtsA. In contrast, septation sites formed in the presence of no FtsA (amber strain) or reversibly inactivated FtsA (ftsA2) completed septation under permissive conditions. Perhaps FtsA is a structural component of the septum, or perhaps it helps to organize the septation complex. In either case an irreversibly inactivated ftsA product could block active FtsA function under permissive conditions. Even blocked septa seem to eventually complete septation in later division cycles, so that FtsA binding may not be permanent in stalled septation sites.

Tormo and Vicente have used their ftsA2 and ftsA3 alleles to investigate the relationship between ftsA

expression and activity with other cell cycle events. In contrast to ftsA(Am) inactivation, which required about 20 minutes before active ftsA was used up, ftsA(ts) mutants cease division immediately at the restrictive temperature (Tormo et al., 1985, 1980). ftsA3 strains required about 25 minutes before division resumed. Division was blocked by chloramphenicol only during the first 10 minutes of this period, implying that dissassembly of the permanently inactivated FtsA and reassembly may have required another 15 minutes. By comparison, ftsA2 temperature induced filaments resumed division 10 minutes after a return to permissive conditions. Division occured in the absence of protein synthesis, albeit at somewhat lower levels.

Tormo et al. (1980) repeated some of Donachie's ftsA timing experiments with the ftsA3 (thermo-irreversible) allele. Their results supported Donachie's conclusions and demonstrated that timing of ftsA expression and activity had similar division cycle requirements.

Tormo et al. (1980) also observed that ftsA3 (thermo-irreversible) temperature-induced filaments can be prevented from dividing by adding nalidixic acid within the first five minutes after a shift to the permissive temperature; addition at later times does not prevent division. They take this as evidence that ftsA expression requires a period of DNA synthesis. While this is one possible explanation, other possibilities must be considered. DNA gyrase, the target of nalidixic acid, affects transcription of many loci through supercoiling (Brahms et al., 1985), and loss of superhelical density in cis could inhibit ftsA expression. Nalidixic acid also induces the SOS response (see Section 1.4), although different inducing signals can bring about different levels of induction of the response (Walker, 1985). SOS induction cannot explain why division proceeds if nalidixic acid is added after five minutes, unless one assumes that FtsA3-blocked septation sites prevent SulA from reaching its FtsZ target. The conclusion that ftsA

expression requires a period of DNA replication does not correlate with the fact that division proceeds normally in cells blocked for initiation of replication (a dnaA(ts) strain, for example). They attempt to demonstrate a requirement for ftsA synthesis and action at the end of chromosome replication using cells aligned for initiation of replication by the alternate thymine starvation-amino acid starvation procedure (Donachie, 1969). However cell cycle conclusions based on procedures that activate one or more of the inducible responses (Walker, 1985) must be viewed with extreme caution.

The discovery that ftsA activity was required only during a brief segment of the division cycle prompted Begg et al (1980) to search for other loci with cell-cycle specific time requirements for action. They UV-irradiated an asynchronous population of cells growing at 30°C, and enriched for ts-mutants by filtering cells that filamented over 3 cycles of 5-minute, 42°C pulses imposed at each mass doubling of the culture, hence the name "temperature-oscillation enrichment", or TOE. Several ftsA alleles were recovered, including TOE-13 (see Chapter 4), but a separate locus was identified by transducing phage complementation in TOE-1. This locus, designated ftsQ, was described briefly in Section 2.2. It has not been characterized as well as ftsA, but preliminary results suggest that ftsQ expression and activity may be required during the same critical period as ftsA (K.J. Begg, personal communication).

2.4 Molecular genetics of the 2-minute region

Detailed characterization of the loci involved in envelope growth and division requires more information on gene products, transcriptional organization, regulatory sequences, coding sequence domains, and ultimately complete

Table 2.1

λ16-2 deletion derivatives: complementation results and gene products

phage	murG	murC	ddl	ftsQ	ftsA	ftsZ	envA
16-2	+	+	+	+	+	+	+
ΔJ		-	-	-	-	-	+
JFL40		-	-	-	-	-	+
envA		-	-	-	-	a	+
ΔB		-	-	-	-	+	+
16-25	-	-	b	+	+	+	+
ΔE	-	-	b	+	+	+	+
JFL41		-	-	+	+	-	-
ΔR2	+	+	+	+	-	-	-
LE3		+	+		-	-	-
ΔR1	+	-	-	-	-	-	-
ΔBE1		-	-	-	-	-	-
assigned proteins:	48K	65K	(30K)	?	50K	45K	31K

a: the 45K protein is expressed at weak levels, and ftsZ complements poorly under a narrow range of conditions. Note that Δ B gives normal ftsZ expression simply by providing the 3'-terminus of ftsA coding sequence.
b: the 30K protein is not expressed, nor is ddl complemented, although it may be marker rescued.
These results are compiled from Lutkenhaus and Wu, 1980; Lutkenhaus et al., 1980; Salmond et al., 1980; and my personal results. Blank spaces in the table represent complementation tests that are not published and that I have not performed myself. The ftsQ locus was not known at the time of the gene product studies, hence the assignment of the 30K protein is ambiguous.

sequencing and biochemical analysis of all the genes and gene products in the system.

Identification of the ftsA gene product was described in Section 2.2. The transducing phage that lead to its identification, λ16-2, was used to construct deletion derivatives (see figure 2.1) that could be used to characterize other loci from murG to envA (Lutkenhaus et al., 1979; Lutkenhaus and Wu, 1980).

The direction of transcription of these loci can be deduced by determining whether gene expression is enhanced or diminished in the presence of high levels of transcription from P_L from within the transducing phage (Ward and Murray, 1979; Lutkenhaus and Wu, 1980). They found that expression from all of these loci was diminished when P_L was turned on, with the exceptions of ftsQ (which was not known at the time), ddl (which could not be distinguished from phage bands) and envA, which appeared to be enhanced by P_L transcription. They concluded that all known genes from murG to ftsZ are transcribed in a clockwise sense with respect to the E. coli chromosomal map, and that envA was transcribed in the opposite direction. However, Sullivan and Donachie (1984b) report that operon fusions with envA have shown it to be oriented in the same direction as the other genes in this cluster. That it appeared otherwise in the phage-expression system reveals the limitations of an indirect method. The orientations of ddl and several other loci were independently confirmed by complementation results (see below).

The complementation pattern of λ16-2 derivatives (compare Table 2.1 with Figure 2.1) confirms the order of the genes and offers clues as to the transcriptional organization of the region. Complementation by a transducing phage generally correlated with expression of a unique protein by that phage in UV-irradiated cells.

murG, mapping at the left end of the chromosomal insert in λ16-2 (see Figure 2.1) corresponds to a 48,000

dalton protein (table 2.1). Phage expressing this protein complement murG. Expression of murG, then, must come either from its own promoter or an exogenous E. coli promoter reading across the attB site. Because the attP site is at the other end of the λ16-2 chromosome insert (Lutkenhaus and Donachie, 1979) and phage promoters are repressed in the lysogenic state, murG must have its own promoter.

Phage complementing murC express a 65,000 dalton product (table 2.1). λΔR1 does not complement murC, although it can marker-rescue certain murC alleles (Lutkenhaus et al., 1980), and it expresses a 45,000 dalton protein that is most likely to be a "run-off" polypeptide bearing only the N-terminus of murC. Therefore, the murC coding sequence can extend at most approximately 540 base pairs to the right of the HindIII site defining one boundary of the chromosomal insert in λΔR1 (assuming an average of 110 daltons per amino acid in E. coli polypeptides), and at least 1230 bp to the left of that site (this data is included in figure 4.5, showing the fine organization of loci on the λ16-2 insert). This result also confirms the orientation of murC. Because murC expression in cloned fragments has not been studied in the presence of a murG deletion, it is impossible to conclude whether murC has its own promoter or whether it is expressed from the murG promoter (see figure 4.5).

Because ftsQ was not known at the time of their experiment, the gene-product assignment of ddl by Lutkenhaus and Wu (1980) is equivocal. Certainly all the phage in their experiment that complement ddl produce a unique 30,000 dalton polypeptide, but these phage also complement ftsQ (results not shown). Not all phage that produce the 30,000 dalton product complement ddl, though they marker rescue ddl alleles; they do all however complement ftsQ. Several recombinant phage are known that complement ftsQ, but not ddl (λJFL41, Lutkenhaus et al., 1980; λFH16, Begg et al., 1980; λGH16, G.F. Hatfull, PhD thesis; and λJFL100,

Donachie et al., 1983). Of these phage, λJFL41 was shown not to produce the 30,000 dalton protein (Lutkenhaus and Wu, 1980). Therefore, the most likely assignment of the 30,000 dalton gene product is to ddl, as was originally suggested, but further results are needed to confirm this assignment (see Chapter 6).

If ddl codes for the 30,000 dalton protein, then why does λ16-25, which extends beyond ddl into murC (Lutkenhaus and Wu, 1980), fail to complement ddl, even though it expresses the 30,000 dalton protein in UV-irradiated cells? The answer is that expression of ddl in λ16-25-infected cells probably occurs from the phage promoter P'_R (Lutkenhaus and Wu, 1980; Murray, 1977), which would be repressed in the lysogen. ddl expression in the lysogen would then depend solely on promoters carried by the chromosomal insert (see below). Then we must conclude that ddl expression depends on a promoter upstream of murC (P_{murC} if it exists, or P_{murG}). Other transducing phage that carry ddl but not the left end of murC fail to complement ddl (results not shown), suggesting that ddl is organized in a transcriptional unit with murC and possibly murG. This possibility will be considered in Chapters 4, 5, and 8.

Several recombinant phage have been constructed carrying the 2.3 kb EcoRI fragment in a lambda replacement vector (λJFL41, λJFL100, λGH16, λFH16, see above). These phage all complement ftsQ (results not shown), however considerable evidence has accumulated that P_{ftsQ} does not lie on this EcoRI fragment (see Chapters 4, 5, and 8). How then can we account for ftsQ expression in lysogens carrying these phage? Three possibilities are that transcription originates from phage, host, or fortuitous junction promoters. Because λ616, the vector used in these constructions (Wilson and Murray, 1979), carries the EcoRI insertion site just to the left of the attP site, P'_R would be the nearest phage promoter that could transcribe across the insert in the prophage state. P'_R however should be

repressed in the prophage (Murray, 1983). Even if small amounts of transcription from P'_R reached the EcoRI site in the prophage, only those constructions with the insert in the proper orientation should be able to express ftsQ. At least one construction, λJFL100, is known to carry the insert in the orientation opposed to P'_R, so that another mechanism seems likely. The translational start for ftsQ in JFL100 lies very near to the attP site (see Chapter 8), therefore a host promoter between bio and attB and directed toward attB could conceivably direct expression of ftsQ in the prophage, although such a promoter has not been described. The orientations of the insert in λJFL41, λFH16, and λGH16 have not been published, therefore one would have to propose that they were oriented in the same direction as the insert in λJFL100 to account for ftsQ expression by an exogenous promoter. A fortuitous fusion promoter cannot be ruled out, though it remains an unlikely possibility.

ftsA complementation by λ16-2 derivatives was straightforward (see Table 2.1) and suggested that ftsA could be expressed independently of sequences upstream of ftsQ. Because no deletion derivatives inactivate ftsQ, it could not be determined whether ftsA has its own promoter or whether it lies in a transcriptional unit with ftsQ. The gene product assigned to ftsA by Lutkenhaus and Wu (1980) was identical to that assigned to ftsA by a similar method (Lutkenhaus and Donachie, 1979; see above).

ftsZ complementation results were somewhat complicated. All phage carrying the 3.2 kb HindIII fragment (see figure 2.1) could complement ftsZ, although λenvA$^+$, which carries only this fragment, complements poorly. These phage also direct synthesis of a unique 48,000 dalton protein, although λenvA$^+$ expresses this protein weakly. Therefore ftsZ expression and complementation are improved if sequences upstream of the leftward HindIII site are added to the insert (as in λΔB). The amount of sequence does not

have to include the ftsA promoter ($\lambda\Delta$B does not complement ftsA), however it must include ftsA coding sequence (the HindIII site cuts ftsA, compare $\lambda\Delta$R2 with λ16-25). We may conclude that ftsZ has its own weak promoter, mapping between EcoRI and HindIII sites and an "enhancer" sequence upstream of the HindIII site. The enhancer improves ftsZ expression and therefore behaves as would be expected for a second promoter. Expression of ftsZ is discussed in detail in Section 2.5 and Chapters 4, 5, and 8.

The only remaining unique protein expressed by λ16-2 has a MW of 31,000, and indeed, only those phage that complement envA directed synthesis of this protein. envA expression is not dependent on any other loci, therefore it must have its own promoter. Both the envA promoter and a promoter in the same orientation just downstream of envA, expressing an unknown genetic function, have been investigated by Sullivan and Donachie (1984b) and will not be considered further here.

2.5 Characterization of FtsZ (SulB)

One of the mutations that suppresses a lexA(ts) mutation (ts-constitutive SOS response) maps to the 2-minute region (sulB, Huisman et al., 1980b). Like sulA strains, sulB strains express other components of the SOS response, but they do not become inhibited for division. Therefore, sulB mutants behave as if the expression or action of a cell division gene SOS-target had become resistant to sulA inhibition.

Lutkenhaus (1983) constructed a λ16-2 derivative carrying a sulB allele, and used this phage to map sulB with respect to the cell division genes in the 2-minute region. He showed that sulB was allelic with ftsZ, and that sulB alleles gave a slightly ts-FtsZ product with a slightly slower mobility than the $FtsZ^+$ protein. ftsZ is a likely

target for an inducible division inhibiting response, because it seems to be involved at an early stage of division. These conclusions were corroborated by an independent investigation (Jones and Holland, 1984) using Tn1000 insertions to map sulB. Both studies found that 3'-terminal ftsA sequences greatly increased ftsZ expression, and Jones and Holland agreed with the conclusion that an ftsZ promoter lies in the distal 40% of the ftsA coding sequence.

The fact that ftsZ(sulB) alleles are dominant to ftsZ$^+$ suggests that FtsZ is normally active either as an oligomer or associated with other polypeptides in a functional division complex. One would then predict that increasing dosage of ftsZ$^+$, and especially ftsZ(sulB) (which is resistant to SulA), could displace FtsZ-SulA in SOS-blocked septation sites. Lutkenhaus indeed found that increased dosages of ftsZ(sulB), and to a lesser extent ftsZ$^+$, allowed septation to continue even when the SOS response was induced. This result also implies, as do the kinetics of SOS division inhibition, that SulA acts by binding to FtsZ protein, rather than to an ftsZ sequence. However, ftsZ repression during an SOS induction cannot be ruled out at this time. The suggestion that ftsZ has at least 2 promoters, one within ftsA coding sequence, implies that regulation of ftsZ expression may be complex. In any case, protein synthesis is required for division in cells recovering from SOS induction (Jones and Donachie, 1973), which may indicate a requirement for new ftsZ expression.

Further clues into the mechanism of SulA inhibition of FtsZ have been gained by studies of a lacZ-ftsZ fusion protein (Ward and Lutkenhaus, 1984). The operon fusion, under lac control, produces a hybrid protein carrying seven N-terminal LacZ amino acids followed by about 90% of the C-terminal FtsZ amino acids. Introduction of the hybrid protein resulted in cessation of division within 30 minutes, but increased dosage of ftsZ$^+$ or ftsZ(sulB) could relieve the division block. These results favor a "mixed multimer"

model for inhibition by SulA and its analogue, the hybrid LacZ-FtsZ protein, but they do not rule out the other possibility, which is that SulA binding to a separate target site blocks FtsZ action. A C-terminal ftsZ(am) mutation yields an amber LacZ-FtsZ fragment which has no effect on division, suggestion that the extreme C-terminus of the FtsZ protein is involved in oligomerization or target site binding.

2.6 Transcriptional activity of the ftsZ "enhancer"

Lutkenhaus has constructed a different lac operon fusion vector, λJFL100 (described with respect to ftsQ in Section 2.4), that is of use in studying ftsZ expression. The insert in λJFL100 carries the entire ftsQ coding sequence, but not its promoter, and the 5'-terminal segment of ftsA up to the HindIII site (equivalent to the insert of pDK340 in Figure 5.3). The promoters on this fragment would then be P_{ftsA} and the putative P_{ftsZ2} "enhancer" to the left of the HindIII site (P_2 in figure 4.5). lacZ expression is under control of these 2 promoter regions in λJFL100, thus beta-galactosidase activity is an index of promoter activity in lysogens.

Donachie has used this system to characterize ftsZ expression (the P_{ftsZ2} component) and possibly ftsA expression (Donachie et al., 1983, 1984). Because ftsA is normally expressed at very low levels (Lutkenhaus and Donachie, 1979; see Chapter 5), P_{ftsA} is unlikely to give a significant contribution to lacZ expression in JFL100.

The most striking feature of P_{ftsZ2} transcription is that it is independent of growth rate (Donachie et al., 1983, 1984). Therefore, the same number of ftsZ transcripts would be produced per septum formed, irrespective of cell size. This behavior is consistent with the thinking that ftsZ is required in a fixed amount per septal structure.

The mode of regulation of P_{ftsZ2} activity to give a constant dose of transcripts per septum is not known, but expression appears to be periodic in synchronous cultures of a λJFL100 lysogen (Donachie et al., 1983). Also, the cAMP-CAP complex seems to be involved in regulation. P_{ftsZ2} transcription is increased in a cya strain, but returns to normal upon addition of exogenous cAMP (Donachie et al., 1984). Because cAMP-CAP is known to modulate other septation activities, this effect on λ P_{ftsZ2} could be primary or secondary.

P_{ftsZ2} transcription is also increased in certain cell division mutants. An ftsA amber mutant causes a five-fold increase in P_{ftsZ2} activity, perhaps because the ftsA product represses P_{ftsZ2} or P_{ftsA}. Other ftsA, ftsQ, ftsZ and ftsI alleles cause less increase, and some alleles (ftsE, lexA, and envA, for example) have no effect. The lexA(ts) result suggests that SOS induction will not affect ftsZ expression. This prediction has been confirmed by Donachie et al. (1983), therefore SfiA does not act at the level of ftsZ expression. Why other septation mutations should increase ftsZ expression is not clear, but presumably it reflects the manner in which synthesis and organization of the septation apparatus is regulated.

2.7 Unresolved questions concerning the organization of the 2-minute region

So far we have generated many clues about how division is organized, but many gaps remain to be filled. In a systematic approach to characterizing the 2-minute region we could begin with the DNA sequence, move to investigating transcriptional regulatory signals, then to studies on transcription and translation in vivo, and finally to biochemical analysis of the gene products. Sequencing studies are being carried out in our lab by Dr. A.C.

Robinson and will be discussed in Chapter 8. I chose to investigate organization at the next level, by analyzing segments of the 2-minute region with respect to their ability to express a specific gene product. I focused on the chromosomal segment between the left HindIII site and the fourth EcoRI site (see Figure 2.1) because this region represents the boundary between a cluster primarily concerned with muropeptide synthesis (ending at ddl) and a cluster primarily concerned with septation (beginning at ftsQ). This segment also contains sequences responsible for expression of the three division genes ftsQ, ftsA, and ftsZ, the latter two of which have been somewhat characterized.

I approached this investigation with several specific questions in mind, generated by the information presented above.

1) Can direct methods confirm that the orientations inferred by Lutkenhaus and Wu (1980) are correct?
2) What are the minimum sequences required for expression and coding of these genes?
3) Which segments carry promoter activity, and do these promoters correlate with expression of specific genes?
4) Do any segments function as transcriptional terminators?
5) Can the 30,000 MW protein ambiguously assigned to ddl be confirmed by direct means?
6) Can the ftsQ product be identified by direct means?

My general approach was to subclone chromosomal segments into a multicopy plasmid vector and then to carry out extensive deletion and complementation analysis (Chapter 4); to subclone segments into a galK operon fusion system for promoter and terminator analysis (Chapter 5); and to subclone the intact ddl and ftsQ genes into an expression vector for gene product identification (Chapter 6). Several incidental observations on effects of manipulating ftsQ and ftsA sequences are presented in Chapter 7. Chapter 8

summarizes my conclusions and correlates them with the sequencing results independently generated by A.C. Robinson.

Chapter 3 Methods and Materials

Most of these methods have been described in Robinson et al., 1984, which makes up Appendix B.

Media: all media are given in Appendix B.

Strains:
W3110 (prototroph), laboratory stock;
C600K$^-$ (galK thr leu thi lac tonA supE), R. Hayward;
DS410 (minA minB prototroph), N. Willetts;
PC1358 (thr leu trp his thyA thi lac gal xyl mH ara tonA phx rpsL ths), E.J.J. Lugtenberg
TOE-1 (ftsQ(ts) thyA argE leu his pro thr thi), K. Begg;
TOE-13 (ftsA(ts) thyA argE leu his pro thr thi), K. Begg;
NFS 6 (as C600K$^-$ plus recA Tc^r gyrA), N. Sullivan

Transducing phage: constructions are described in Chapter 2 and in Lutkenhaus and Wu (1980).

Biochemicals and enzymes: see Appendix B.

DNA techniques and recombinant constructions: see Appendices A and B. Restriction digests were performed either according to the manufacturers recommendations or, for routine analysis, in universal buffer (33mM Tris-acetate (pH 7.9), 10mM magnesium acetate, 66mM potassium acetate, and 0.5 mM dithiothreitol).
Restriction fragments were isolated by separating them on 1% agarose gels in Tris-acetate buffer (5mM sodium acetate, 1mM EDTA and 40 mM Tris [pH 7.5]); the desired band was cut from the gel and the agarose was dissolved in 10 mM potassium phosphate (pH 6.8) saturated with potassium iodide; the sample was loaded onto a hydroxyapatite column and washed through with 50 mM potassium phosphate (pH 6.8); bound DNA was eluted with 400 mM potassium phosphate (pH 6.8); the

DNA-containing fractions were pooled and loaded onto a Sephadex G-50 column and the column was run with dH_2O; DNA-containing fractions were pooled and ethanol precipitated.

Colony hybridization: see Appendix B.

Galactokinase assays: see Appendix B and McKenney et al. (1981). Assay results were analyzed as follows: relative activities between clones assayed at the same time could be compared directly, but activities measured in repeated experiments tended to fluctuate. The fluctuations were such that relative activities between clones remained constant, but that these relationships were lost when a series of repeated assays were simply averaged together. Therefore it is useful to calculate a number related to all of the assay activities measured at the same time, which could be compared to a similar number calculated for a repeated experiment. This number is taken to be the mean of all galactokinase activities that were measured in the same assay repetition, termed the "group mean". Group means calculated for each repeat of the enzymatic assay experiment can then be normalized to each other, and the original measurements may then be normalized relative to their normalized group mean. Data processed in this fashion preserves the same relationships between clones that are seen as trends across a series of repeated galactokinase activity determinations. It is this averaged, normalized data that is presented in Tables 5.1, 5.2, and 5.3.

Minicell-expression system: pHUB2 recombinants were transformed into a DS410 strain already carrying pRK248. Minicells were prepared by banding on three successive sucrose gradients (sucrose gradients prepared by freezing 20% w/v sucrose in M9-glu media and thawing prior to use). 2 x 10^{10} cells were resuspended in M9-glu and incubated for 30

min at 30°C to allow degradation of parent cell transcripts. 10 uCi of ^{35}S-methionine was added and the mixture incubated for 4 hours at 42°C. The mixture was chased with 40 ug of cold methionine and incubated another 15 min at 42°C. Cells were then boiled in loading buffer (0.6 g SDS; 1 ml 2-mercaptoethanol; 4 ml glycerol; 1.25 ml 0.5 M Tris, pH 6.8, diluted to 10 ml with dH_2O). The sample was run on a 7 to 20% polyacrylamide gradient gel, and fixed gels were dried and set up for autoradiography.

Chapter 4 Subcloning and deletion analysis of the *murC-ddl-ftsA-ftsZ* region

4.1 Subcloning from λΔE

The chromosomal sequence of interest is carried by the λ16-2 deletion derivative λΔE (see figure 2.1). Figure 4.1 shows the convenient restriction fragments for subcloning. pBR325 carries unique EcoRI, BamHI, and HindIII sites (see Figure 4.2) and hence was a suitable vector for the initial subclonings, which are described in detail in Appendix A.1. pKO1 is the vector used for the gal-operon fusion experiments (see Figure 5.1; Chapter 5), and all fragments were eventually subcloned into this vector. The complementation results shown in Figure 4.5 include both pBR325 and pKO1 clonings. A positive complementation was indicated by the ability of the transformant to form colonies at 42°C, and in the case of *ftsQ* and *ftsA*, to do so without filamentation.

An EcoRI cloning was attempted to insert the four chromosomal EcoRI fragments into pBR325 (see Appendix A). Only three of the fragments were recovered, due to the fact that the 2.5 kb *envA*$^+$ fragment is not stable in high copy number vectors (Sullivan and Donachie, 1984b). The 840 and 540 bp EcoRI recombinants were designated pDK5 and pDK7 respectively. 2.28 kb EcoRI recombinants were recovered but were not used as they previously had been constructed by G. Hatfull (Robinson et al., 1984; G. Hatfull, PhD thesis). Neither pDK5 nor pDK7 complemented *ddl* (results not shown).

Similarly, a BamHI cloning was used to insert the 1.18 kb BamHI fragment into pBR325 (see Appendix A.1). Recombinants were recovered carrying the insert in both orientations, and both of these complemented *ddl*. One of these, pDK20, is shown in figure 4.5. Orientation of the insert is defined by the clockwise, or left to right, transcription

Figure 4.1

Subcloning from from the transducing phage λΔE

The extended rectangle represents the chromosomal sequences carried by λΔE, shown in Figure 2.1. These sequences include the 3'-terminus of murC and extend to the normal right end of the λ16-2 insert.

Relevant restriction sites are indicated, and their corresponding fragments are shown above and below the phage diagram.
H=HindIII, top line
B=BamHI, middle line
E=EcoRI, lower line

The 2.28 kb EcoRI fragment size has been confirmed by sequencing (Robinson et al, 1984, in Appendix B). It is referred to in the rest of this thesis as the 2.3 kb EcoRI fragment.

The 1.18 kb BamHI fragment was sized by Smith and Birnstiel mapping (see text for details). It is referred to in the rest of this thesis as the 1.2 kb BamHI fragment.

Recombinant constructions are described in detail in Appendix A.

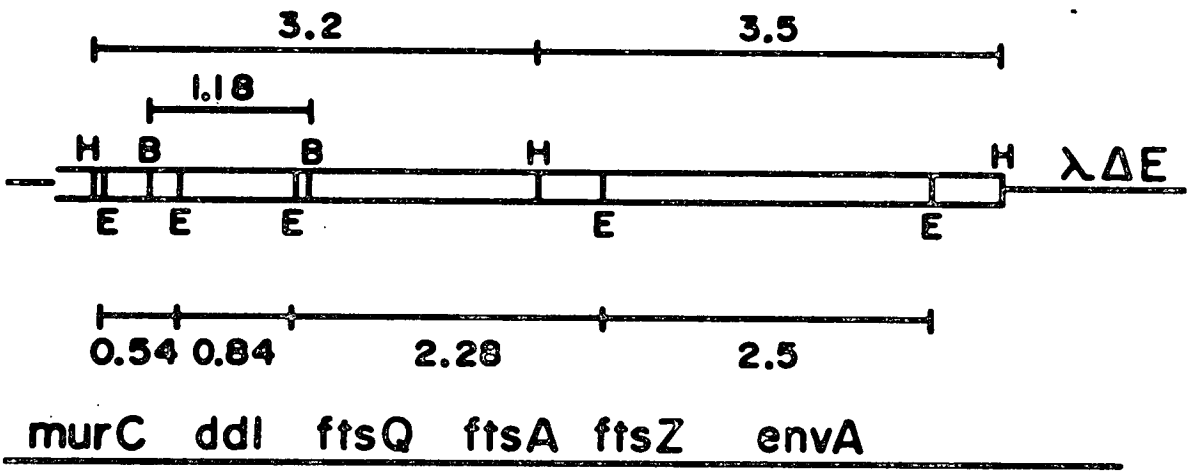
3.2
3.5
1.18
H
B
B
H
H
λΔE
E
E
E
E
E
0.54
0.84
2.28
2.5
murC
ddl
ftsQ
ftsA
ftsZ
envA

FIGURE 4.1

Figure 4.2

pBR325

The map of pBR325 as reported by Bolivar (1978). Antibiotic resistance markers are limited by arrows. Relevant restriction sites are indicated:

A=AvaI

B=BamHI

E=EcoRI

H=HindIII

P=PstI

Pv=PvuII

S=SalI

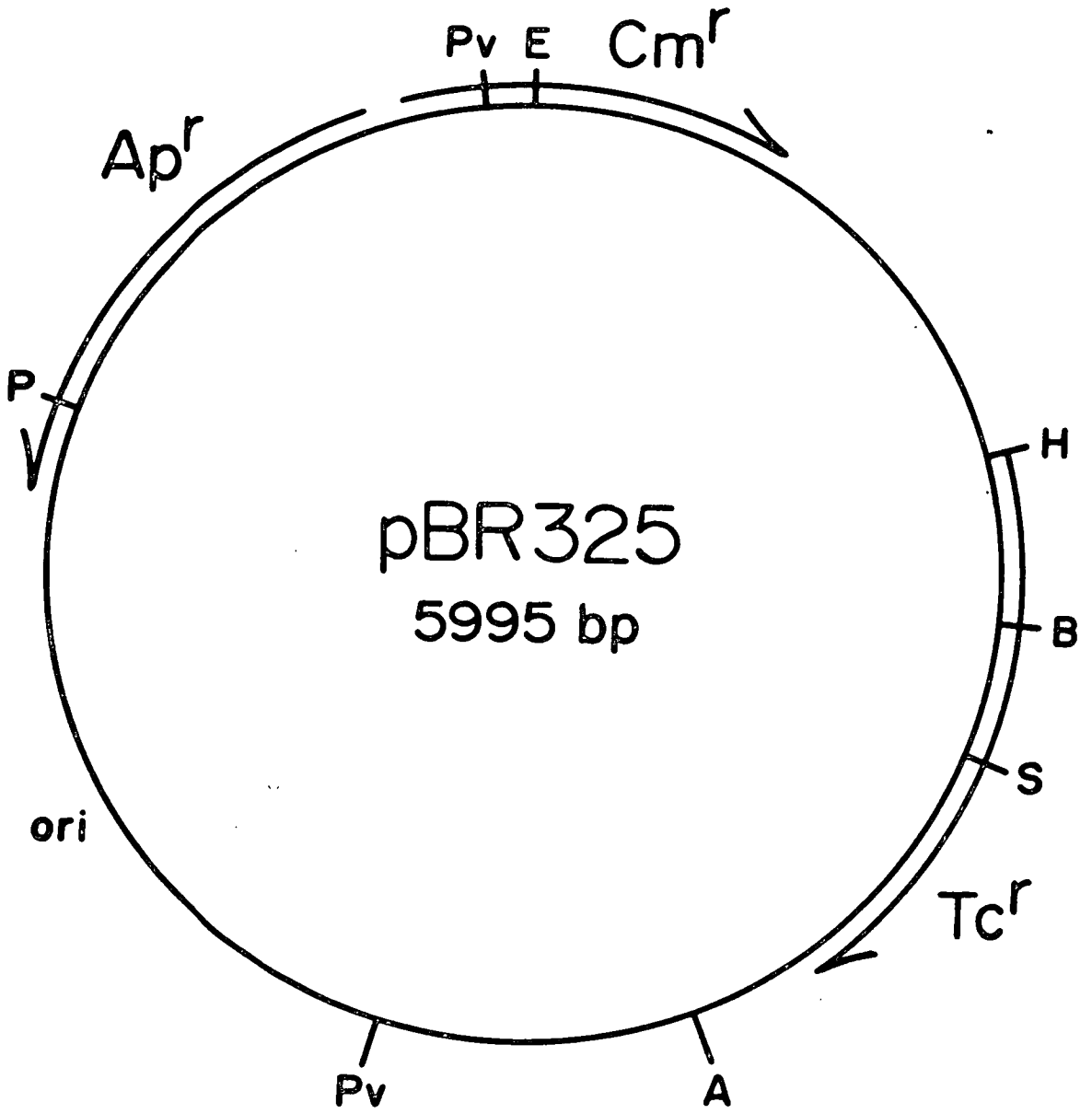

FIGURE 4.2

shown by 2 minute loci, and is usually described in relation to a vector marker such as Tc^r or galK. The Tc^r gene transcript in pBR325 crosses the BamHI site in only one direction, therefore it could not be responsible for ddl expression in both orientations. These complementation results suggest that ddl does in fact carry its own promoter on the 1.2 kb BamHI fragment, as opposed to being entirely dependent on a promoter upstream from murC. This putative promoter likely would be located on the 210 bp BamHI-EcoRI fragment, assuming no overlapping coding sequences, because the 30,000 MW polypeptide tentatively assigned to ddl would require approximately 820 bp of coding sequence. Recall that murC must extend at least 545 bp to the right of the HindIII site, placing the murC terminus on the same BamHI-EcoRI segment as P_{ddl} (illustrated in Figure 4.5). The ddl 3'-terminus could extend over the EcoRI site onto the 104 bp EcoRI-BamHI segment (at the right of the 1.2 kb BamHI fragment), but it would have to lie close to the ftsQ 5'-terminus, which also maps to this segment.

A HindIII subcloning from $\lambda\Delta$E into pBR325 was also attempted numerous times, but no recombinants were recovered. Note that the 3.5 kb HindIII fragment carries envA. This fragment would not then be stable in a high copy number vector (Sullivan and Donachie, 1984b). Reasons why the 3.2 kb HindIII fragment also might not be stable are discussed in Chapter 7.

4.2 Smith and Birnstiel mapping of the 1.18 kb BamHI fragment

In an effort to generate a series of deletion derivatives from recombinants containing the 1.2 kb BamHI fragment, I constructed a detailed restriction map of the region using the method of Smith and Birnstiel (1976). pDK20

Figure 4.3

Master agarose gel for Smith and Birnstiel mapping

Lanes:

A: pBR322 AluI size standards: 910, 722, 655, 521, 403, 281, 257, 226, 100, 90, 63, 57, 49, 46, 19, 15, and 11 bp

B: lambda cI857 HindIII size standards: 23.15, 9.42, 6.56, 4.38, 2.32, 2.02, 0.56, and 0.125 kb

C: BamHI

D: EcoRI

E: SalI

F: MspI

G: AluI

H: lambda cI857 HindIII

I: Sau3A

J: TaqI

K: XhoI

L: PstI

M: AvaI

N: lambda cI857 HindIII

O: pBR322 AluI

The end-labeled 3.2 kb HindIII-PvuII fragment of pDK20 is present in each lane. The 1.5 and 0.35 kb bands mark the 1.2 kb BamHI fragment boundaries within the original end-labeled fragment. All bands falling between these markers originate from restriction sites on the 1.2 kb BamHI fragment. All other bands originate from sites within the pBR325 vector. The pBR325 fragments calculated from band mobilities correspond closely to restriction site predictions from the pBR325 sequence. Restriction sites mapping to the right end of the insert (see Figure 4.4) correspond closely with preliminary sequence data for this region (A.C. Robinson, personal communication). The Sau3A lane shows primarily the 350 bp band, although good partial digests were seen on a previous gel (without size standards). The reason why the Sau3A digest apparently continued in stop buffer at -20°C is not known. See text for details of the end-labeling procedure.

Enzymes that do not cut: BglII, HindIII, KpnI, PvuII, SmaI

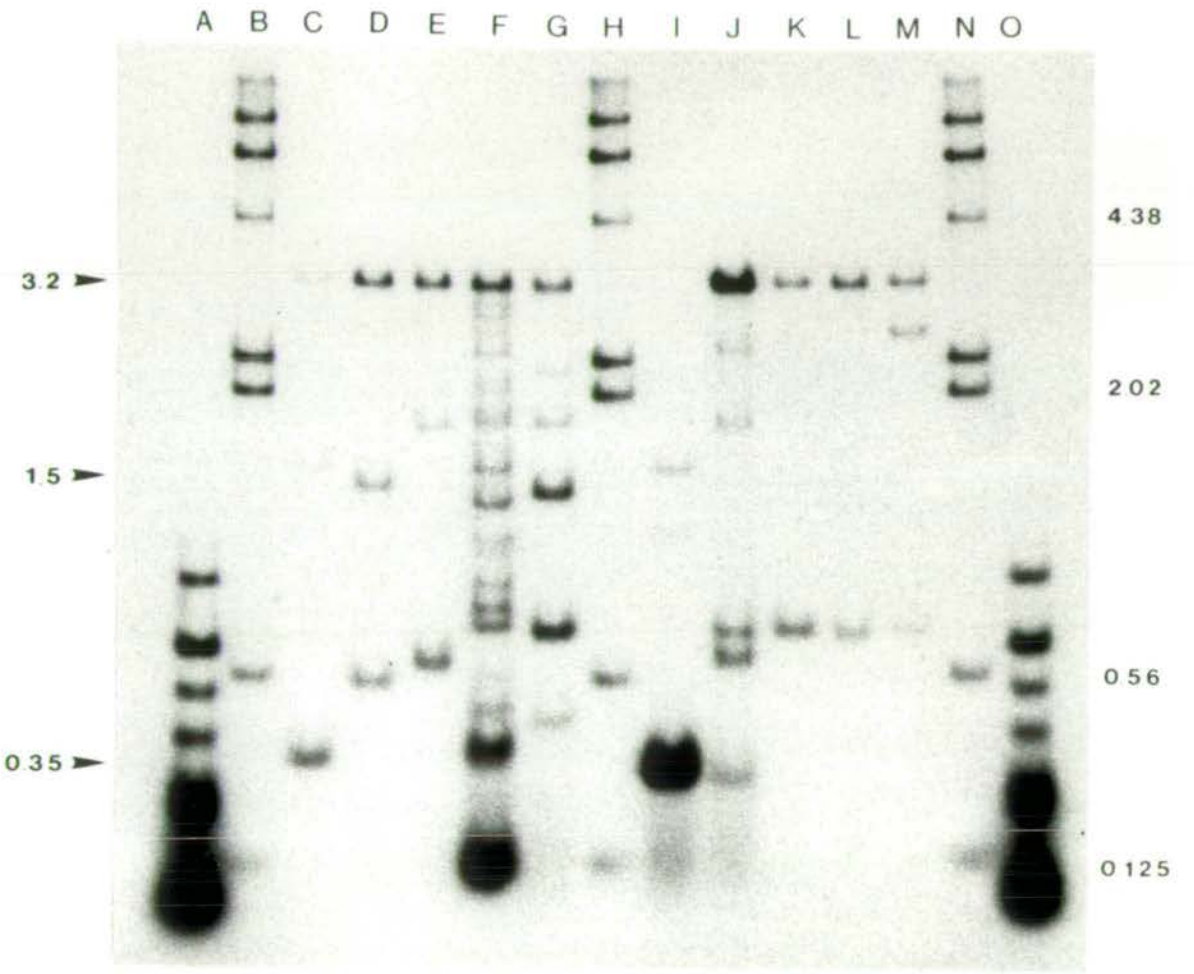

FIGURE 4.3

carries useful restriction sites for the end-labeling and fragment isolation procedures.

A fragment of pDK20 DNA carrying the BamHI insert was labeled at a single end as follows: pDK20 DNA was digested to completion with HindIII and then labeled at both ends by treatment with CIP and polynucleotide kinase plus [γ^{32}P]-ATP. The linearized plasmid was digested to completion with PvuII to yield fragments of 1350, 2610, and 3220 bp. The latter fragment carried the BamHI insert, and bore the single HindIII-terminal label. Fragments were separated on an agarose gel, and the desired band was cut out. The purified fragment was then used in the restriction mapping experiment.

A series of partial digests of the purified end labeled fragment were generated using the appropriate restriction endonucleases, and these fragments were run out on both agarose and polyacrylamide gels. An autoradiogram of an agarose gel is shown in figure 4.3. Band mobilities were analyzed by the modified linear regression method of Southern (1979) and the results used to generate the restriction map shown in figure 4.4. This map complements the detailed restriction maps of the 2.2 kb BamHI-EcoRI segment, constructed by A. Robinson (Robinson et al., 1984), and the 2.5 kb EcoRI fragment, constructed by N. Sullivan (Sullivan and Donachie, 1984b).

4.3 Subcloning the 1.2 kb BamHI fragment into pKO4 and construction of deletion derivatives

pKO4 is a derivative of pKO1 constructed by cloning a 10 bp BamHI linker into the SmaI site of pKO1 (see Figure 5.1). The 1.2 kb BamHI fragment was subcloned into pKO4 as described in Appendix A.2. Recombinants were recovered with the insert in the same orientation as galK (pDK30) as well

Figure 4.4

A detailed restriction map of the 1.2 kb BamHI fragment

The top scale corresponds to the 1.2 kb BamHI fragment, shown directly below.

The bottom scale corresponds to the regional restriction map, and the BamHI fragment is shown in relation to this map.

Only relevant restriction sites are indicated:

A=AvaI	Al=AluI
B=BamHI	Bg=BglII
E=EcoRI	H=HindIII
K=KpnI	M=MspI
P=PstI	Pv=PvuII (mistakenly indicated as Pr
S=SalI	T=TaqI in this figure)
X=XhoI	

See the text for more details.

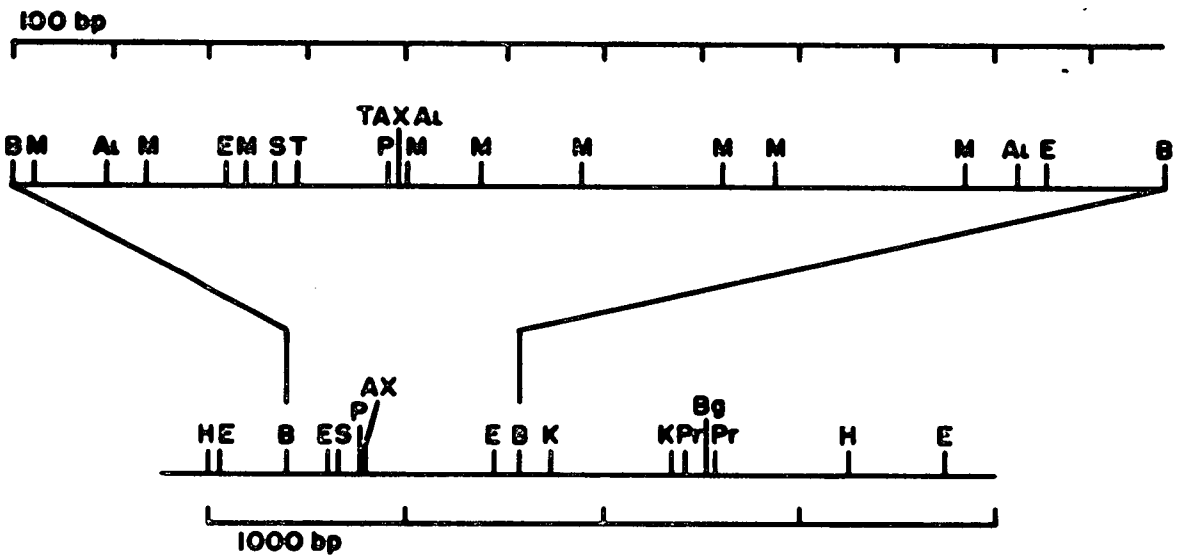
100 bp
TAXAL
BM AL M EM ST P M M M M M M AL E B
AX
P
Bg
HE B ES E B K KPr Pr H E
1000 bp

FIGURE 4.4

as in the opposite orientation (pDK31). Both recombinants complemented ddl, as predicted (see figure 4.5).

Figure 4.4 shows that a SalI and an XhoI site lie approximately 120 bp apart on the BamHI fragment. These restriction sites generate complementary sticky ends, and a SalI-XhoI deletion-religation generates a new TaqI site. Because these sites lie toward the proposed 5' end of the ddl coding sequence, deletion of the 120 bp fragment should destroy ddl complementation. Figure 4.5 shows that pDK32, the SalI-XhoI deletion derivative (see Appendix A.3), does not in fact complement ddl.

Another series of derivatives was constructed by partial and complete EcoRI digestion of pDK30 (see Appendix A.3). pDK30 carries two EcoRI sites on the insert and a third on the vector 315 bp upstream of the vector BamHI insertion site, so that an EcoRI digest yields fragments of 520 and 840 bp. Deletion of the 520 bp fragment gave pDK34; the 840 bp fragment, pDK35; and both fragments, pDK33 (see Figure A.2). None of these plasmids complement ddl, as predicted.

4.4 Subcloning pDK5 and pDK7 EcoRI fragments into pKO1

The EcoRI fragments carried by pDK5 and pDK7 (see Section 4.1) were also subcloned into pKO1 (see Appendix A.2). The 840 bp EcoRI fragment was recovered in both orientations, designated pDK10 and pDK11 for inserts in the same direction as galK, and in the opposite direction, respectively. The 520 bp fragment was also recovered in both orientations, designated pDK50 and pDK51 for inserts in the same and in the opposite directions as galK, respectively. None of these recombinants complemented ddl, as expected from the limits of ddl predicted in Figure 4.5. The remote possibility that the entire coding sequence for ddl is carried on the 840 bp EcoRI fragment, with pDK5 failing

Figure 4.5

Organization of gene expression between murC and ftsZ

The genetic and physical map of a portion of the 2-minute region is shown at the top. The scale bar is in units of kb. Only the major restriction sites are shown (symbols are as presented in Figure 4.4). Recombinant clones and deletion derivatives are shown below, with bars indicating the chromosomal sequences present. PGH300 carries the same 2.3 kb EcoRI fragment as pDK302, but in the opposite orientation. pDK40 carries the 2.3 kb EcoRI fragment rearranged as a 2.3 kb BamHI insert. Complementation results are indicated below the genetic symbols as (+) (colony growth without filamentation at 42°C) or (-) (filamentation or no growth at 42°C). See text for discussion of these complementation results. The map at the bottom indicates the genetic boundaries relative to restriction sites for each locus. Solid lines indicate sequences strongly implicated as coding for the gene product shown. Dashed lines indicate sequences for which the genetic limits are less well defined, such as those calculated from gene product measurements. See text for details.

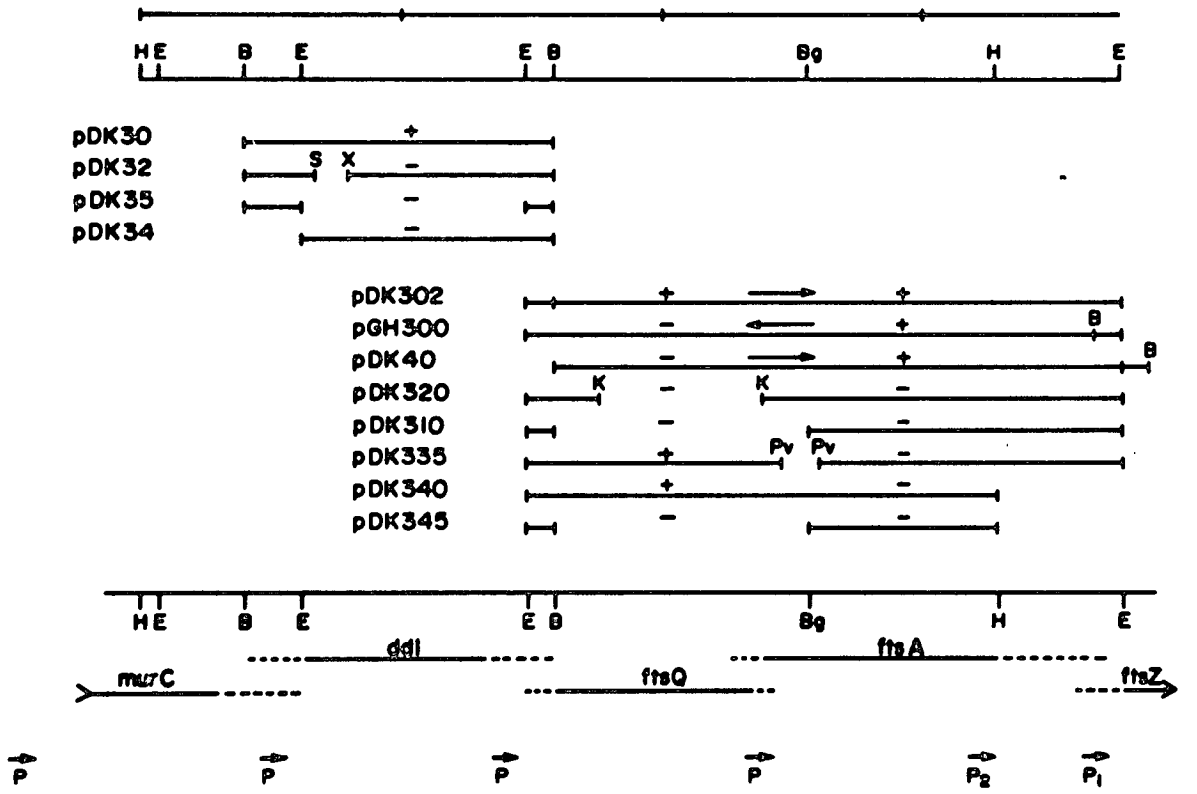
H E
B
E
E B
Bg
H
E
pDK30
pDK32
pDK35
pDK34
S
X
pDK302
pGH300
pDK40
pDK320
pDK310
pDK335
pDK340
pDK345
K
Pv
ddl
ftsA
murC
ftsQ
ftsZ
P
P
P
P
P2
P1

FIGURE 4.5

to complement due to lack of a promoter, can now be rejected as pDK10 carries the same EcoRI insert in the path of transcription from a vector promoter, P_4 (R. Hayward, personal communication; Sullivan and Donachie, 1984a; Morita and Oka, 1979), and still fails to complement ddl.

4.5 Subcloning the 2.3 kb EcoRI fragment into pKO1 and construction of deletion derivatives

G. Hatfull has subcloned the 2.3 kb EcoRI fragment from pGH4 (Robinson et al., 1984) into pKO1 (see Appendix A.4; G. Hatfull, PhD thesis). He recovered the insert in the same orientation as galK, designated pGH301, and in the opposite orientation, designated pGH300. Unfortunately, pGH301 carries a double copy of the pKO1 vector. Because this arrangement could give unpredictable effects on copy number and galK expression in the operon fusion experiments (see Chapter 5), I deleted the extra copy of the vector in pGH301 (described in Appendix A.4). The single vector version was designated pDK302. Like pGH301, pDK302 complements both ftsQ and ftsA. pGH300, however, only complements ftsA (see figure 4.5). The simplest explanation for these results is that P_{ftsQ} is not carried on the 2.3 kb EcoRI fragment. pDK302 complements ftsQ because the vector promoter P_4 transcribes across the EcoRI site towards galK, while pGH300 does not complement ftsQ because no transcription crosses the EcoRI site from the other direction. We must therefore predict that P_{ftsQ} lies to the left of the EcoRI site. Results further confirming this prediction are discussed in Chapter 5.

The deletion derivatives constructed from pGH301 by G. Hatfull (Robinson et al., 1984; G. Hatfull, PhD thesis) needed to be reconstructed also. KpnI, PvuII, BamHI-BglII, and HindIII deletions were all constructed using the restriction sites shown in Figure 4.4 and the vector HindIII

site located 290 bp downstream from the vector EcoRI insertion site (see Figure 5.1). These constructions are described in Appendix A.5 and illustrated in Figure 4.5.

pDK335 complements ftsQ (see figure 4.5), therefore the 3'-terminus must lie to the left of the first PvuII site. pDK340 complements ftsQ while pDK310, pDK320, and pDK345 fail to complement, as predicted by this boundary assignment. The 5'-boundary of ftsQ is discussed below.

pDK320 fails to complement ftsA, therefore the 5'-boundary of ftsA must extend over the right KpnI site. The conclusion that ftsA is cut by HindIII is supported by the fact that pDK340 does not complement ftsA. If the 5'-terminus of ftsA is close to the KpnI site, as it must be from ftsQ coding capacity requirements (see Chapter 6), then an FtsA product of 50,000 MW, requiring approximately 1,360 bp of coding sequence, would place the 3'-terminus of ftsA approximately 450 bp beyond the HindIII site. Results presented in Chapter 6 indicate that this is probably a slight overestimate for the size of ftsA; in any case ftsA must extend nearly to the right end of the 2.3 kb EcoRI fragment. The complementation results of pDK310, pDK335, and pDK345 are consistent with this assignment of ftsA boundaries.

The rightward EcoRI site cuts ftsZ sequences. If we assume that ftsA and ftsZ coding sequences do not overlap, then very little of the 5'-terminus of ftsZ should extend onto the 2.3 kb EcoRI segment.

4.6 Subcloning the 2.3 kb EcoRI fragment as a BamHI fragment into pKO4 and construction of deletion derivatives

The only indication presented thus far that ftsA has its own promoter comes from the fact that pGH300 complements ftsA but not ftsQ. More direct evidence that ftsA

expression is not dependent on ftsQ sequences is provided by another series of constructions (see below) in which ftsQ has been destroyed by moving its 5'-terminus on the 104 bp EcoRI-BamHI fragment to the other end of the 2.3 kb fragment. The primary reason, however, for constructing the rearranged fragment is that the most convenient insertion site in the available terminator assay vectors is a BamHI site (see pHR9, figure 5.4; Section 5.5).

The 2.3 kb EcoRI fragment was isolated from pDK302 as described in Appendix A.6. The purified fragment was circularized by self-ligation and then digested with BamHI to generate a rearranged fragment with BamHI ends (shown as pDK40, see figure 4.5). This fragment was cloned into pKO4 and recovered in both orientations, designated pDK40 with the insert in the same direction as galK, and pDK41 in the opposite direction.

Neither pDK40 or pDK41 complement ftsQ (see Figure 4.5), consistent with the 5'-terminus of ftsQ mapping to the left of the BamHI site. This places the leftward end of ftsQ on the 104 bp EcoRI-BamHI segment, as shown in Figure 4.5.

pDK40 and pDK41 both complement ftsA, in spite of the fact that the 5'-terminus of ftsQ has been removed. This is further evidence that ftsA must have an independent promoter. A similar result is given by pNS28, an analogous recombinant constructed by N. Sullivan (Robinson et al., 1984), in which the 104 bp EcoRI-BamHI fragment has been deleted.

One curious phenotype displayed by ftsA strains carrying pDK40 or pNS28 is that, even though they divide normally, confirming that ftsA is complemented, the cells grow as ovoids rather than rods. This result is discussed further in Chapter 7.

A series of deletion derivatives were constructed from pDK40 similar to those made in pDK302 (see Appendix A.7). Although these constructions were valuable in the operon fusion experiments, results from their complementations only

confirmed the conclusions already made in this chapter and added no new information. These results are shown in Figure 5.3.

Conclusions for the results presented thus far are summarized in Figure 4.5. In every case they were consistent with earlier hypotheses presented in Chapter 2, with the exception that ddl appears to have an independent promoter. More direct evidence supporting these conclusions is presented in the next chapter.

Chapter 5 Identification and characterization of transcriptional control signals between murC and ftsZ

5.1 Rationale

Operon fusions have proven to be an immensely valuable tool for investigating gene expression. Preliminary applications for our system include demonstration of promoter activity in the regions predicted by complementation results, quantitation of promoter activity, confirmation of orientation of transcription and identification of terminators that could limit polycistronic transcription. One convenient operon fusion system is the pKO series of vectors constructed by McKenney et al. (1981), which is described next.

5.2 The pKO system

The general strategy of the pKO system is to place putative transcriptional regulatory sequences upstream of the galK gene such that galK transcription is dependent on these sequences. Galactokinase activity, as measured from cell extracts, is then taken as an index of transcriptional activity. Simple qualitative analysis of transcriptional control sequences is possible by transforming recombinant pKO derivatives into a galK$^-$ strain and plating on MacConkeygalactose-ampicillin media. Clones expressing galK become red on this media and clones that cannot express galK remain white. This is the basis behind selection in promoter and terminator constructions.

Figure 5.1 shows the parent vector of the pKO system, pKO1. This vector carries four major domains: the galK coding sequence and its 168 bp leader; pBR322 sequence carrying oriV and the beta-lactamase gene; lambda sequence

Figure 5.1

pKO1 (adapted from McKenney et al., 1981)

Arrows represent the Ap and galK markers and show their directions of transcription. The rectangle between the EcoRI and HindIII sites carries the lambda terminator t_o. pKO4 is a pKO1 derivative constructed by inserting a 10 bp BamHI linker into the SmaI site. X_1, X_2, and X_3 represent the translational stop codons in each of the reading frames. The 5'-terminus of galK is indicated by AUG. An exogenous promoter, P_4 is associated with oriV, and transcribes in a clockwise sense (see text for details). Only relevant restriction sites are indicated, and the symbols are given in the legend to Figure 4.3.

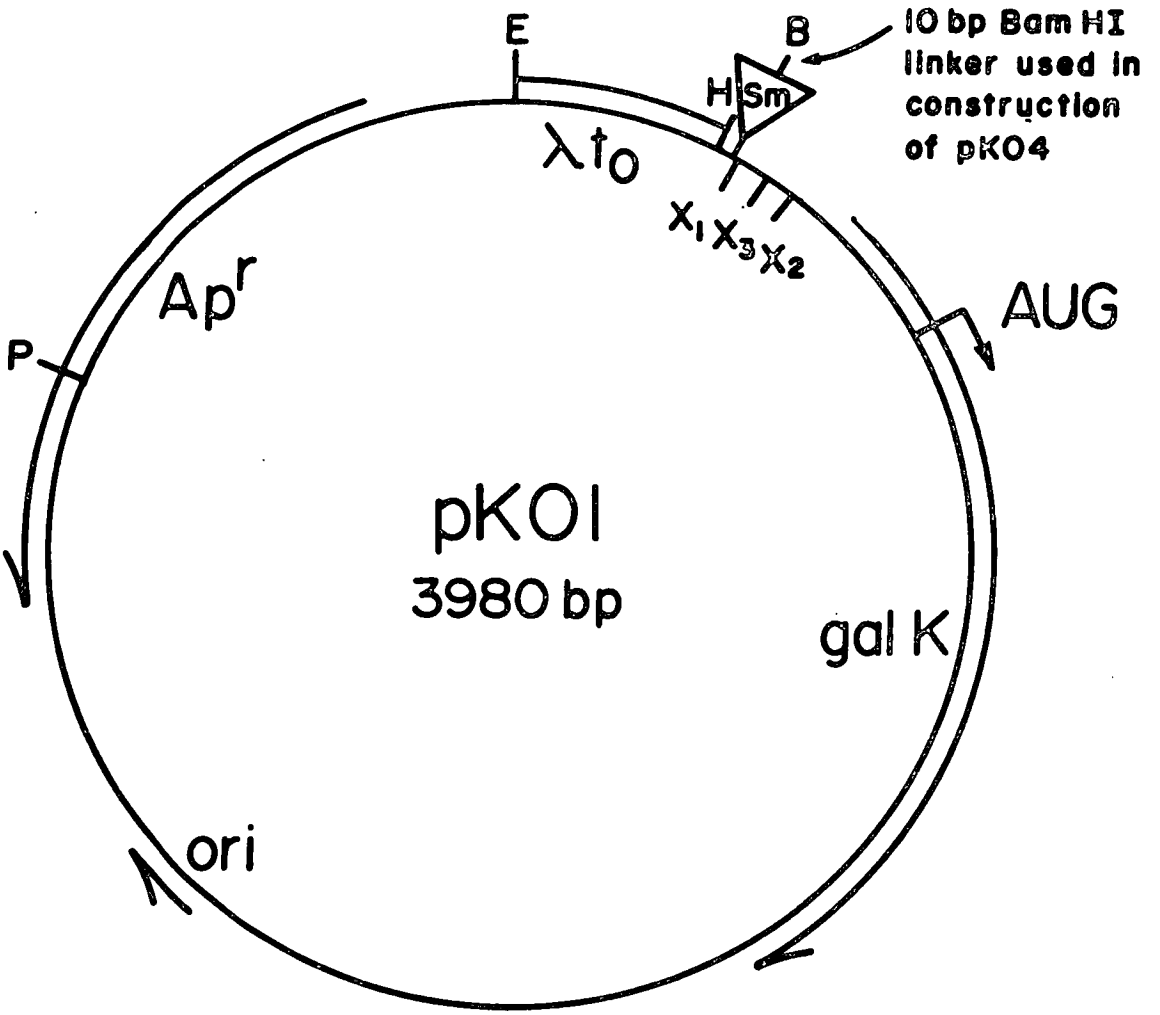
E
B
H
Sm
10 bp Bam HI linker used in construction of pKO4
λt0
X1 X3 X2
AUG
Apr
P
pKO1
3980 bp
gal K
ori

FIGURE 5.1

bearing the O gene terminator, λt_o; and an engineered sequence from the gal-operon carrying translational stop codons in all three reading frames and a SmaI cloning site (McKenney et al., 1981). The stop codons are necessary to uncouple translation, originating from translational start sequences within the insert, from transcription directed by that insert. This is important because upstream translational control sequences can have significant and unpredictable effects on translational efficiency of downstream sequences (de Boer, 1984; Kastelein et al., 1983). galK has its own translational start site, and the 168 bp leader sequence assures a relatively constant polarity effect on galK transcription and translation (McKenney et al., 1981).

The λt_o sequence was included because transcription from the P_4 vector promoter appears to cross the EcoRI site towards galK (R. Hayward, personal communication; Close and Rodriguez, 1982). λt_o does not block galK expression by P_4 completely, although it does prevent pKO1 from complementing galK. A pKO1 derivative with a λt_o deletion increases galactokinase activity approximately 40%, which allows galK complementation (Sullivan and Donachie, 1984a). A strong terminator cloned into the EcoRI site does eliminate galK expression (see Table 5.1 and 5.3, clones with inserts opposed to galK). Therefore pKO1 carries no promoters to the right of the EcoRI site.

One practical consequence of P_4 and λt_o in pKO1 is that promoters inserted at the EcoRI site will have to read through λt_o, and constructions that delete λt_o will have about 40% more P_4 activity contributing to galK expression. These factors must be considered in interpreting galK fusion results.

There are several limitations of the pKO system that also must be identified. Foremost for our purposes is that it is a multicopy system. This implies that, in comparing different constructions, copy number equivalence must be established. Copy number determinations are difficult in

practice, although the commonly used beta-lactamase assay gives a rough estimate. Beta-lactamase assays have been done on several pKO constructions (N. Sullivan and D. Kenan, unpublished results), and they were equivalent within the limits of the assay. We make the guarded conclusion that most, if not all, of our pKO constructions are maintained at equivalent copy numbers, although galactokinase assays in a single copy system would be necessary for accurate quantitative measurements of promoter activity. Single copy constructions can be obtained by crossing galK fusions into an appropriate phage vector, but this was not felt necessary in our preliminary efforts to identify promoters and classify them as "weak", "moderate", or "strong".

Another drawback to a high copy system is that it is likely to titrate out effector molecules expressed at constituitively low levels. Although this may help us to identify promoters that would otherwise be repressed in low copy numbers, identification of promoters requiring activators and characterization of regulatory circuits would need to be done in a single copy system.

A final drawback to the pKO system is that the galK assay, in our hands, proved to be somewhat inconsistent. However, even though the same plasmid often gave quite different galactokinase activities from assay to assay, the relative activities between plasmids in the same assay remained constant within limits of roughly 10%. Simple statistical methods described in Chapter 3 allow separate assays of the same group of plasmids to be averaged without obscuring relationships between plasmids.

5.3 Promoter activity between murC and ftsQ

The construction of pDK10 and pDK50 (pKO1 clonings) and pDK30 and its derivatives (pKO4 clonings) is described

Figure 5.2

pDK30 and related recombinants: complementation results and galactokinase activity

The top line represents a scale of 1000 bp. Immediately below is the regional map showing the most important restriction sites. Symbols are explained in the legend to Figure 4.3. Rectangles represent the chromosomal inserts for each construction. Arrows to either side show the location of the lambda terminator domain of pKO1, if present, in relation to the insert. The direction given by these arrows represents the orientation of both the chromosomal insert and the galK marker downstream. Constructions with inserts oriented away from galK are not shown, but pDK31, pDK51, and pDK11 all gave the same ddl complementation results as their counterparts (pDK30, pDK50, and pDK10) and none produced galactokinase activity. ddl complementation was determined by colony formation at 42°C. galK complementation was identified by red colony phenotype on MacConkey-galactose agar. Galactokinase activity is expressed relative to pDK30 from the data shown in Table 5.1. The SalI-XhoI fragment is deleted in pDK32.

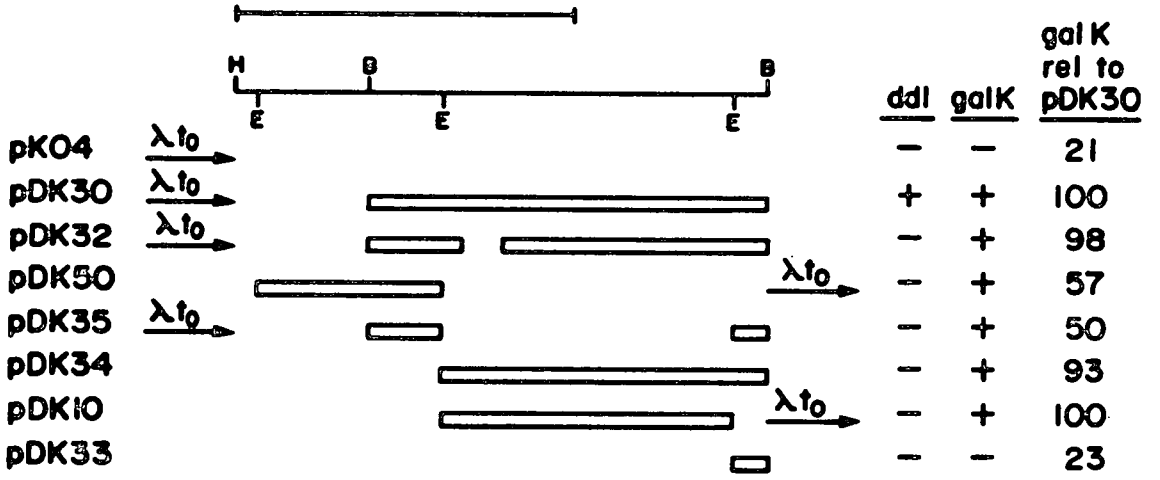
H
B
B
E
E
E
pK04
pDK30
pDK32
pDK50
pDK35
pDK34
pDK10
pDK33
λ t0
λ t0
λ t0
λ t0
λ t0
ddl
galK
galK rel to pDK30
– – 21
+ + 100
– + 98
– + 57
– + 50
– + 93
– + 100
– – 23

FIGURE 5.2

in Appendix A.2 and A.3, and complementation results are discussed in Sections 4.3 and 4.4. Here we describe the transcriptional activity directed by these inserts.

The galK complementation results in Figure 5.2 show that all the inserts carry promoter activity except the 104 bp EcoRI-BamHI fragment carried by pDK33. The 5'-terminus of ftsQ lies on this fragment, further confirming that P_{ftsQ} lies to the left of the EcoRI site. pDK10, which lacks the 5'-terminus of ddl, and therefore carries no upstream promoters, expresses 100% of the activity of pDK30. The most likely location for this activity is to the right of the ddl 3'-terminus, which, by gene boundary estimates (see Figure 4.5) places P_{ftsQ} very close to the EcoRI site. The slightly lower galactokinase levels of pDK34 are within the limits of error, but may also reflect an influence from the translational start site for P_{ftsQ} on the 104 bp BamHI fragment. Remember that P_{ftsQ} in pDK10 reads through λt_o, so that its activity should be corrected to about 140 relative units. The fact that promoter activities in the pKO system do not add up may reflect either errors in measurement or genuine effects of inserted sequences, but the discrepancies are not significant for our purposes. By comparison with P_{gal}, a moderately strong E. coli promoter (McKenney et al., 1981; Rosenberg et al., 1982), P_{ftsQ} is a relatively weak promoter with approximately 20% of P_{gal} activity (see Table 5.3).

Although P_{ftsQ} can account for all of the measured promoter activity carried by pDK30, another promoter seems to lie at the left end of the 1.2 kb BamHI segment. pDK50 carries 57% of the activity of pDK30. Comparison with pDK35, having equivalent activity shows that a promoter is located on the 210 bp BamHI-EcoRI segment. This corresponds well to a prediction for P_{ddl} based on the fact that the murC 3'-terminus and ddl 5'-terminus are both located on the same segment (see Figure 4.5).

Table 5.1

pDK30 and related constructions: galactokinase assays

fusion	galactokinase activity*
pKO4	15 ± 3
pDK30	73 ± 11
pDK31	0
pDK32	72 ± 8
pDK50	42 ± 2
pDK51	0
pDK35	37 ± 6
pDK34	68 ± 4
pDK10	73 ± 8
pDK11	0
pDK33	17 ± 3

* galactokinase units were originally expressed as nanomoles of galactose phosphorylated per minute per OD_{650}. Each plasmid-bearing strain was assayed a minimum of four times, and the results were normalized using the statistical method described in Chapter 3. Therefore these values have relative significance only, and should not be compared to other galactokinase data. See page 70 for discussion of pDK11, pDK31, and pDK51

pDK32 carries a deletion that destroys ddl complementation but should not affect the promoters at either end of the insert. Figure 5.2 shows that pDK32 carries the same promoter activity as pDK30, consistent with this prediction.

These results confirm that both P_{ddl} and P_{ftsQ} transcribe in a clockwise sense relative to the E. coli genetic map. Both of the EcoRI fragments and the BamHI fragment were cloned in the opposite orientation as well (pDK51, pDK11, and pDK31; see Table 5.1) and these constructions uniformly gave no galK expression. Whether the block to P_4 readthrough in these inserts is due to opposing transcription (Ward and Murray, 1979) or transcriptional terminators in the non-coding strand is not known (see Section 5.5 for further discussion).

5.4 Promoter activity between ftsQ and ftsZ

Construction of pDK302 (pKO1 cloning), pDK40 (pKO4 cloning) and their derivatives is described in Appendix A.4, A.5, A.6, and A.7 and some complementation results are given in Sections 4.5 and 4.6.

galK complementation results in Figure 5.3 show that all inserts carry promoter activity except the BamHI-BglII fragment of pDK315. The pDK33 EcoRI-BamHI insert also shows no promoter activity (discussed above), and a related construction, pNS37, carrying these two segments intact from the EcoRI site to the first PvuII site, again shows no promoter activity (Robinson et al., 1984). The pNS37 insert does, however, complement ftsQ, presumably due to transcription from the vector promoter P_4 (see above). This result confirms that P_{ftsQ} lies entirely to the left of the EcoRI site, but it also fails to demonstrate P_{ftsA}, which was mapped to this segment by genetic methods. Possible explanations are that ftsA expression requires a weakly expressed activator, which is titrated by the high

Figure 5.3

pDK302 and related recombinants: complementation results and galactokinase activity

The top line represents a scale of 1000 bp. Immediately below is the regional map showing relevant restriction sites. Symbols are explained in the legend to Figure 4.3. Rectangles represent the chromosomal inserts for each construction. Arrows to either side show the location of the lambda terminator domain in pKO1, if present, in relation to the insert. The direction given by these arrows shows the orientation of the galK gene downstream. Note that all inserts are oriented in this same direction except for that of pGH300. pDK302 and pGH300 carry the same insert in opposite orientations as indicated by the central arrows over their insert rectangles. pDK41, which is not shown, carries the insert of pDK40 oriented away from galK, gives complementation results identical to those of pDK40 and produces no galactokinase activity. ftsQ and ftsA complementation was determined by colony formation without filamentation at 42°C. galK complementation was tested as described in the legend to Figure 5.2. Galactokinase activity is expressed relative to pDK302 and pDK40 from the data shown in Table 5.2.

FIGURE 5.3

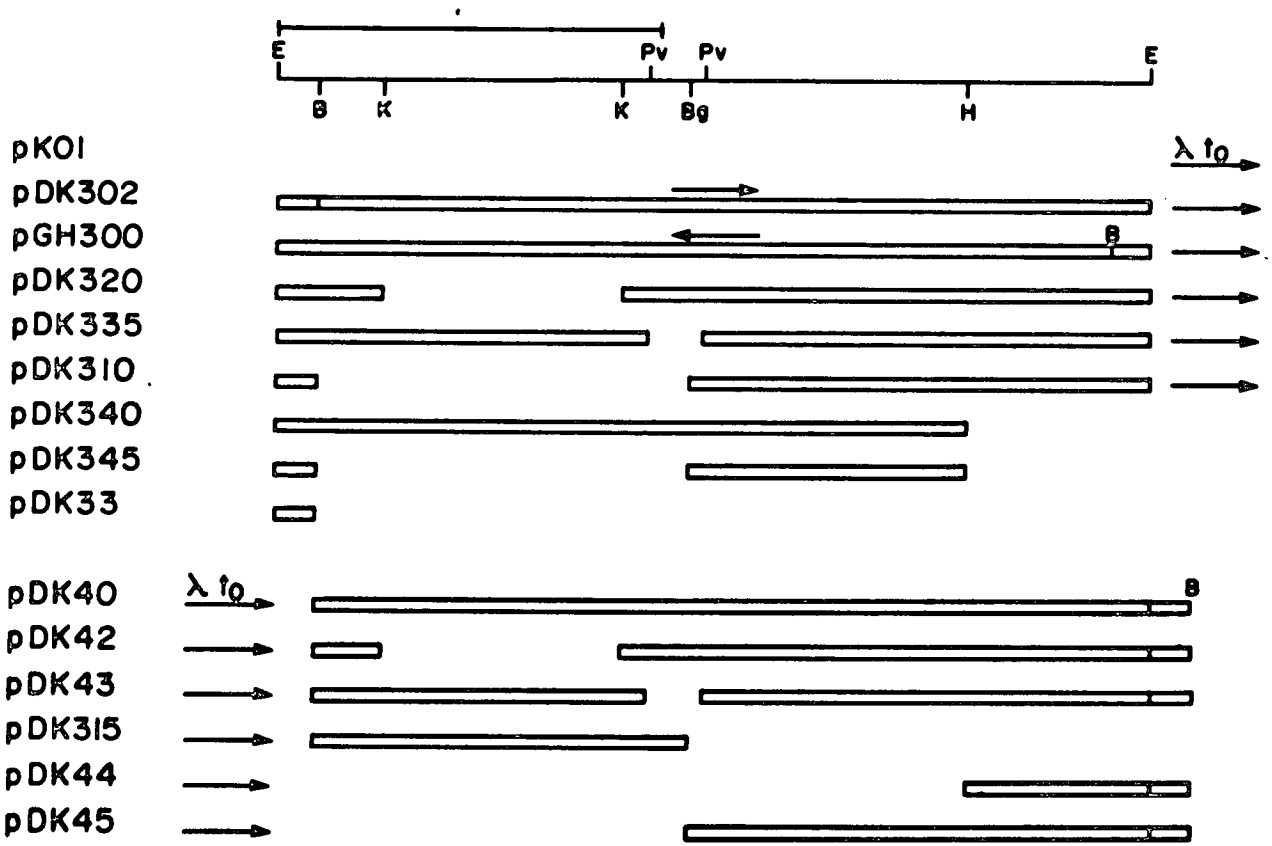

	ftsQ	ftsA	galK	galK rel to pDK302
pKO1	−	−	−	22
pDK302	+	+	+	100
pGH300	−	+	−	0
pDK320	−	−	+	92
pDK335	+	−	+	95
pDK310	−	−	+	95
pDK340	+	−	+	59
pDK345	−	−	+	36
pDK33	ND	ND	−	ND
				rel to pDK40
pDK40	−	+	+	100
pDK42	−	−	+	89
pDK43	−	−	+	102
pDK315	−	−	−	5
pDK44	−	−	+	74
pDK45	−	−	+	93

copy number; or that ftsA is transcribed only at very low levels, perhaps periodically, insufficient to complement galK. One of the failures of our use of the pKO system has been its inability to demonstrate P_{ftsA}.

The results discussed above indicate that all promoter activity measured in the 2.3 kb EcoRI fragment originates to the right of the second PvuII site (see figure 5.3). The possibility still remains that sequences to the left of this PvuII site will affect transcription from rightward promoters. This was shown not to be the case by comparing pDK345 with pDK320, pDK335, and pDK302, and similarly comparing pDK45 with pDK43, pDK42, and pDK40: all have essentially equivalent galactokinase activities. We can conclude that all promoter activity measured from pDK302 and similar constructions is directly related to ftsZ transcription.

The fact that pDK345 and pDK44 both display promoter activity indicates that ftsZ has at least two functional promoters, designated P_2 and P_1 in Figure 4.5, and that the ftsZ "enhancer" postulated by Lutkenhaus and Wu (1980) is actually the promoter, P_2. Direct analysis of P_2 activity and indirect analysis of P_1 (compare pDK345 with pDK310, after subtracting the pKO1 activity from each, see Figure 5.3) indicate that P_2 has only about 25% of the activity of P_1. Indirect analysis of P_2 and direct analysis of P_1 (compare pDK44 with pDK45, as above) indicate that P_2 has about 30% of the activity of P_1. These results suggest that P_1 is the most efficient promoter for expression of ftsZ, although results discussed in Chapter 2 show that ftsZ expression normally relies on P_2 as well. Independent results obtained by N. Sullivan with different clones measuring P_1 and P_2 directly showed that they had roughly equal activities (Sullivan and Donachie, 1984a), therefore it is probably best to conclude nothing more than that P_1 and P_2 have somewhat similar, relatively weak promoter activities in a multicopy system.

Table 5.2

pDK302, pDK40, and related constructions: galactokinase assays

fusion	galactokinase activity*
pKO1	45 ± 8
pDK302	200 ± 30
pGH300	0
pDK320	190 ± 20
pDK335	200 ± 20
pDK310	190 ± 20
pDK340	120 ± 20
pDK345	74 ± 7
pKO4	24 ± 20
pDK40	340 ± 40
pDK41	0
pDK42	300 ± 20
pDK43	350 ± 40
pDK315	16 ± 20
pDK44	250 ± 30
pDK45	310 ± 70

* Galactokinase units are as described in Table 5.1. Note that pDK302-group and pDK40-group data have been normalized within their respective groups and hence cannot be compared to each other or to any other sets of galactokinase data. Each group was assayed a minimum of five times, and the data was analyzed as described in Table 5.1.

The fact that the constructions discussed above place P_2 to the left of the HindIII site firmly locates this *ftsZ* promoter within *ftsA* coding sequence. The significance of this conclusion will be discussed in Chapter 8.

5.5 Terminator activity between *murC* and *ftsZ*

The pKO system can also be used to study terminators by cloning potential terminator sequences between P_{gal} and *galK* and measuring the amount of P_{gal} readthrough that persists. A pKO1 derivative, designated pKG1800 (McKenney et al., 1981) was constructed by replacing the 190 bp EcoRI-HindIII fragment in pKO1 with a 1085 bp EcoRI-HindIII fragment from the *gal* operon carrying *Pgal*. Note that P_{gal} actually consists of three promoter regions, two operator regions, and two different transcriptional start sites, (Irani et al., 1983), and that gal repressor is titrated by the multiple copies of P_{gal}. Therefore, transcription from P_{gal} is constituitive in pKG1800 transformants (McKenney et al., 1981). The vector used in our experiments, pHR9 (see Figure 5.4), was derived from pKG1800 by cloning a 10 bp BamHI linker into the SmaI site (Newman et al., 1982).

Limitations of the pHR9 system include those discussed in Section 5.2 for pKO1, plus another problem. The P_{gal} fragment carries the *galE* translational start, meaning that BamHI inserts will be translated as they are transcribed. Because there is a two-thirds chance that translation originating from *galE* will be out of phase with respect to the correct reading frame for an inserted gene, it is possible that ribosomes could continue past the normal translational stop into terminator sequences and alter the termination event. Therefore, the presence of the *galE* translational start means that some functional terminators could be inhibited. Terminator assays cannot then be

Figure 5.4

pHR9 (adapted from McKenney et al., 1981)

Arrows represent the Ap and galK markers and show their directions of transcription. The rectangle between the EcoRI and HindIII site carries chromosomal sequences from the gal promoter and operator regions. The 5'-terminus of galE and its translational start are indicated by AUG (galE). X_1, X_2, and X_3 represent the translational stop codons in each of the reading frames. The 5'-terminus of galK is indicated by AUG (galK). Only relevant restriction sites are indicated, and the symbols correspond to those given in the legend to Figure 4.3.

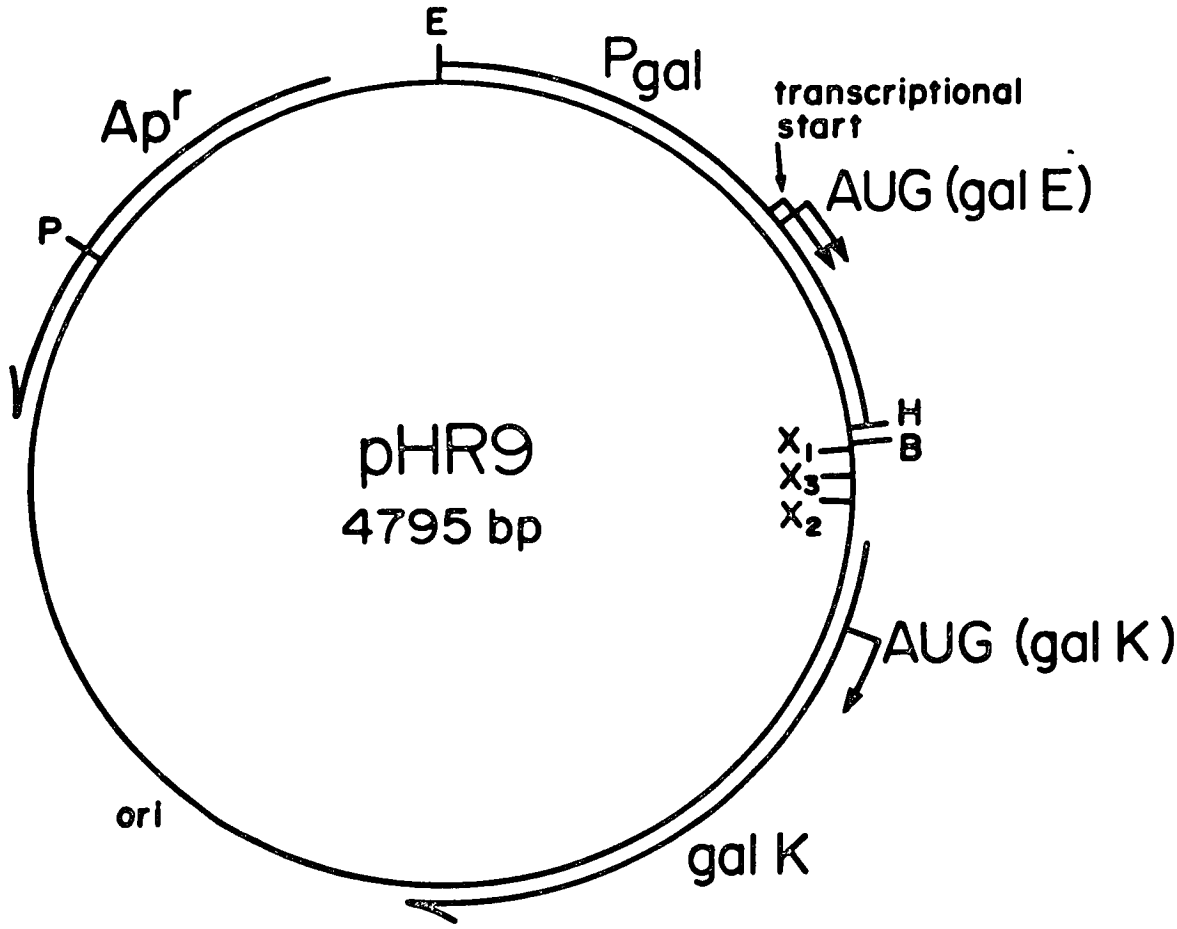
E
Pgal
transcriptional start
AUG (gal E)
Ap^r
P
pHR9
4795 bp
H
B
X1
X3
X2
AUG (gal K)
ori
gal K

FIGURE 5.4

interpreted with confidence unless translation from galE can be prevented from crossing the terminator, or preferably, any part of the insert.

McKenney (personal communication) has suggested one way to stop galE translation from proceeding into the insert. His sequence of the P_{gal} region shows that filling-in the HindIII sticky ends and religating will introduce a stop codon (TAG) into the galE reading frame. However, there are two reasons to suspect that McKenney's sequence contains errors, meaning that the altered HindIII site may not in fact put a stop codon in the galE reading frame. First, preliminary sequencing results of the P_{gal}-BamHI segment (by J. Wright) has identified one missense and three deletion errors in the McKenney sequence (R. Hayward, personal communication). While these results are still preliminary and only include the distal 40% of this sequence, they do suggest that the galE translational phase across the BamHI site is uncertain. Second, pDK114, a construction missing the 5'-terminus of ftsQ (described below) is able to complement ftsQ, suggesting strongly that a fortuitous galE-ftsQ fusion enables transcription of ftsQ from P_{gal} and translation from galE. The ftsQ translational phase across the BamHI site is known (Robinson et al., 1984), which would put the correct galE translational phase as (+1 bp) from that predicted by the McKenney sequence.

galE translation, then, remains a problem in interpreting pHR9 results, and it probably cannot be eliminated by filling in the HindIII site. However, translation in non-coding reading frames would not likely proceed far before encountering a stop codon, and larger pHR9 inserts such as those used in my experiments would be unlikely to allow galE translation to reach a downstream terminator site. This has been confirmed by sequence data for the 2.3 kb EcoRI fragment (see Chapter 8; Robinson et al., 1984). In fact, translation out of phase with ftsQ would be

Figure 5.5

pHR9 constructions: galactokinase activity

The top line represents a scale of 1000 bp. Immediately below is the regional map showing the most important restriction sites. Symbols are explained in the legend to Figure 4.3. Rectangles represent the chromosomal inserts for each construction. The arrows to the left of the rectangles represent the gal promoter and its direction of transcription. This is also the direction of transcription for most of the inserts and for the galK marker downstream. Those inserts oriented away from galK are indicated by leftward arrows above the insert rectangles. pDK113, which is not shown, carries the same insert as pDK112 but oriented away from galK. This construction produces no galactokinase activity. Galactokinase activity is expressed relative to pHR9 from the data shown in Table 5.3. Percent readthrough is calculated as described in the text, and refers to the component of galactokinase activity produced by P_{gal} transcripts passing through the insert. Complementation results are shown separately in Table 5.4 to emphasize their importance.

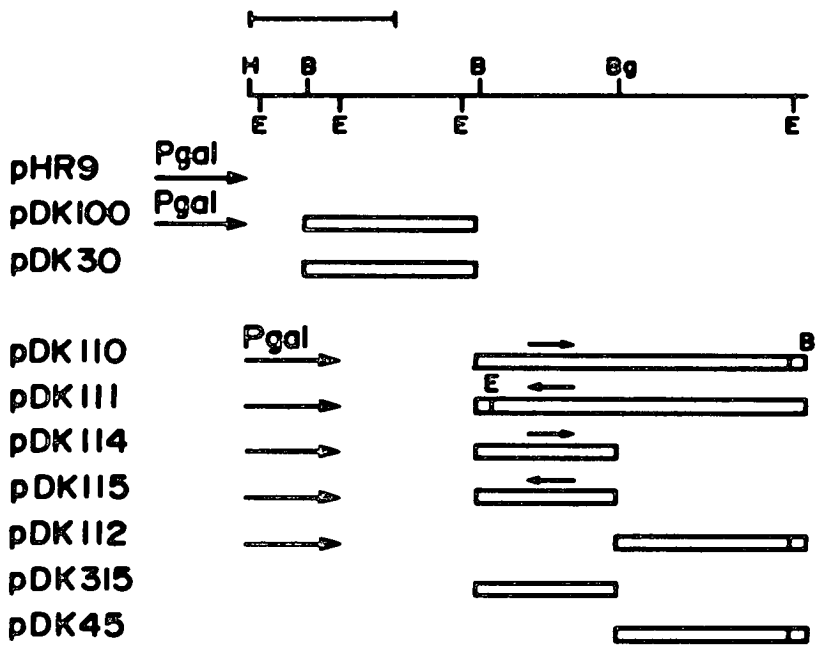

	gal K rel to pHR9	percent read through
pHR9	100	100
pDK100	99	76
pDK30	23	
pDK110	ND	ND
pDK111	0	0
pDK114	53	50
pDK115	0	0
pDK112	67	30
pDK315	3	
pDK45	37	

FIGURE 5.5

Table 5.3

pHR9 constructions: galactokinase assays

fusion	galactokinase activity*
pHR9	500 ± 120
pDK100	490 ± 40
pDK101	0
pDK30	113 ± 40
pHR9	820 ± 40
pDK110	ND
pDK111	0
pDK112	540 ± 70
pDK113	0
pDK45	300 ± 40
pDK114	430 ± 90
pDK115	0
pDK315	30

* Galactokinase activity was analyzed as described in Table 5.1. The pDK100 and pDK110 groups were not assayed together, therefore their normalized values should not be directly compared. pDK110 transformants grew poorly in minimal media and thus were not assayed. All assays were repeated at least three times with the exception of pDK315, for which only one assay was performed. This clone, however, consistently gives a weak galactokinase activity equivalent to that of pKO4, and the pKO4 assays that were done with the pDK110 group confirm that the value given for pDK315 is likely to be accurate (data not shown).

predicted to stop 15 bp past the BamHI site in pDK114 for the ftsQ(+1) phase and 112 bp past the BamHI site for the ftsQ(+2) phase. Similarly in pDK112, translation out of phase with ftsA would be predicted to stop at 87 bp past the BglII site in the ftsA(+1) phase and 31 bp past the BglII site in the ftsA(+2) phase. Sequence data is not yet available for the ddl reading frame, but the ftsQ-ftsA results suggest that translation from galE out of phase with ddl would not reach the end of the 1.2 kb insert in pDK100.

We can conclude that galE translation probably does not affect termination efficiency in my pHR9 constructions, but other effects such as differential rates of transcript degradation (Kastelein et al., 1983) among the various constructions cannot be predicted. One effective solution would be to delete or mutagenize the galE start site, although one would have to take care to avoid disrupting the nearby gal-promoter sequences.

Construction of pDK100, pDK101, pDK110, pDK111, pDK112, pDK113, pDK114, and pDK115 is described in Appendix A.8 and A.9. Figure 5.5 and Table 5.3 show galactokinase assays and Table 5.4 shows complementation results.

It is striking that all pHR9 constructions with the inserts in the opposite direction relative to galK give no galK expression. These clones are pDK101, pDK111, pDK113, and pDK115, each corresponding to the same inserts carried by their next-lowest number counterparts in Figure 5.5. Although this effect was seen in opposition to P_4 (pKO1 and pKO4 constructions), P_{gal} is approximately 100 times stronger (personal observation). Even pDK115, carrying the undemonstrated P_{ftsA}, prevents P_{gal} readthrough, suggesting that the mechanism involves more than opposing transcription. Because all genes in this region seem to be transcribed in the same direction, a mechanism to block RNA polymerase from binding to or transcribing the non-coding strand might be advantageous. The presence of terminators in the non-coding strand could account for this behavior,

Table 5.4

Complementation of pDK100, pDK110, and their related constructions*

clone	ddl	ftsQ	ftsA	galK
pHR9	-	-	-	+
pDK100	+			+
pDK101	+			-
pDK30	+			+
pDK110		ND	ND	+
pDK111		-	+	-
pDK40		-	+	+
pDK112		-	-	+
pDK113		-	-	-
pDK45		-	-	+
pDK114		+	-	+
pDK115		-	-	-
pDK315		-	-	-

* Complementation was scored as positive if the transformant was able to form colonies at 42°C, and, in the case of ftsQ and ftsA, without filamenting. galK complementation was described in Figure 5.2.

and remains a strong possibility. The 2.3 kb EcoRI fragment sequence reveals many domains of dyad symmetry (Robinson et al., 1984; see Chapter 8), perhaps reflecting a complex arrangement of expression control signals and putative protein binding sites.

If the fact that the pDK115 insert, carrying the undemonstrated P_{ftsA}, blocks P_{gal} is surprising, then it seems even more surprising that P_{ftsA} is able to express *fts*A in opposition to P_{gal} (see pDK111 complementation results, Table 5.4). This result is the strongest indirect evidence we have generated that P_{ftsA} exists. See Chapters 7 and 8 for further discussion of P_{ftsA}.

Efficiency of termination for an inserted fragment is estimated by subtracting the promoter activity of that fragment (measured in pKO4, for example) from the promoter activity given by a fusion with that fragment inserted between P_{gal} and *gal*K (expressed in units relative to pHR9 galactokinase activity). The result is termed "percent readthrough" in Figure 5.5.

Non-terminator sequences can affect P_{gal} transcripts passing through the insert in ways that mimic termination, and these possibilities must be considered in interpreting pHR9 results. An RNA polymerase pause site, for example, could decrease the number of P_{gal} transcripts successfully completed. Similarly, almost any insert cloned between P_{gal} and *gal*K will give a slight polar effect on transcription (between 10-20%, McKenney et al., 1981). Larger fragments will presumably give more significant polar effects. Finally, it must be remembered that transcription may be influenced by translational events (attenuation, for example), and isolation of a terminator from other sequences that regulate gene expression may not necessarily reflect behavior *in vivo*. All of these subtle complications could be investigated in detail with techniques of molecular genetics, but simple cloning of relatively large fragments

into pHR9 should be adequate to answer the question of whether strong terminators function between murC and ftsZ.

pDK110 carries the rearranged 2.3 kb BamHI insert (see Figure 5.5). Cells carrying pDK110 grow poorly, and the plasmid is unstable (see Chapter 7). If ftsA expression is destroyed by subcloning the pDK110 insert as BamHI-BglII fragments (see Appendix A.8) then no deleterious effects are noted. This suggests that ftsA is responsible for the deleterious effect, and that overproduction of ftsA by P_{gal} transcription is harmful to the cell (see Chapter 7 for further discussion). A practical consequence is that termination in the 2.3 BamHI fragment must be studied by inactivating ftsA, such as occurs with the pDK112 and pDK114 constructions described below.

pDK112 carries sequences that make up the ftsA 3'-terminal to ftsZ 5'-terminal junction (see Figure 5.5). Comparison of pDK112 and pDK45 galactokinase activity shows that this insert allows approximately 30% readthrough from P_{gal}. While this result confirms that no strong terminators lie between ftsA and ftsZ, it does not rule out the possibility that a less efficient terminator occupies this region. Taking 20% termination as a reasonable polarity effect for a fragment of this size (see above), 50% of the transcripts remain to be accounted for. In any case, we can conclude that ftsA and ftsZ may be expressed from the same transcript in at least some circumstances. Similarly, comparison of pDK114 and pDK315 galactokinase activities shows 50% readthrough. Using the same arguments as above, we can conclude that no strong terminators lie between ftsQ and ftsA, and that these genes may be expressed from the same transcript.

pDK100 carries sequences between the murC 3'-terminus all the way to the ftsQ 5'-terminus, including the whole of ddl. Comparison with pDK30 shows that the 1.2 kb BamHI insert allows 76% readthrough from P_{gal}, suggesting that no strong terminators lie between murC and ftsQ. The 24%

termination that is seen is entirely within the limits of "normal" polarity described by McKenney et al. (1981). By extension, we can make the guarded conclusion that no strong terminators are found between murC and ftsZ, and that all of these loci could be transcribed together. Note that terminators lying on the leftward BamHI site, the BglII site, and the rightward EcoRI site would have been destroyed by these clonings, although these regions all lie within coding sequence and therefore are not likely to carry terminators. Possible roles for termination in control of gene expression in the murC-ftsZ cluster will be discussed in Chapter 8.

Chapter 6 Gene expression directed by the 1.2 kb BamHI and 2.3 kb EcoRI fragments

6.1 Rationale

Lutkenhaus and Wu utilized an indirect method to assign gene products to the 2-minute loci carried by λ16-2. While their results were valuable in initiating a molecular genetics approach to this region, many of them have awaited confirmation by more direct methods. This chapter describes the use of a system for expression of genes directed by specific restriction fragments, thereby allowing direct correlation with their products.

6.2 The pHUB2 system

Figure 6.1 shows the pHUB2 vector (Bernard et al., 1979), carrying pBR322 sequences with the tetracycline-resistance gene and several unique restriction sites; a pBR322-modified segment carrying the kanamycin-resistance marker; and a lambda segment carrying P_L. The vector must be maintained in a lambda lysogen, or a strain otherwise carrying the cI function, to prevent transcription from P_L from blocking replication of the plasmid. If the lysogen is cI857, then transcription from P_L can be induced simply by raising the temperature.

In our application of the pHUB2 system, fragments bearing complete genes with intact translational start sites and ribosomal binding sites were cloned downstream from P_L. Recombinant vectors were transformed into a minicell-producing strain, DS410, which carried cI857 expressed by a different plasmid, pRK248 (Bernard et al., 1979). Minicells which were harvested at 30°C were pulse-labeled with [^{35}S]-methionine at 42°C, and then total minicell protein

Figure 6.1

pHUB2 (adapted from Bernard et al., 1979)

The Kn and Tc markers are shown inside the vector diagram. Only relevant restriction sites are shown, and these correspond to the symbols used in Figure 4.3, except for Hp=HpaI. The leftward lambda promoter, P_L, is shown and its direction of transcription is represented by the arrow. Transcription from P_L interferes with replication, so that pHUB2 must be maintained in a strain that expresses the cI repressor. See text for further details.

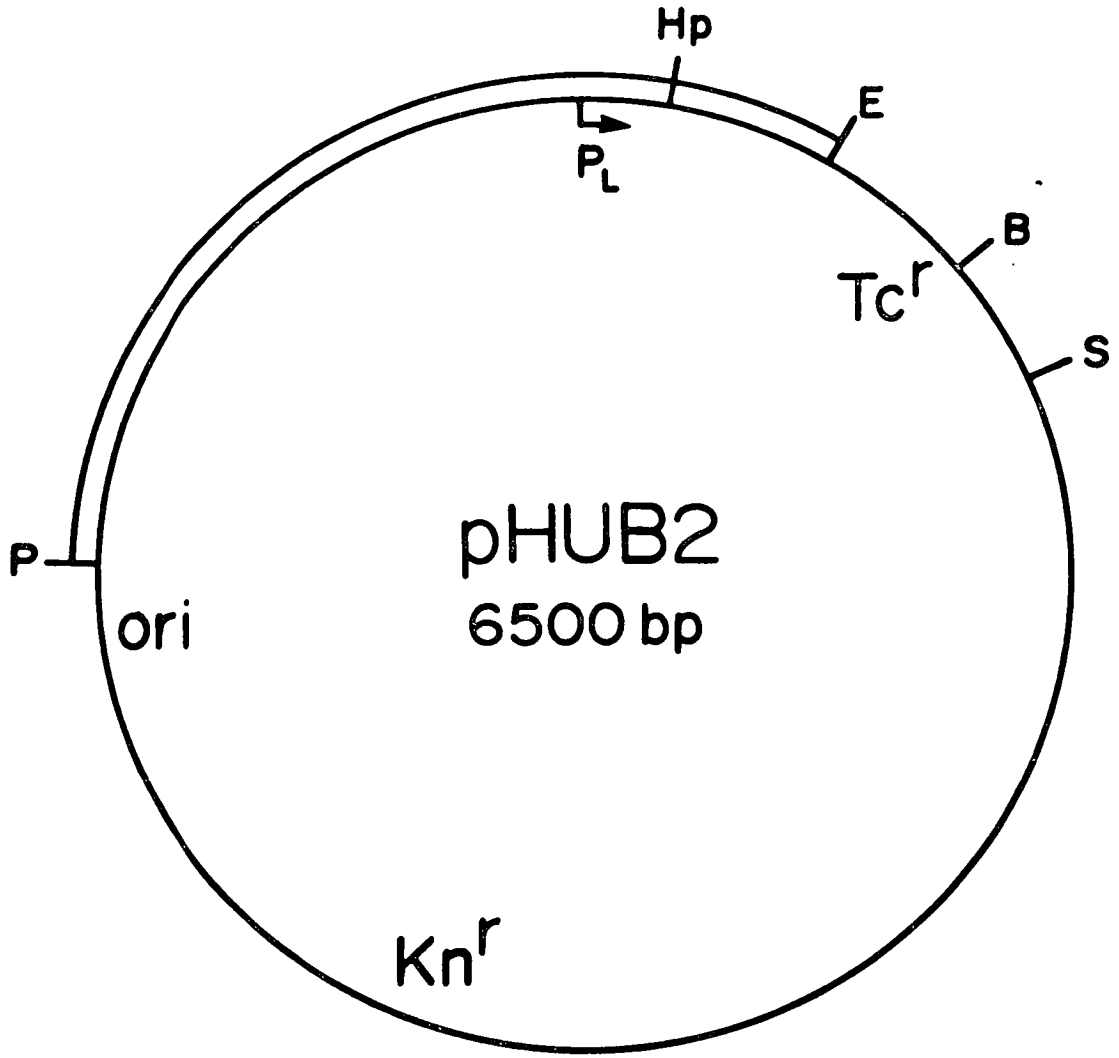

FIGURE 6.1

was run out on a 7-20% polyacrylamide gradient gel. Autoradiograms revealed proteins expressed by pRK248 and pHUB2 derivatives. Gene products were assigned to cloned genes by comparison with gene products from a construction in which the same insert was oriented in opposition to P_L, and hence unable to express its products due to opposing transcription (Ward and Murray, 1979; see below).

6.3 The Ddl, FtsQ, and FtsA proteins

The constructions of pDK60 and pDK61, carrying the 1.2 kb BamHI fragments in both orientations, and pDK70, carrying the 2.3 kb EcoRI fragment in the same orientation as P_L, are described in Appendix A.10. pDK70 is equivalent to pNS23, which was the recombinant used in these experiments. Unfortunately, the 2.3 kb EcoRI-pHUB2 recombinant in the orientation opposed to P_L was not isolated before the expression experiment, and an alternative method of destroying expression from that fragment was employed (see below).

Figure 6.2 is an autoradiogram showing the polypeptide products of pDK60, pDK61, pRK248, pHUB2, and pNS23. Comparing the pDK60 and pDK61 lanes with the controls shows a single unique band of 32,000 dalton expressed at high levels by pDK60. This construction places *ddl* in the same orientation as P_L. pDK61, with *ddl* expression opposed to P_L, does not express the 32,000 dalton product. Therefore, the unique band corresponds to the *ddl* gene product. This result is consistent with the 30,000 dalton *ddl* product proposed by Lutkenhaus and Wu (1980), with the slight difference possibly attributable to the use of different PAGE systems or anomalous migration (Banker and Cotman, 1972).

Similarly, comparison of the pNS23 lane with pHUB2 and pRK248 lanes reveals two unique polypeptides of 46,000 and 35,000 daltons expressed by pNS23. The 46,000 dalton

Figure 6.2

Gene products expressed by the 1.2 kb BamHI and 2.3 kb EcoRI fragments

A 7-20% gradient SDS-PAGE autoradiogram

Lanes:
A: size standards: Phosphorylase b (94 K); BSA (67 K); Ovalbumin (43 K); Carbonic anhydrase (30 K); Soybean trypsin inhibitor (20.1 K); alpha-Lactalbumin (14.1 K)
B: pNS23
C: pRK248
D: size standards
E: pHUB2
F: pDK61
G: pDK60
H: size standards

Unlabeled size standards were detected by staining in Coomassie blue and marking their positions on the autoradiogram (pencil marks in the size standard lanes are faintly visible). All band sizes are in units of kilodaltons. All bands are seen more clearly on the original autoradiogram, which is available upon request from the author.

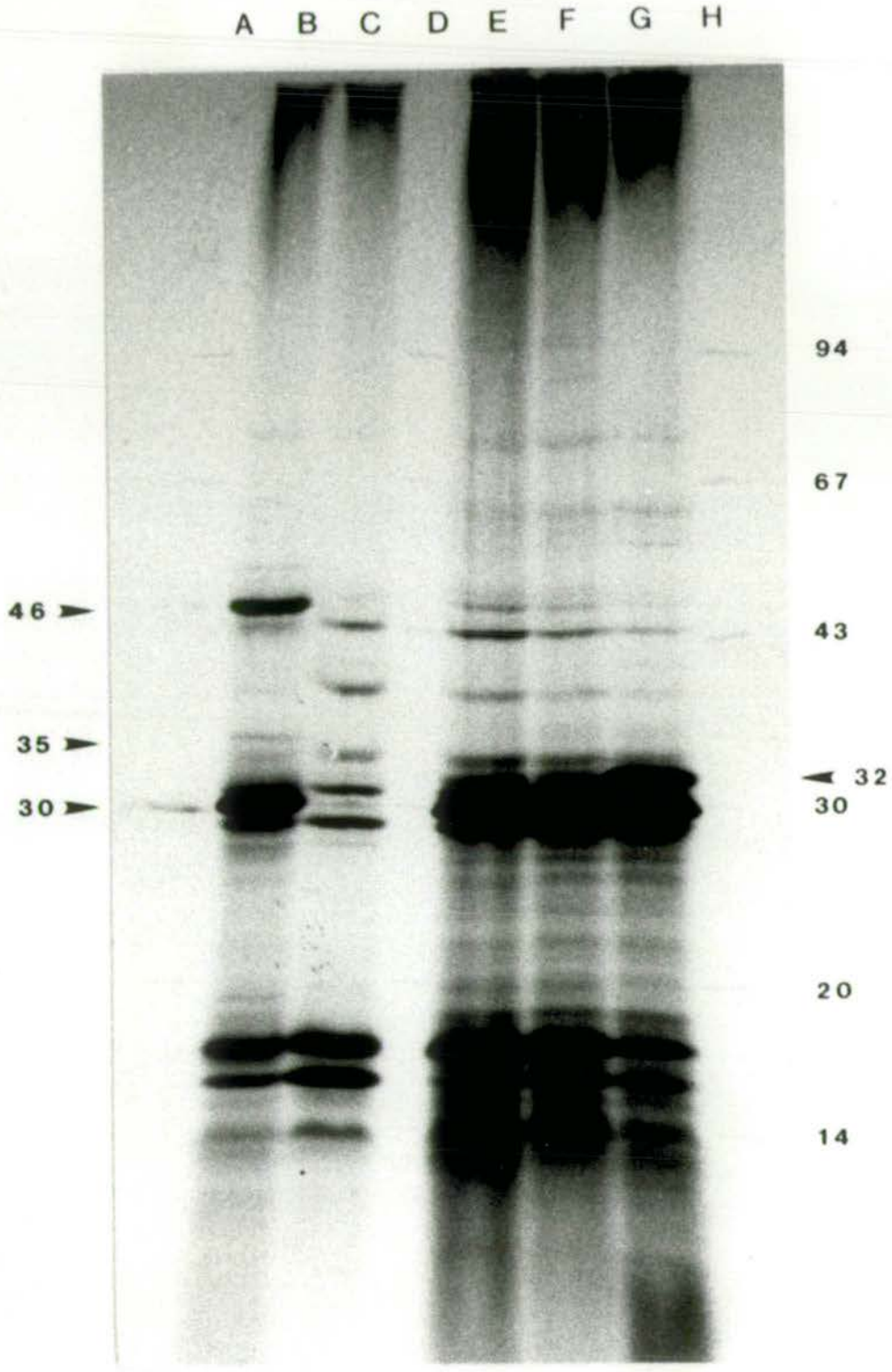

FIGURE 6.2

species is nearest in size to FtsA, reported as a 50,000 dalton polypeptide by Lutkenhaus and Wu (1980) and Lutkenhaus and Donachie (1979). Robinson et al. (1984), however, report that the calculated molecular weight of FtsA, based on sequence data, is 46,416. A KpnI deletion derivative of pNS23 (constructed by V. Derbyshire), destroying both ftsA and ftsQ complementation (see the comparable insert of pDK320 in Figure 5.3), does not express the 46,000 dalton protein, suggesting strongly that it does in fact correspond to FtsA. Again, the larger previous measurements may be attributable to anomalous migration or differences between SDS-PAGE systems.

The 35,000 dalton product expressed by pNS23 was also destroyed by the KpnI deletion mentioned above. This implies either that the protein is expressed by ftsQ, or that it is a degradation product of the 46,000 dalton ftsA product. Cloning the 2.3 kb rearranged BamHI fragment into pHUB2 should destroy ftsQ expression in the minicell expression system and thereby help to distinguish between the above possibilities. If the 35,000 dalton protein is the ftsQ product, then it must also be explained why it is expressed at such low levels in spite of the P_L fusion. Possibilities include some type of post-transcriptional regulation, unstable transcripts, or unstable protein. The fact that ftsQ appears to be expressed at low levels may explain why it was not detected in the transducing-phage-directed system of Lutkenhaus and Wu (1980).

Chapter 7 Effects of manipulating ftsQ and ftsA sequences

7.1 Effects of high levels of transcription across ftsA and ftsQ

An operon fusion which placed the rearranged 2.3 kb BamHI fragment under transcriptional control from P_{gal}, recombinant pDK110, was described in Section 5.5. Cells carrying pDK110 grew poorly, presumably due to a deleterious effect of increased transcription across ftsQ and ftsA sequences. The pDK110 insert is known to express ftsA in both orientations in pKO4 (see Figure 5.3) and subcloning the fragment into pHR9 using restriction sites that destroy ftsA prevents deleterious effects. One of these subcloning products, pDK114, is able to complement ftsQ even though the insert lacks the ftsQ 5'-terminus (see Figure 5.5). ftsQ expression in pDK114 is probably made possible by translation from the galE translational start sequences provided by the pHR9 vector (see Section 7.4). Even though complementation tests are not possible with pDK110 due to poor viability of host cells, we may reasonably assume that pDK110 also expresses ftsQ because this construction reproduces the galE-ftsQ domain of pDK114. Therefore, pDK110 lethality may not be simply due to high levels of ftsA expression. A simple experiment to test whether ftsA is deleterious in the absence of ftsQ would be to isolate a transposon-inactivated ftsQ in pDK302, and then to clone the altered insert into pHR9. Note that a straightforward transposon insertion into pDK110 would be undesirable, because pDK110 mutations appear to be strongly selected (see below).

Regardless of whether ftsA or an ftsQ-ftsA effect is responsible for pDK110-induced lethality, effects on the host cell are interesting. The initial pDK110 cloning and transformation into C600K$^-$(recA) produced small red

colonies among normal-sized white and red colonies. When the small red colonies were streaked out, the plates grew mostly small red colonies but also many normal-sized red colonies and rare white colonies. Their plasmid DNA was not analyzed, but all four galactokinase assays attempted on larger red colonies gave much lower levels of galK expression than pHR9. This suggests that promoter-down mutations were selected in pDK110. It was not possible to assay the small red colonies, which carried pDK110, because they would not grow in minimal media.

To demonstrate that pDK110 is unstable, C600K$^-$(recA) transformants were selected on NB-Ap at 30°C and streaked once on NB-Ap. A single colony was then innoculated into a non-selective broth medium at 30°C and 37°C. Every 24 hours, the culture was subcultured 1:10,000, and dilutions of the overnight culture were plated onto NB agar. 100 colonies were then patched onto NB and NB-Ap plates, and the percentage of Ap^S was scored. The curing curve is shown in Figure 7.1.

The reason for attempting pDK110 curing at both 30°C and 37°C is that C600K$^-$(recA) does not grow at 42°C, and pDK110 transformants appear healthier at 30°C than at 37°C (see below). Unfortunately, I failed to monitor optical density in this experiment, so that differences in curing at 30°C and 37°C with respect to generations of cells cannot be inferred from these data. The experiment does, however, demonstrate a very strong selection against pDK110 in nonselective media, while pDK40, carrying the same insert, and pDK302, carrying the intact 2.3 kb EcoRI fragment, do not appear to be selected against at all. The significance of these results will be discussed in Section 7.2.

C600K$^-$(recA)-pDK110 transformants grew as short-to-medium length filaments at 30°C. Division was grossly aberrant in these cells, demonstrated by the fact that filaments of many different sizes were produced as well as a small number of minicells (results not shown). Many of the

Figure 7.1

Curing of pDK110

The lower scale is in increments of days in nonselective media. Solid symbols show the percentage of ampicillin resistant colonies in C600K$^-$(recA) transformants of pDK40, pDK302, and pKO1 at both 30°C and 37°C. Open squares show the percentage of ampicillin resistant colonies in pDK110 transformants at 37°C, and open circles show the same cells at 30°C. Optical density was not followed, so that curing cannot be expressed in terms of generations of cells. However, cells growing at 37°C appeared much less healthy than cells growing at 30°C. See the text for further details.

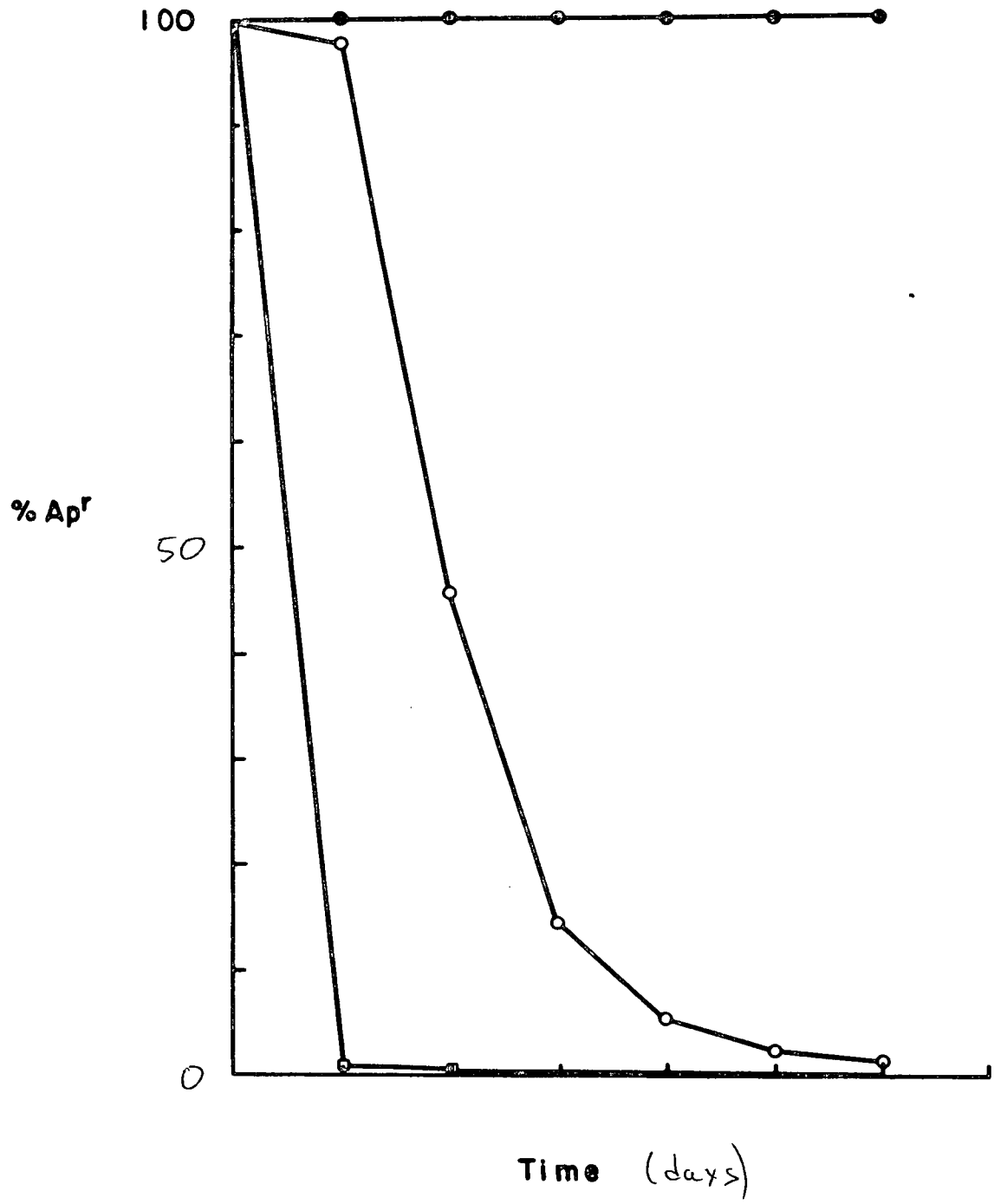

FIGURE 7.1

filaments displayed bulges at regular intervals along their length, presumably at sites of nascent septa. These bulges are reminiscent of penicillin bulges described by Spratt (1977), occurring as the result of both PBP3 and PBP2 inhibition. At 37°C these cells lysed rapidly, and occasionally, emerging spheroplasts were evident. While this evaluation of pDK110 effects is too hasty for serious speculation of their basis, it is striking that ftsA (or ftsA-ftsQ) overproduction causes morphological changes reminiscent of those produced by defects in class 2, class 7, and class 9 morphogenes. A more careful analysis of these effects may reveal important aspects of ftsA involvement in cell division.

7.2 Cloning ftsQ and its promoter in high copy number vectors

ftsQ has been cloned without its promoter, as an EcoRI fragment, into several different high copy number vectors. Likewise, its promoter has been successfully cloned into the same vectors. ftsQ has even been cloned in high copy number under transcriptional control from P_{gal}, which is approximately 5-10 times stronger than P_{ftsQ} (recombinant pDK114, see Figure 5.5). However, repeated attempts to clone the 3.2 kb HindIII fragment, bearing P_{ftsQ} and ftsQ in their natural association (see Figure 4.1), into a high copy vector have been unsuccessful.

At this point it is useful to consider ways of demonstrating that a recombinant construction is not stable. If the source of DNA used for the cloning yields more than one possible insertion fragment, then recovery of all possible recombinants except for one suggests that the construction which is missing is not stable. In the case of the λΔE-HindIII cloning, the 3.5 kb fragment carries envA and is thus itself unstable, hence there is no internal control for a successful cloning. Recovery of the arms of the lambda

vector as an insertion into the plasmid vector would again suggest that the other fragments were unstable, although I never attempted clonings under conditions that would favor recovery of the arms of lambda.

Another approach would be to clone the fragment into a low copy vector, such as pSC101, and then use this recombinant as the source for cloning into a high copy vector. Recovery of only pSC101 vector insertions into the high copy vector would indicate that the fragment was unstable. I refrained from using pSC101 because of the lack of a convenient selection for recombinants. However, Stoker et al. (1982) report several new,low copy vectors specifically designed for cloning deleterious cell surface and division genetic elements, and these vectors should allow cloning of the 3.2 kb HindIII fragment.

I did attempt a similar approach which involved cloning the fragment into pNS10, a variable copy number vector carrying both the ColE1 origin (oriV) and the pSC101 origin. This vector is maintained at high copy number in a polA(ts) strain at 30°C and at low copy number at 42°C (Sullivan and Donachie, 1984b). Unfortunately, I failed to produce a 3.2 kb HindIII fragment-pNS10 recombinant despite repeated efforts. Because pNS10 is maintained at approximately four copies at 42°C, it is unlikely that a 3.2 kb HindIII recombinant would be unstable due to extra copies of ftsQ. Therefore, I feel that failure to clone this insert into pNS10 probably represents complications of the cloning experiment rather than an unstable low copy construction.

Another approach which I attempted was the reconstruction of a P_{ftsQ}-ftsQ association by cloning the appropriate inserts together. pNS28 carries the 2.2 kb BamHI-EcoRI segment containing most of the coding sequence for ftsQ but lacking its 5'-terminus and promoter. Note that this insert is the same as for pDK40 (Figure 5.3), except that pNS28 lacks the 104 bp EcoRI-BamHI fragment to the right of the insert. The missing ftsQ sequences,

however, are carried by the 1.2 kb BamHI fragment of pDK20 (see Figure 4.5). Therefore, I attempted to clone the BamHI fragment into pNS28. Recovery of only fragments oriented such that ddl is expressed anti-parallel to ftsQ would indicate that the reverse orientation produced an unstable construction. I did, in fact, recover the insert in the opposite orientation (designated pDK81, see Appendix A.10 and Figure 7.2), but I recovered only one recombinant in over 70 clones screened. Time constraints prevented me from repeating this experiment.

In conclusion, I have not been able to demonstrate that the 3.2 kb HindIII fragment is unstable in a high copy vector, although I have generated some circumstantial evidence to this effect. There are also published results which suggest that ftsQ is not stable when cloned with its promoter in high copy. Nishimura et al. (1977) screened the Clarke and Carbon bank of random E. coli chromosome-ColE1 recombinants (Clarke and Carbon, 1976, 1977) in search of cell surface growth and cell division genetic markers. Several loci, including ftsA, were missing from this bank. Unfortunately, ftsQ was not sought because it was unknown at the time. 2000 clones were screened, with a theoretical 99% probability of locating a specific marker after screening 1440 clones. Since ftsA is known to be stable in various high copy constructions, the average insert size in this collection is 14 kb, and ftsQ and ftsA are very closely linked, the absence of ftsA could reflect a selection against the intact ftsQ locus.

7.3 Morphological effects of uncoupling ftsA expression from ftsQ

As noted earlier, pDK40 transformants grow as ovoids of various sizes. Because ftsA strains transformed with pDK40 formed normal-sized colonies at 42°C and did not grow

as filaments, the 2.3 kb BamHI fragment complements ftsA. ftsQ(ts)-pDK40 strains, however, formed typical filaments at 42°C. pNS28, an independently constructed recombinant (discussed in Section 7.1) carries the same sequences in the P_4-ftsQ-ftsA domains as pDK40. Likewise pNS28 complements ftsA but not ftsQ. Although an ftsA(ts)-pNS28 transformant was reported by Robinson et al. (1984) to grow and divide normally at the restrictive temperature, on closer examination I observed that pNS28 produces the same ovoid phenotype as pDK40.

One explanation for the ovoid morphology is that activity of FtsQ and FtsA might be coordinated such that increasing the gene dosage of ftsA relative to ftsQ produces an unbalanced FtsA activity. However, this possibility may be ruled out by the observation that pGH300, which also complements ftsA but not ftsQ, produces normal rod-shaped cells. The difference between pGH300 and pDK40 is that the latter has P_4 reading across the insert (see Figure 7.2). Therefore, we may postulate that the ovoid morphology results from unbalanced ftsA expression by the weak vector promoter. P_4 transcription in pDK302 would produce a transcript with complete ftsQ-ftsA coding and translational regulatory sequences (see Figure 7.2). In pDK40, however, the 5'-terminus of ftsQ is removed so that ftsQ translation would not be possible from P_4 transcripts. Therefore, activity of the ftsA ribosomal binding site could not be modified by ftsQ translation. pGH300 would produce a P_4 transcript that terminates in the insert, while P_{ftsA} would allow independent expression of ftsA in the opposite direction. Note that P_{ftsA} presumably would be responsive to morphogenetic regulatory signals; hence pGH300 transformants appear rod-shaped. P_4 would not be regulated in this manner, thus pDK40 transformants express ftsA out of harmony with morphogenetic requirements. Balance appears to be restored if ftsQ is associated with ftsA on the same transcript, as in pDK302. These results suggest that ftsQ

Figure 7.2

ftsA transcription and translation in pDK40 and similar constructions

For each construction, upstream vector sequences are represented schematically as a single line and inserted sequences are shown as rectangles. Only relevant restriction sites are indicated, and these correspond to the symbols explained in Figure 4.3. Transcripts are represented as originating at either P_4 or P_{ftsA} and continuing in the direction of the star. Translational starts are shown under *ftsQ* and *ftsA*. The *ftsQ* 5'-terminus is not present at the left BamHI site of pDK40 as indicated by x*ftsQ*. P_4 transcripts do not continue through the insert in pGH300, as indicated by ---x. pDK81 carries the *ddl* fragment oriented away from the downstream *ftsQ*-*ftsA* fragment, and therefore duplicates aspects of both pDK40 and pGH300 constructions. See text for details.

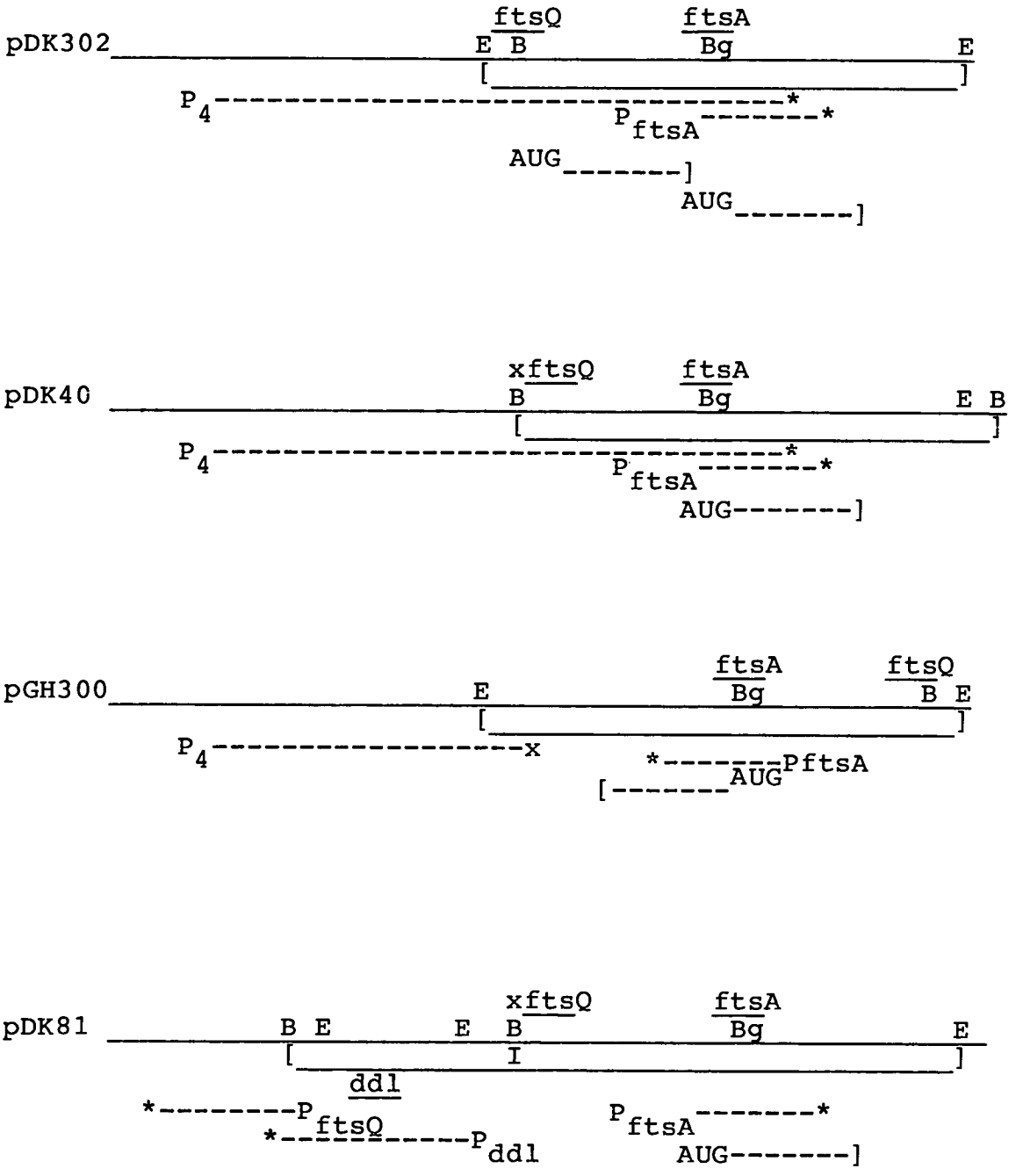
pDK302
ftsQ
ftsA
E B
Bg
E
P4
PftsA
AUG
AUG
pDK40
xftsQ
ftsA
B
Bg
E B
P4
PftsA
AUG
pGH300
ftsA
ftsQ
E
Bg
B E
P4
x
PftsA
AUG
pDK81
xftsQ
ftsA
B E
E B
Bg
E
I
ddl
PftsQ
PddlPftsA
AUG

Figure 7.2

and ftsA may normally be expressed, in at least some situations, from the ftsQ promoter, and that translation of the two may then be coupled (see Chapter 8).

Translational coupling has been demonstrated in several operons where coordinate expression of adjacent loci is important (cf. Schumperli et al., 1982; Baughman and Nomura, 1983). The mechanism is not known in detail, but apparently ribosomes terminating near the ribosomal binding site of an adjacent gene are well situated to re-initiate translation there. The role of translational coupling in expression of ftsQ and ftsA remains to be determined. I have shown that expression of ftsA in pDK40 strains does lead to aberrant morphology, similar to that seen with pbpA or rodA deficiencies and dacA overproduction. The pDK110 results discussed above also indicate that even co-expression of ftsQ and ftsA can disrupt morphogenesis if they are transcribed by the moderately strong P_{gal}. Note that ftsQ alone can apparently be transcribed at high levels with no ill effect (as in pDK114), although the low levels of FtsQ seen with the pHUB2 expression vector suggest the possibility that ftsQ is subjected to post-transcriptional regulation. The significance of ftsQ-ftsA coupling is considered further in Chapter 8.

7.4 The galE-ftsQ operon fusion

pDK315 and pDK114 carry the same 971 bp BamHI-BglII insert (see Figure 5.5), yet pDK114 complements ftsQ and pDK315 does not. Both constructions lack the ftsQ 5'-terminus, although pDK114 provides the galE 5'-terminus and ribosomal binding site approximately 420 bp upstream of the BamHI insertion site. Thus, pDK114 most likely complements ftsQ through synthesis of a GalE-FtsQ hybrid protein. As discussed in Chapter 5, the galE sequence provided by McKenney is at odds with the translational phase across the

BamHI site predicted by a functional galE-ftsQ fusion, although independent galE sequencing results suggest that McKenney's sequence contains some errors. Even so, we can assume that most of the sequence is correct and can therefore predict some of the properties of a putative GalE-FtsQ hybrid product. Such a fusion would yield a protein carrying approximately 140 N-terminal amino acids from GalE, 1 amino acid specified by the BamHI linker, and the C-terminal 249 amino acids from FtsQ (based on the proposed ftsQ sequence, Robinson et al., 1984). Only 27 N-terminal FtsQ amino acids would be deleted in this construction.

Because expression of the hybrid product is under P_{gal} control, it should be possible to demonstrate the predicted 43,000 dalton product at relatively high levels in minicells, and also to eliminate expression by placing a transposon within the galE coding sequence. Such an experiment should be able to demonstrate that the fusion protein is expressed and would then confirm the galE translational phase.

The fact that a GalE-FtsQ hybrid protein preserves FtsQ activity has certain implications for ftsQ function. FtsQ is probably not a membrane or periplasmic protein, because its N-terminus can be replaced by the N-terminus of GalE, a cytoplasmic protein, without effect. The N-terminal domain also must not be essential for FtsQ activity. There is no evidence that FtsQ functions in a structural or enzymatic complex. The simplest explanation for ftsQ complementation is that the product is an enzyme whose catalytic activity does not involve the N-terminal domain.

The possibility of constructing other ftsQ fusions offers encouragement for investigations into ftsQ expression and the biochemical activity of its product. A useful P_{gal}-galE-ftsQ-ftsA fusion would be readily constructed as follows: The 840 bp EcoRI fragment, carrying ddl coding sequence (see Figure 4.1), could be inserted into the single EcoRI site of pDK114 in the proper orientation. The ddl-

P_{gal}-galE-ftsQ fusion could then be crossed onto a λ16-25(ftsQ$^-$) derivative (see Figure 2.1; λ16-25 would require a transposon-inactivated ftsQ locus). The resulting construction would place ftsQ, and presumably ftsA, under P_{gal} expression. Controlled induction of P_{gal} could then be used to probe effects of overproduction of ftsQ and ftsA, division cycle requirements for their expression, and effects of uncoupled expression of each product alone. This sort of approach may elucidate some of the interesting phenotypes seen with ftsQ-ftsA manipulations. Other useful operon fusions are discussed in Chapter 8.

8.1 Summary of the molecular genetics of the 2-minute region and correlation with sequencing results

In Chapter 2, I set out my specific goals for investigating the molecular genetics in the murC-ddl-ftsQ-ftsA-ftsZ cluster. As I proceeded with my work, A.C. Robinson sequenced the 2.3 kb EcoRI fragment and part of the 1.2 kb BamHI fragment. Our results complement each other and have been included in a recent publication (Robinson et al., 1984) which is found in Appendix B. This paper contains only a portion of my results, and another paper correlating my molecular genetics results for the ddl region with A.C. Robinson's ddl sequence is in process. An overview of my conclusions and their relationship to the sequence data is presented in the following paragraphs.

Two aspects of the 2-minute region organization stand out in Figure 8.1: All genes are oriented clockwise, and there is little space between genes. First consider orientation. All genetic, operon fusion, and sequence results agree with the hypothesis that the loci between murG and envA are transcribed in a clockwise sense. There is conflicting genetic data for envA, but direct promoter fusions have confirmed that it too is transcribed in a clockwise fashion. Other regional loci not carried by λ16-2 have also been shown to be oriented in the same direction, including secA (Oliver and Beckwith, 1982) and ftsI (Nakamura et al., 1983). Thus, it seems probable that most if not all loci in the 2-minute morphogenetic cluster are transcribed in the same direction. This remarkable organization could reflect either a general mechanism for coordinating expression of these products or a series of divergent sequence duplications. Both of these possibilities are consistent with my results and the sequence data, and will be considered further below.

Figure 8.1

Organization of the murC-ddl-ftsQ-ftsA-ftsZ region

Figure 8.1 is simply an enlargement of the bottom of Figure 4.5, and has been placed in the figure pocket inside the rear cover so that it may be removed along with the sequence and kept at hand while reading the text. Note that this figure summarizes primarily genetic results, and as such does not distinguish the two groups of multiple putative promoters identified by the sequence for ftsA and ftsZ. Therefore, the ftsA promoter in this figure corresponds to two promoter sequences, P_1 also represents two putative promoter sequences, and hence ftsZ has a total of three putative promoters. It is for this reason that my genetic assignment of promoters does not correspond exactly to the conventions used for the sequence assignments of promoters by Robinson et al. (1984).

Neidhardt et al. (1983) report that E. coli chromosomal coding capacity is 70% utilized on average, assuming one polypeptide per sequence domain. Yet, Figure 8.1 shows that coding capacity in the 2-minute region must be closer to being 100% utilized. In fact, the sequence of ftsQ and ftsA domains (Robinson et al., 1984) as well as of ddl (A.C. Robinson, personal communication) shows that these domains utilize almost 100% of the regional coding capacity. Why there should be such constraints on space in the 2-minute region is not immediately obvious, but it may reflect the means by which expression of these loci is regulated. One mechanism that would require tight linkage of adjacent loci is translational coupling.

Even though a mechanism of coordinate expression accounts well for the organization of the 2-minute cluster, it is difficult to reconcile with the observation that each of these loci is capable of independent expression in most genetic manipulations attempted. Figure 8.1 reminds us that each locus carries an independent promoter; although polycistronic transcripts have not yet been demonstrated, the absence of strong terminators between murC and ftsZ implies that different subsets of 2-minute loci can be expressed from a series of discrete transcripts. Which transcripts are actually produced would depend on relative individual promoter activities. Perhaps different sets of genes need to be expressed coordinately at different stages of the division cycle, or possibly weak booster promoters within an operon allow fine tuning of expression of critical products. So far we have not observed a classical operon organization in the 2-minute cluster, although a detailed analysis of transcripts produced by this region should reveal much about how these genes are expressed.

Lutkenhaus and Wu (1980) present strong genetic evidence that ddl normally requires intact murC sequences for efficient expression. This may indicate a requirement for a promoter upstream of the murC 5'-terminus, or it may

reflect a mechanism of translational regulation involving murC sequences. I have demonstrated that ddl is expressed from its independent promoter in a high copy vector, but it is not known why this promoter is inadequate in single copy systems. Possible reasons include weak P_{ddl} activity which adds up in a multicopy system or titration of a repressor. The ddl 5'-terminal sequence has not been completed as of the time of this writing, although sequence confirmation of P_{ddl} should be available in the near future (A.C. Robinson, personal communication).

All genetic tests of ftsA expression reveal that this locus may be expressed from its own promoter, however P_{ftsA} activity could not be demonstrated in a high copy galK fusion system. Possible explanations include that ftsA is normally expressed at very low levels (only 400 molecules per cell, Lutkenhaus and Donachie, 1979), that P_{ftsA} requires a titratable activator, or that ftsA represses its own synthesis. The latter possibility would explain why a P_{ftsA}-P_{ftsQ}-lacZ fusion increases beta-galactosidase activity in an ftsA(am) background, and why this fusion appears to express the same number of transcripts per septum, assuming that FtsA is used up only in septation.

The 2.3 kb EcoRI segment sequence does reveal two possible promoter sequences upstream of ftsA (based on consensus sequences, Hawley and McClure, 1983), lying within ftsQ coding sequence (see Appendix B, page 551, and Table 2, page 552.). Characterization of their activity will probably require manipulations in a single-copy lacZ fusion vector such as λJFL100. At least one precedent for a promoter internal to an upstream gene is seen in the trp operon (Horowitz and Platt, 1982). Location of promoter sequences within adjacent coding sequence imposes severe constraints on the evolution of these promoters and indicates that the translational coupling between ftsQ and ftsA must be important for survival. The morphogenetic perturbations that I have found to occur when an uncoupled

ftsA locus is transcribed by a weak exogenous promoter suggests that expression of ftsQ and ftsA is normally coordinated. Coupling could be confirmed by transcriptional analysis and the single-copy P_{gal} fusion proposed in Section 7.4.

The ftsQ sequence has identified a possible promoter to the left of the ftsQ EcoRI site, as predicted by the genetic and fusion results (see Figure 8.1 and Appendix B). The emerging ddl sequence also reveals that the ddl stop codon and ftsQ initiation codon are separated by only one bp (A.C. Robinson, personal communication). Therefore, P_{ftsQ} lies within ddl coding sequence and these 2 loci are probably also translationally coupled. It is somewhat surprising that ddl and ftsQ should be coupled, as the former is specifically involved in muropeptide synthesis while the latter specifically affects septation. The only explanation that can be offered here is that balanced cell surface growth may require that ddl and ftsQ be expressed together over certain time periods or growth conditions, while ftsQ and ftsA must be coordinately expressed during other times or conditions. This behavior would be consistent with a model in which P_{ftsQ} and P_{ftsA} function only in certain situations, while a promoter upstream of ddl, including some or all of the mur loci, is active under a different set of conditions. The fact that no terminator activity was detected between murC and ftsQ is consistent with polycistronic transcription of ddl and ftsQ. Again, transcriptional analysis would confirm or disprove this model.

All of the promoter activity detected on the 2.3 kb EcoRI fragment lies on the right side of the fragment between the BglII and EcoRI sites and is split into two independent foci by the HindIII site. This organization is represented as the ftsZ P_2 and P_1 promoters in Figure 8.1. The 2.3 kb EcoRI sequence does in fact show a single promoter-like sequence (see Table 2, page 552 in Appendix B) approximately 200 bp to the left of the HindIII site,

consistent with the predictions of Jones and Holland (1984). Note that this promoter, designated P_{ftsZ2} in this thesis, is designated ftsZ p3 in Robinson et al. (1984). Because my nomenclature scheme is based primarily on genetic evidence and has only allowed for two ftsZ promoters, I will use the Robinson et al. designations for the remainder of this discussion. The sequence also reveals 2 promoter-like sequences on the 482 bp HindIII-EcoRI segment, corresponding to P_1 in Figure 8.1. All three of these putative promoters lie within ftsA coding sequence, although ftsA and ftsZ do not appear as closely linked as the two upstream loci. The 63 bp sequence separating ftsA and ftsZ carries an 8 bp inverted repeat predicted to form a stem-loop secondary structure immediately beyond the -10 sequence of ftsZ p1. Its function is not known, but it presumably reflects a mechanism for regulating ftsZ transcription by the three upstream promoters. These promoters have not been well studied in isolation from each other, and again, transcriptional analysis would be of benefit in further characterizing their function.

Other regions of dyad symmetry are seen to be associated with ftsZ p2 and ftsZ p3 as well as ftsA p2. Furthermore, the symmetrical elements near ftsA p2 and ftsZ p3 are remarkably similar, with 11 of 13 bp surrounding the centers of symmetry being identical. Again, these symmetrical elements could well represent regulatory sites for promoter activity. None of the possible stem-loop structures bear any relation to typical simple-terminator sites (Platt and Bear, 1984), however stem-loops formed in either the DNA template or the nascent RNA chain could conceivably impede RNA polymerase progression and thereby account for some of the 50-70% readthrough decreases measured for the ftsQ-ftsZ segment in my terminator assay system.

Direct measurements of the sizes of ddl, ftsQ and ftsA products confirmed the assignments made by Lutkenhaus and Wu. I have also identified the FtsQ protein as a 35,000

dalton product, although it is expressed with low efficiency from a P_L-fusion. The sequence predicts that *ftsQ* codes for a 31,434 dalton polypeptide, and differences between predicted and measured sizes may be due to anomalous migration of the protein on SDS-PAGE gels. Note that my measurement of FtsA as a 46,000 dalton protein closely matches the sequence prediction of 45,416 daltons, whereas previous measurements had reported FtsA as having a size of 50,000 daltons (Lutkenhaus and Donachie, 1979; Lutkenhaus and Wu, 1980). The measurement of 32,000 daltons for Ddl may be compared with the *ddl* sequence when it is completed.

8.2 Prospects for future studies

The need for transcriptional data was mentioned repeatedly in Section 8.1. Specific approaches include S1-mapping of transcriptional starts and analysis of the different classes of transcripts produced by the 2-minute loci. Because we still lack biochemical assays for most of the cell division genes, transcriptional analysis would give much useful information regarding the expression of these genes. Also, expression mutations can readily be constructed, isolated, and characterized using both the sequence data and the series of promoter-*galK* fusions that have been constructed.

Determining the regulatory mechanisms of cell division gene expression will probably require more subtle manipulations than have been used previously. Even though cells continue to grow and divide normally in spite of gross rearrangements of cell division genes, the fact that many of these loci appear coupled in expression suggests that their compensated patterns of gene expression may not reflect normal regulatory pathways of division gene expression. Therefore, single copy operon fusions will be most useful. Moreover, this technique would preferably place a *lacZ*

marker within the chromosomal locus to be studied in a manner that preserves the organization of adjacent loci.

Further use of the galE-ftsQ fusion in placing ftsQ and ftsA under P_{gal} control was outlined in Section 7.4. Another useful constructions would be to fuse the C-terminal ends of ftsQ and ftsA (or indeed, any locus to be investigated) to the N-terminus of lacZ (Silhavy et al., 1984). Such hybrid proteins generally retain beta-galactosidase function and often retain the activity of the gene product of interest. This approach could then be used to overcome the general absence of cell division factor assays, and would open the way for biochemical characterization of these gene products.

One construction in particular, described by Germino and Bastia (1984), allows rapid purification of many lacZ fusions. Their vector incorporates a collagen linker between the fusion site and lacZ. Genes inserted in the correct translational phase usually express beta-galactosidase activity, allowing the hybrid protein to be purified to near homogeneity over a beta-galactosidase affinity column. The beta-galactosidase domain may then be removed by treatment with collagenase and the protein of interest purified to homogeneity by HPLC. Isolating purified FtsQ and FtsA proteins would be a first step in identifying other components of the septation apparatus, again by affinity chromatography using a column bound with FtsQ or FtsA.

Elucidation of the mechanisms underlying E. coli cell division will ultimately require a concerted effort spanning the spectrum from biophysical analysis of the involved DNA sequences to biochemical characterization of their gene products and physiological integration into a functional system. A molecular genetics approach such as I have described in these pages is providing the ground work for a concerted investigation into cell division.

Appendix A

Recombinant constructions.

All recombinant constructions were planned and verified using Smith and Birnstiel restriction maps (see Figure 4.4) of the 1.2 kb BamHI and the 2.3 kb EcoRI fragments. The sequence of the 2.3 kb EcoRI fragment (Robinson et al., 1984) further confirmed relevant constructions.

A.1 Subcloning from λΔE into pBR325

λΔE contains several convenient restriction fragments (see Figure 4.1) for subcloning into a high-copy number plasmid vector such as pBR325 (see Figure 4.2).

λΔE DNA was digested to completion with EcoRI and ligated with EcoRI-digested pBR325. The ligation mix was transformed into C600K$^-$ and cells were plated on NB-Ap-Tc plates. Transformants were screened for sensitivity to Cm. $Ap^rTc^rCm^s$ recombinants were screened for EcoRI insertions by restriction analysis of miniprep DNA. Recombinants were recovered carrying the 540, 840, and 2300 bp EcoRI fragments (gels not shown), but the 2500 bp EcoRI fragment was not seen. Sullivan and Donachie (1984b) report that this fragment is unstable when cloned in multiple copies (although it can be cloned in lambda vectors, see Figure 2.2) and attribute the instability to a deleterious effect of high levels of envA expression. The 2300 bp EcoRI fragment was previously cloned into pBR325 by Graham Hatfull (pGH4, see Robinson et al., 1984), hence the identical recombinants recovered in this experiment were studied no further. The 540 bp and 840 bp EcoRI recombinants were designated pDK7 and pDK5 respectively (pDK5 shown in Figure A.1).

Figure A.1

Restriction analysis: pDK5, pDK10, pDK11

Lanes:

A: λcI857-EcoRI;	B: pDK5-EcoRI;	C: pBR325-EcoRI;
D: pDK10-EcoRI;	E: pDK11-EcoRI;	F: pDK10-PstI
G: pDK11-PstI;	H: pHR1800-EcoRI;	I: λcI857-HindIII

All band sizes are in units of kb. λcI857-HindIII size standards are marked on the right; arrows mark fragments yielded by recombinants. Lanes B and C show that pDK5 consists of the pBR325 vector and the 840 bp EcoRI insert. Lanes D and E show that pDK10 and pDK11 carry the same fragment as an insert into pKO1. Lanes F and G confirm the orientations of pDK10 and pDK11. Lane H is irrelevent to this analysis.

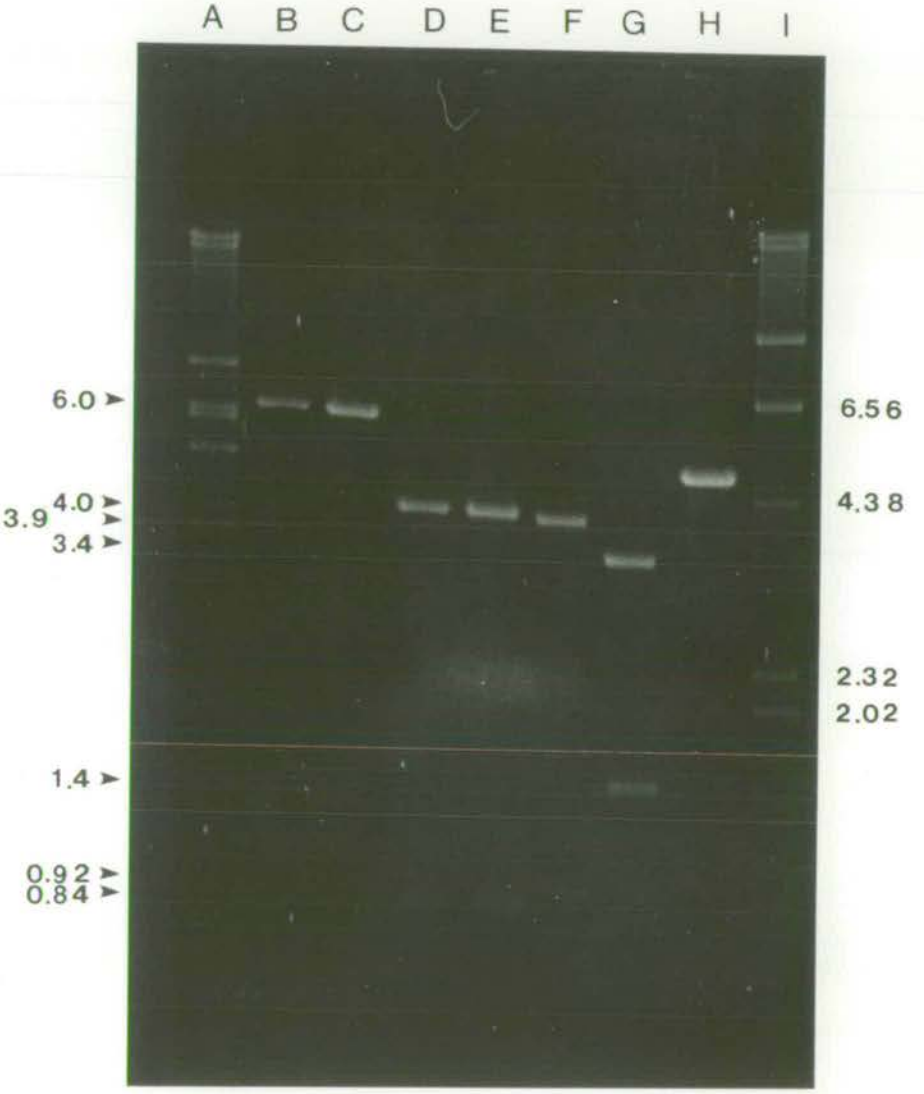

FIGURE A.1

$\lambda\Delta$E contains only 2 BamHI sites in the chromosomal insert, but several sites also lie in the phage vector. To simplify cloning, $\lambda\Delta$E DNA was digested to completion with HindIII, yielding 3200 bp and 3500 bp HindIII fragments (see Figure 4.1). These chromosomal fragments were separated from the high molecular weight vector arms by sucrose gradient centrifugation. The isolated HindIII fragments were then digested to completion with BamHI and ligated with BamHI-digested pBR325. The ligation mix was transformed into C600K$^-$ and cells were plated onto NB-Ap-Cm plates. Transformants were screened for sensitivity to Tc. $Ap^rCm^rTc^s$ recombinants were screened for BamHI insertions by restriction analysis of miniprep DNA. The 1180 bp BamHI fragment was recovered as a recombinant, designated pDK20 (see Figure A.7).

A HindIII subcloning of $\lambda\Delta$E was attempted numerous times (see Figure 4.1 and chapter 7), but no recombinants were recovered. The 3.5 kb HindIII fragment is not expected to be stable in high copy number because of the deleterious effects of envA (Sullivan and Donachie, 1984b). See chapter 7 for a discussion of why the 3.2 kb fragment also may not be stable in high copy number.

A.2 Subcloning from pBR325 constructions into pKO1 and pKO4

The vector pKO1 is illustrated in Figure 5.1. pDK5 DNA was digested to completion with EcoRI and ligated with EcoRI-digested pKO1. The ligation mix was transformed into C600K$^-$ and plated onto MacConkey-gal-Ap plates. Both red and white transformants were recovered, and these were screened for EcoRI insertions by restriction analysis of miniprep DNA (see Figure A.1). Recombinants of the 840 bp EcoRI fragment were recovered with both the red and white phenotypes (designated pDK10 and pDK11 respectively). The fragments were oriented with a PstI digest (see Figure A.1).

pDK10 was found to have the 840 bp EcoRI fragment oriented such that left to right in Figure 4.1 (and all Figures showing genetic organization of the 2-minute region) lies in the same direction as transcription of the galK gene in pKO1 (PstI yielding fragments consistent with the predicted sizes of 920 and 3900 bp). pDK11 was found to lie in the opposite orientation (PstI digest yielding fragments corresponding to the predicted sizes of 1420 and 3400 bp). The insert of pDK10 is shown in Figure 5.2.

The pDK7 insert was subcloned into pKO1 in a similar fashion to give pDK50 (red) and pDK51 (white). These recombinants were oriented with PstI-BamHI double digests. pDK50 was found to carry the 540 bp EcoRI fragment in the same orientation as galK, shown by a PstI-BamHI double digest yielding fragments closely corresponding to the predicted values of 1070 and 3450 bp (gel not shown). pDK51 was found to carry the insert in the opposite orientation (with PstI-BamHI double digestion yielding fragments corresponding to the predicted values of 960 and 3560 bp). The insert of pDK50 is shown in Figure 5.2.

pDK20 DNA was digested to completion with BamHI, the digest was electrophoresed on an agarose gel, and the 1.2 kb fragment band was cut out of the gel. The purified fragment was ligated with BamHI digested pKO4 (a derivative of pKO1 with a 10 bp BamHI linker in the SmaI site, see Figure 5.1). The ligation mix was transformed into C600K$^-$ and cells were plated onto MacConkey-gal-Ap plates. Both red and white transformants were recovered, and these were screened for BamHI insertions by restriction analysis (see Figure A.2). Recombinants were recovered with both red (pDK30) and white (pDK31) phenotypes. The inserts were oriented with an EcoRI digest (see Figure A.2). The insert in pDK30 was found to lie in the same direction as galK, shown by an EcoRI digest producing fragments closely corresponding to the predicted values of 520, 840, and 3790 bp. pDK31 was found to carry the insert in the opposite orientation (with

Figure A.2

Restriction analysis: λΔE, pDK10, pDK11, pDK30, pDK31, pDK32, pDK33, pDK34, and pDK35

Lanes: A: pDK10-EcoRI; B: pDK11-EcoRI C: λΔE-EcoRI
D: pDK30-EcoRI; E: pDK33-EcoRI F: pDK34-EcoRI
G: pDK35-EcoRI; H: λcI857-HindIII I: λΔE-BamHI
J: pDK30-BamHI; K: pDK31-BamHI L: pDK32-BamHI
M: λcI857-HindIII

All fragments are measured in units of kb. λcI857 size standards are given on the right. Arrows mark fragments yielded by recombinants. This gel ran slightly skew, but these relationships held for numerous other gels (not shown). Lane C shows the EcoRI digest of λΔE. Lanes A and B show that pDK10 and pDK11 carry the 840 bp EcoRI fragment inserted into pKO1. Lanes D, E, F, and G compare pDK30 and its EcoRI deletion derivatives (see text for discussion). The pDK30-EcoRI digest also confirms orientation of the insert. Lane I shows the BamHI digest of λΔE, and lanes J and K confirm that pDK30 and pDK31 carry the 1.2 kb BamHI insert. Lane L shows the mobility of the SalI-XhoI deletion derivative in relation to the intact 1.2 kb BamHI fragment.

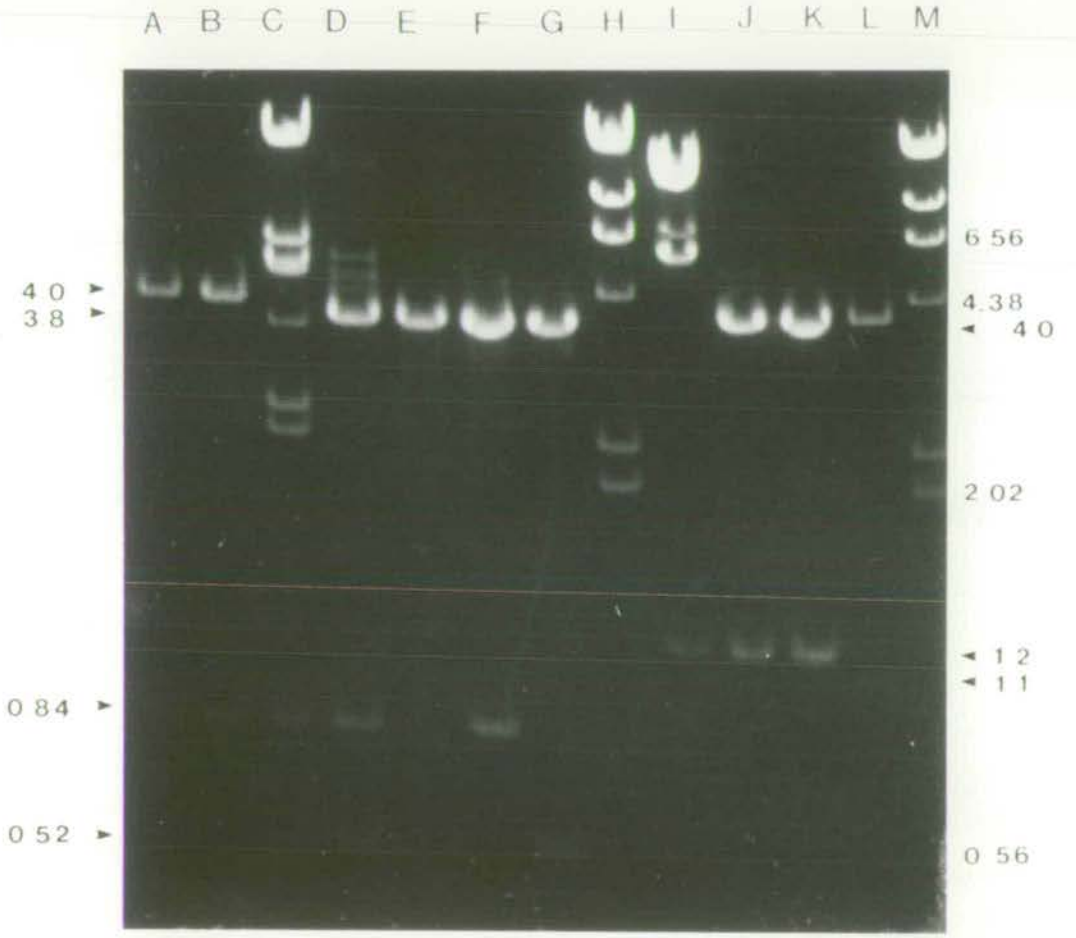

FIGURE A.2

a PstI digest producing fragments corresponding to the predicted values of 1850 and 3320 bp, gel not shown). The insert of pDK30 is shown in Figure 5.2.

A.3 Construction of deletion derivatives of pDK30

pDK30 carries several restriction sites that can be used to create deletions internal to, or at the ends of the 1180 bp BamHI insert. pDK32 represents a SalI-XhoI deletion (see Figure 4.5 for the physical map of these restriction sites). Religation of SalI and XhoI sticky ends forms a TaqI site and destroys the recognition sequences for both of the original enzymes. pDK32 DNA is not, in fact, cut by either SalI or XhoI, nor by PstI, which site lies on the deleted fragment (gel not shown). Figure A.2 shows that the BamHI insert of pDK32 is smaller by about 120 bp, as predicted.

pDK33 represents a deletion of both EcoRI fragments of pDK30. Note that the lambda O gene terminator (λt_o) has also been deleted from the pKO4 vector in this construction (see Figure 5.1). This construction gives only a single EcoRI fragment of 3780 bp, as predicted (see Figure A.2).

pDK34 and pDK35 represent deletions of only one of the two EcoRI fragments (with sizes of 520 and 840 bp). pDK30 DNA was partially digested with EcoRI and was then religated in dilute solution. The ligation mix was transformed into C600K$^-$ and plated onto MacConkey-gal-Ap plates. Predominantly red transformants were recovered, and EcoRI analysis showed them to contain either the 520 bp EcoRI fragment (pDK34) or the 840 bp EcoRI fragment (pDK35, see Figure A.2). All of the pDK30 deletion derivatives are represented in Figure 5.2.

A.4 Construction of pDK302

Figure A.3

Restriction analysis: pDK302 and pGH301

All fragment sizes are in kb

A:

Lanes: A: pGH301-HindIII B: λcI857-HindIII
C: pDK302-HindIII D: pDK302-undigested
E: pGH301-undigested

Lane A shows that the pGH301 construction carries 2 copies of the pKO1 vector in the same orientation, and Lane E shows the low mobility of the undigested plasmid. Lanes C and D show that pDK302 carries a single copy of the vector and insert, and confirms the orientation of the insert.

B:

Lanes: A: pDK302-EcoRI B: pDK302-HindIII
C: λcI857-HindIII

Lane A shows the 2.3 kb EcoRI insert and the pKO1 vector. Lane B confirms the orientation of the insert.

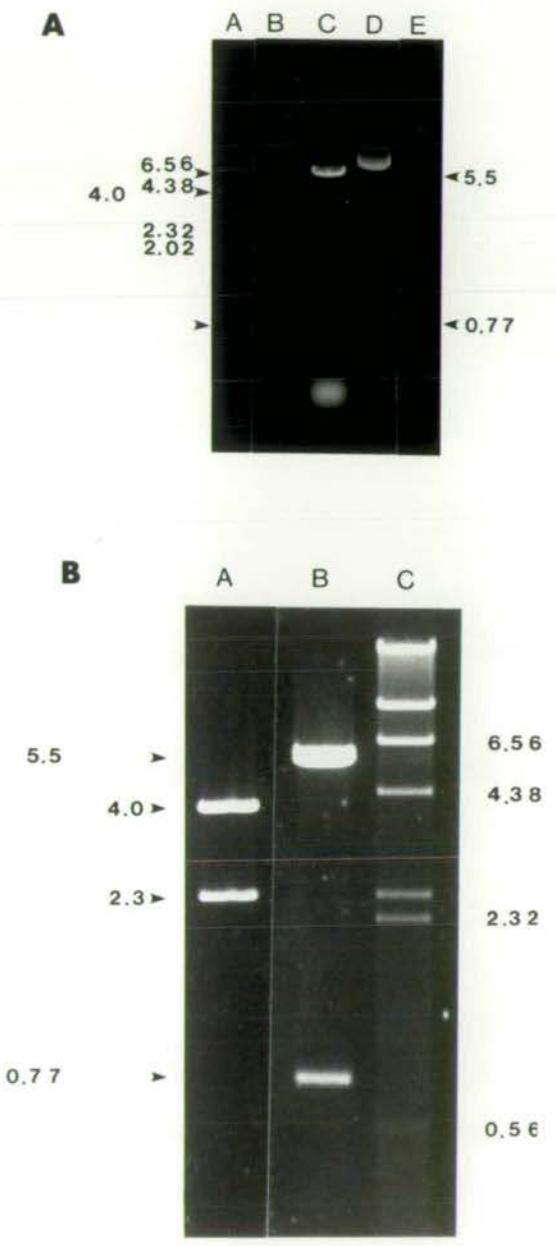
A
A B C D E
6.56
4.38
4.0
2.32
2.02
5.5
0.77
B
A B C
5.5
4.0
2.3
0.77
6.56
4.38
2.32
0.56

FIGURE A.3

Graham Hatfull subcloned the 2.3 kb EcoRI fragment from pGH4 (Robinson et al., 1984) into pKO1 (Graham Hatfull, PhD thesis), yielding pGH301 (with the insert in the same orientation as galK) and pGH300 (with the insert in the opposite orientation). However, pGH301 carries 2 copies of the pKO1 vector, lying in the same orientation (Graham Hatfull, PhD thesis). Because 2 vector copies could have unpredictable effects on copy number and galK expression, it was deemed necessary to reconstruct a single-copy version of pGH301. To this end, pGH301 DNA was digested to completion with EcoRI and then religated. The ligation mix was transformed into C600K$^-$ and plated onto MacConkey-gal-Ap plates. Both red and white transformants were recovered. Some of the red clones were screened for EcoRI insertions by restriction analysis of miniprep DNA. Samples of unrestricted DNA were also screened for unusually high molecular weight CCC, linear, and circular forms of the plasmids (see Figure A.3). A recombinant, pDK302, was chosen with the 2.3 kb insert oriented in the same direction as galK in a single copy pKO1 vector. Orientation was shown by a HindIII digest, yielding fragments closely corresponding to the predicted values of 5490 and 770 bp (see Figure A.3). The insert of pDK302 is represented in Figure 5.3.

A.5 Construction of deletion derivatives of pDK302

The 2.3 kb EcoRI fragment contains 2 KpnI sites, 2 PvuII sites, and 1 BamHI and BglII site. The pKO1 vector carries none of these sites, and deletions were easily constructed by digestion of pDK302 with the appropriate enzymes and religation in dilute solution. C600K$^-$ transformants all had the red phenotype, and recombinants were screened for deletions by restriction analysis.

The BamHI-BglII deletion derivative was designated pDK310. This plasmid was not cut by BamHI, BglII, or KpnI,

and generated an EcoRI fragment about 900 bp smaller than that of pDK302 (gels not shown), consistent with a deletion of the 971 bp BamHI-BglII fragment. The KpnI deletion derivative was designated pDK320. This plasmid was linearized by KpnI, but was missing the 620 bp KpnI fragment (gel not shown). An EcoRI digest confirmed that the EcoRI insert was smaller by about 600 bp in pDK320 (gel not shown). The PvuII deletion derivative was designated pDK335. This plasmid was linearized by PvuII, and was missing the 147 bp PvuII fragment. An EcoRI digest confirmed that the EcoRI insert was smaller by about 180 bp in pDK335 (gel not shown). The inserts of these constructions are shown in Figures 4.6 and 5.3.

The insert in pDK302 and the pKO1 vector each carry a HindIII site, allowing for deletion of a 770 bp HindIII fragment carrying the right terminus of the insert. pDK340 is the designated HindIII deletion derivative, and C600K$^-$ cells harboring this plasmid were red on MacConkey-gal-Ap plates. Both EcoRI and HindIII linearize pDK340 and give a single band having a mobility consistent with the predicted value of 5500 bp (gels not shown). The insert of pDK340 still carries a BamHI and a BglII site, allowing a further deletion of the 971 bp BamHI-BglII fragment. This recombinant was designated pDK345 and was found to be linearized by EcoRI and HindIII giving single bands consistent with a predicted size of 4520 bp (gels not shown). Both of the inserts of pDK340 and pDK345 are represented in Figures 4.5 and 5.3.

A.6 Cloning the 2.3 kb EcoRI fragment as a BamHI fragment

Several of the available vectors in the pKO system utilize BamHI sites. This, plus the ease of constructing further useful deletion derivatives of the 2.3 kb EcoRI fragment, made it desirable to construct a slightly altered

fragment with BamHI ends. To accomplish this, pDK302 DNA was digested to completion with EcoRI and the 2.3 kb fragment was isolated from an agarose gel. The purified fragment was circularized by ligation in dilute solution, then the ligation mix was digested to completion with BamHI. These manipulations had the effect of moving the 104 bp EcoRI-BamHI fragment from the left terminus of the fragment to the right terminus, generating BamHI ends (see Figures 4.5 and 5.3 for representations of these alterations). The rearranged fragment was then ligated with BamHI digested pKO4. The ligation mix was transformed into C600K$^-$ and cells were plated onto MacConkey-gal-Ap plates. Both red and white colonies were recovered. Recombinant plasmids were screened for BamHI insertions by restriction analysis of miniprep DNA. A plasmid designated pDK40 (red) was found to carry the 2.3 kb BamHI insert oriented in the same direction as galK. Orientation was shown by a HindIII digest, giving fragments closely corresponding to the predicted values of 4550 and 1720 bp (see Figure A.4). An EcoRI digest (see Figure A.4) further confirmed that the insert in pDK40 is as shown in Figure 5.3. Another plasmid designated pDK41 (white) was found to carry the 2.3 kb BamHI insert in the opposite orientation. Orientation was shown by an EcoRI digest giving fragments consistent with the predicted values of 5860 and 420 bp (gel not shown).

A.7 Construction of deletion derivatives of pDK40

The insert in pDK40 carries 2 KpnI sites and 2 PvuII sites, allowing deletion of a 620 bp KpnI fragment and a 147 bp PvuII fragment in a fashion similar to those deletions made in pDK302. The KpnI deletion derivative, designated pDK42, gave a single KpnI fragment of approximately 5660 bp, as predicted, and in comparison to a pDK40 KpnI digest, pDK42 showed no 620 bp KpnI band (gel not shown). BamHI

Figure A.4

Restriction analysis: pDK40

All fragment sizes are in kb. λcI857-HindIII size standards are shown on the right. Arrows mark recombinant fragments.

Lanes: A: pDK40-BamHI; B: pDK40-EcoRI
C: pDK40-HindIII E: λcI857-HindIII
Lane A shows that pDK40 carries the rearranged 2.3 kb BamHI fragment in a pKO4 vector, and lanes B and C confirm orientation of the insert.

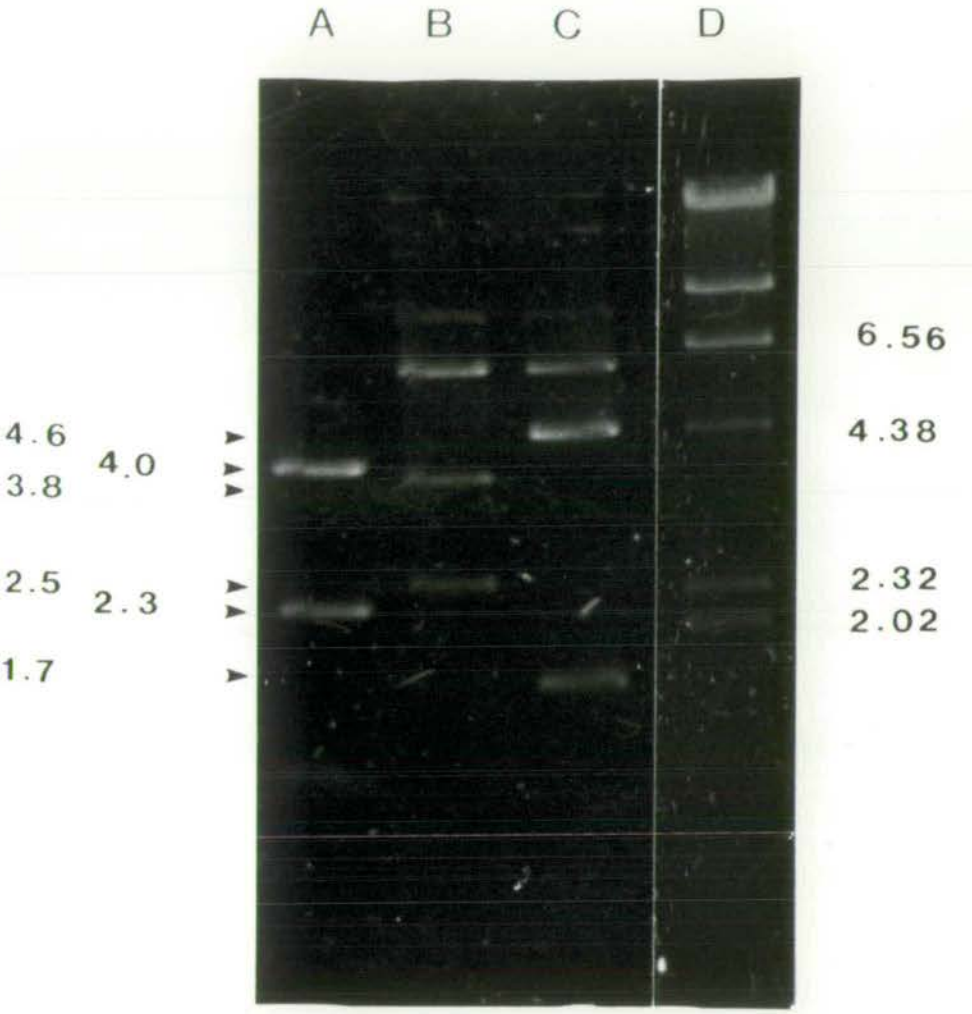

FIGURE A.4

digestion of pDK42 gave fragments closely corresponding to the predicted sizes of 3990 and 1665 bp, confirming that the 2.3 kb BamHI insert of pDK40 had lost a 620 bp KpnI fragment in pDK42 (gels not shown, see Figure 5.3). Finally, pDK42 gave exactly the same BamHI restriction pattern as an EcoRI digest of pDK320, as expected (gel not shown).

The PvuII deletion derivative, designated pDK43, was linearized by PvuII. A BamHI digest gave fragments closely corresponding to the predicted sizes of 3990 and 2140 bp, consistent with a deletion of the 147 bp PvuII fragment (gels not shown, see Figure 5.3).

Whereas the EcoRI inserts in pKO1 are upstream of the HindIII site, pKO4 BamHI inserts are downstream of that site. Therefore a HindIII deletion derivative of pDK40 will preserve that portion of the insert (the 482 bp HindIII-EcoRI segment) that was deleted in the pDK302 HindIII derivative, pDK340 (see Figure 5.3). The HindIII deletion derivative of pDK40, designated pDK44, was linearized both by HindIII and BamHI, giving fragments consistent with the predicted size of 4550 bp. The pDK44 digest was also missing the 1724 bp HindIII fragment, as predicted (gels not shown).

The BglII site internal to the BamHI insert in pDK40 allows construction of 2 further deletion derivatives, removing each end of the insert. pDK40 DNA was partially digested with BamHI. Further digestion was carried to completion with BglII. These DNA fragments were religated in dilute solution, the ligation mix was transformed into C600K$^-$, and cells were plated onto MacConkey-gal-Ap plates. Both red and white colony phenotypes were recovered. Recombinants were screened for deletions with EcoRI restriction analysis of miniprep DNA. One recombinant, pDK45 (red), gave a restriction pattern consistent with deletion of the 971 bp BamHI-BglII fragment (see Figure 5.3). pDK45 was linearized by BamHI, giving a single fragment closely corresponding to the predicted size of 5300

bp; it was cut by EcoRI to give 2 fragments closely corresponding to the predicted sizes of 3780 and 1520 bp. Another recombinant, pDK315 (white), gave a restriction pattern consistent with deletion of the 1314 bp BglII-BamHI fragment. pDK315 was linearized by EcoRI, HindIII, BamHI, and PvuII, all giving single fragments closely corresponding to the predicted value of 4960 bp. In addition, a KpnI-PvuII double digest yielded a fragment of 890 bp, confirming the orientation of the BamHI-BglII fragment (gels not shown). These constructions are illustrated in Figure 5.3.

A.8 Cloning the 2.3 kb BamHI fragment into pHR9

The 2.3 kb BamHI fragment, prepared as described in section A.6, was ligated with BamHI digested pHR9 (see Figure 5.4). The ligation mix was transformed into C600K$^-$ and cells were plated onto MacConkey-gal-Ap plates. Both red and white transformants were recovered. Recombinants were screened for BamHI insertions by restriction analysis of miniprep DNA. The only recombinants recovered from this ligation were in the opposite orientation to galK, designated pDK111 (white). An EcoRI digest of pDK111 gave fragments closely corresponding to the values predicted for this orientation, 5860 and 1220 bp (gel not shown; construction illustrated in Figure 5.5).

pDK111 DNA was digested with BamHI and then religated in an effort to clone the insert in the same orientation as galK. The ligation mix was transformed into C600K$^-$ and cells were plated onto MacConkey-gal-Ap plates. Both red and white transformants were recovered, but the red colonies showed 2 types of morphology: one type was typical of C600K$^-$(pHR9) at 37°C, the other type produced exceptionally small colonies. It was this second morphological class that carried a recombinant with the 2.3 kb BamHI insert in

Figure A.5

Restriction analysis: pDK110

All fragment sizes are in kb. λcI857-HindIII size standards are shown on the right. Arrows indicate recombinant fragments.

Lanes: A: pDK110-BamHI B: pDK110-EcoRI
C: pDK110-HindIII E: λcI857-HindIII

Lane A shows that pDK110 carries the rearranged 2.3 kb BamHI fragment in a pHR9 vector, and lanes B and C confirm orientation.

Figure A.6

Restriction analysis: pDK112, pDK45, and pDK114

Lanes: A: pDK114-EcoRI B: pDK114-HindIII
C: λcI857-HindIII D: pDK45-EcoRI
E: pDK45-BamHI F: pDK112-EcoRI
G: pDK112-BamHI

Lanes A and B show that pDK114 carries a single EcoRI and BamHI site. Lanes F and G show that pDK112 carries a single BamHI site, and is oriented as shown in Figure 5.3.

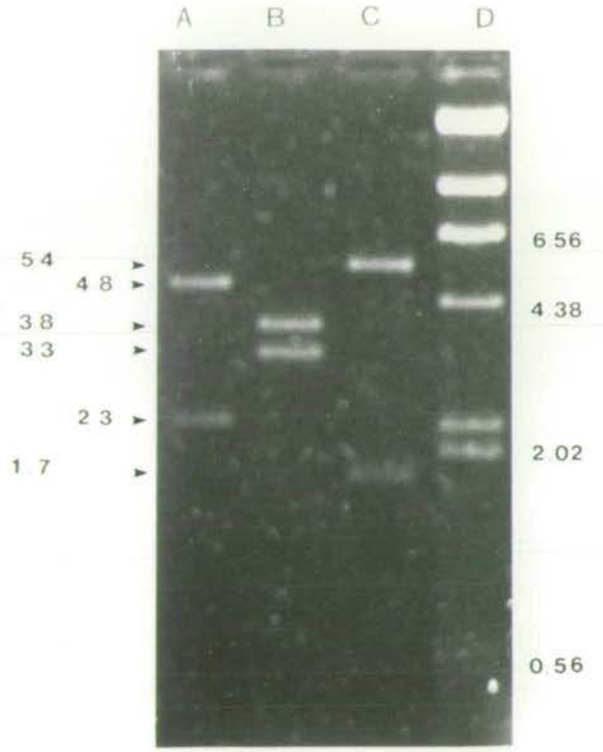

FIGURE A.5

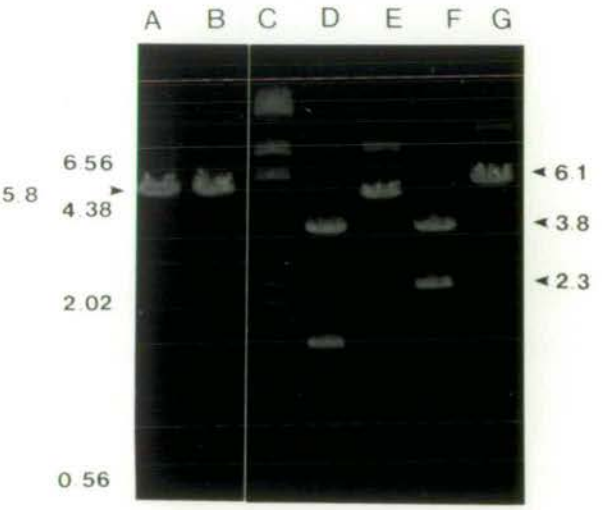

FIGURE A.6

the same orientation as galK, downstream from P_{gal}. This construction was designated pDK110. A full plasmid prep was prepared for restriction analysis, with difficulty because cells harboring pDK110 grew poorly. Figure A.5 shows a restriction analysis of pDK110. A BamHI digest confirms that the 2.3 kb BamHI fragment is cloned into the 4795 bp vector. An EcoRI digest gives fragments closely corresponding to the predicted values of 3780 and 3300 bp. A HindIII digest also confirms this orientation with fragments of 5360 and 1720 bp as predicted.

Unfortunately, pDK110 was useless for its original purpose, which was to assay terminators, because of its deleterious effects on the cells that carry it. Chapter 7 discusses this deleterious effect in more detail, but for the present task of subcloning the 2.3 kb fragment for terminator assays, it was deemed likely that overproduction of ftsA was responsible for this effect. Thus, subcloning the 2.3 kb BamHI fragment as BamHI-BglII fragments would destroy ftsA expression (see Figure 5.3, clones pDK45 and pDK315) and should allow readthrough from P_{gal} without harmful effect to the cell. BamHI-BglII deletions from pDK110 were not felt to be desirable because of the strong selection for mutations in pDK110. Accordingly, the cloning was done using a 2.3 kb BamHI fragment purified from pDK41 (using the method described in section A.2). The purified BamHI fragment was digested to completion with BglII and ligated with BamHI digested pHR9. The ligation mix was transformed into $C600K^-$ and cells were plated onto MacConkey-gal-Ap plates. Both red and white transformants were recovered. The white transformants were screened by restriction analysis for insertions. Both the 971 BamHI-BglII recombinant (designated pDK115) and the 1314 bp BglII-BamHI recombinant (designated pDK113) were recovered and found to carry their inserts in the opposite orientation to galK. pDK113 gave a BamHI digest corresponding to the predicted single fragment size of 6110 bp. A HindIII digest gave

fragments closely corresponding to the predicted sizes of 610 and 5500 bp and a BamHI-PstI double digest of 1870 and 4240 bp. Both digests confirm the orientation of pDK113. pDK115 gave an EcoRI digest corresponding to the predicted single fragment size of 5780 bp. Orientation was confirmed with an EcoRI-BamHI double digest, giving fragments consistent with the predicted sizes of 2090 and 3680 bp.

None of the white colonies screened revealed the BamHI-BglII fragments cloned in the same orientation as galK. Colony hybridization was employed to simplify screening the numerous red colonies for these recombinants. 250 Ap^r colonies were patched out onto LB plates and nitrocellulose filters were prepared according to the method described in chapter 3. The purified 2.3 kb BamHI fragment was used as a probe. Several colonies bound the radioactive probe, and these were screened for insertions by EcoRI restriction analysis of miniprep DNA. Both the 971 bp BamHI-BglII and the 1314 bp BglII-BamHI fragments were recovered in the same orientation as galK (designated pDK114 and pDK112, respectively, see Figure 5.5). Figure A.6 shows restriction analysis of these clones. A BamHI digest of pDK112 gave a single fragment corresponding to the predicted value of 6110 bp, and an EcoRI digest gave fragments consistent with the predicted values of 2330 and 3780 bp, thereby confirming the orientation. Both EcoRI and BamHI digests of pDK114 gave the predicted single fragment size of 5780 bp. These constructions are illustrated in Figure 5.5.

A.9 Cloning the 1.2 kb BamHI fragment into pHR9

The 1.18 kb BamHI fragment was isolated as described in section A.2. The purified fragment was ligated with BamHI-digested pHR9, the ligation mix was transformed into $C600K^-$ and cells were plated onto MacConkey-gal-Ap plates. Both red and white transformants were recovered.

Figure A.7

Restriction analysis: pHR9, pDK100, pDK101, pDK20, pDK30, pDK31

Band sizes are in kb. λcI857 size standards are shown on the right. Arrows indicate recombinant phenotypes.

A:

Lanes: A: pHR9-BamHI B: pDK100-BamHI C: pDK101-BamHI
D: pDK20-BamHI E: pDK30-BamHI F: pDK31-BamHI
G: pKO4-BamHI H: λcI857-HindIII

Lanes B and C show that pDK100 and pDK101 both carry the 1.2 kb BamHI fragment in the pHR9 vector. The other lanes show relationships between different vectors carrying the 1.2 kb BamHI insert. Partial digests are evident in lanes B, C, D, and F.

B:

Lanes: A: pDK100-PstI B: pDK101-PstI C: λcI857-HindIII

Lanes A and B show that pDK100 and pDK101 both carry the 1.2 kb BamHI fragment in the orientations shown in Figure 5.5. Partial digests are evident in lanes A and B.

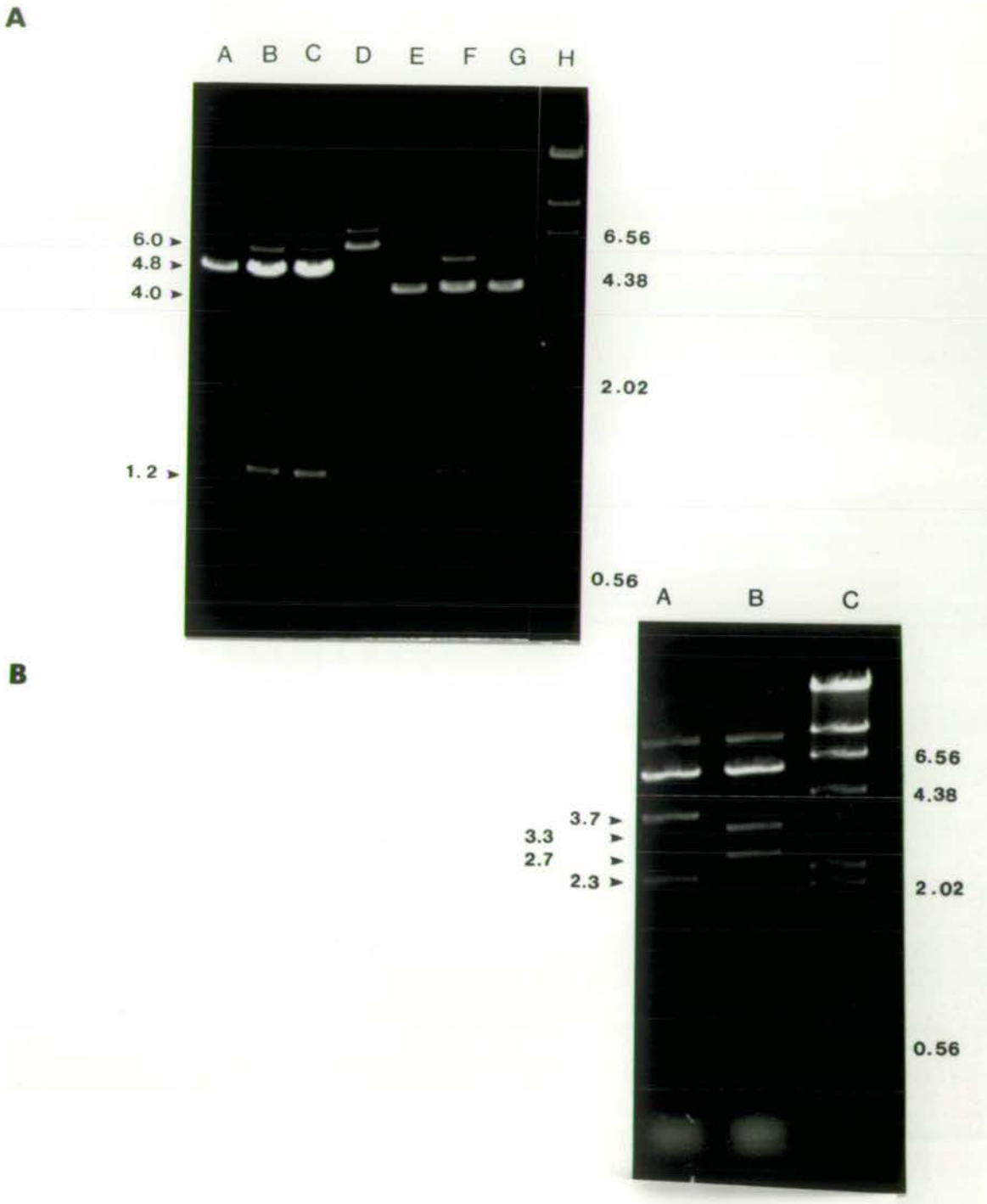
A
A B C D E F G H
6.0
4.8
4.0
1.2
6.56
4.38
2.02
0.56
B
A B C
3.7
3.3
2.7
2.3
6.56
4.38
2.02
0.56

FIGURE A.7

Recombinants were screened for BamHI insertions by restriction analysis of miniprep DNA. A red colony was found to carry a recombinant with the insert in the same orientation as galK, designated pDK100, and a white colony carried a recombinant with the insert in the opposite orientation, designated pDK101. Figure A.7 shows the restriction analysis results for pDK100 and pDK101. BamHI digestion of both recombinants yields the 4790 bp vector and the 1180 bp inserts, and the insert is seen to be the same size as that of pDK20, from which it was derived. PstI digestion of pDK100 yields fragments closely corresponding to the predicted sizes of 3720 and 2260 bp, while PstI digestion of pDK101 yields fragments consistent with the predicted sizes of 2670 and 3310 bp. Other restriction analysis of pDK100, including HindIII and EcoRI-HindIII double digestion, further confirmed the orientation of this insert (results not shown). These constructions are illustrated in Figure 5.5.

A.10 Cloning into pHUB2

pHUB2 (see Figure 6.1) is an expression vector that employs P_L for transcription of downstream inserts. It has convenient EcoRI and BamHI restriction sites for cloning the 2.3 kb EcoRI and the 1.18 kb BamHI fragments. See chapter 6 for the uses of these constructions.

The 1.18 kb BamHI fragment was isolated as described in section A.2. The purified fragment was ligated with BamHI digested pHUB2, the ligation mix was transformed into a C600K$^-$ λwt lysogen, and cells were plated onto NB-Kn plates. Transformants were screened for insertional inactivation of the Tc^r gene by patching onto NB-Kn-Tc plates. Kn^{r}Tc^s transformants were screened by restriction analysis of miniprep DNA. Figure A.8 shows the results of BamHI and PstI digestion of 2 of the recombinants that were

Figure A.8

Restriction analysis: pHUB2, pDK60, pDK20, pDK61, and pDK50

All fragment sizes are in kb. λcI857 size standards are shown on the right. Arrows indicate recombinant fragments.

Lanes: A: pHUB2-BamHI B: pDK60-BamHI C: pDK20-BamHI
D: pDK61-BamHI E: pHUB2-PstI F: pDK60-PstI
G: pDK61-PstI H: pDK50-BamHI-HindIII
I: λcI857-HindIII

Lanes B and D show that pDK60 and pDK61 both carry the 1.2 kb BamHI fragment, and lanes F and G confirm their orientation as described in Chapter 6.

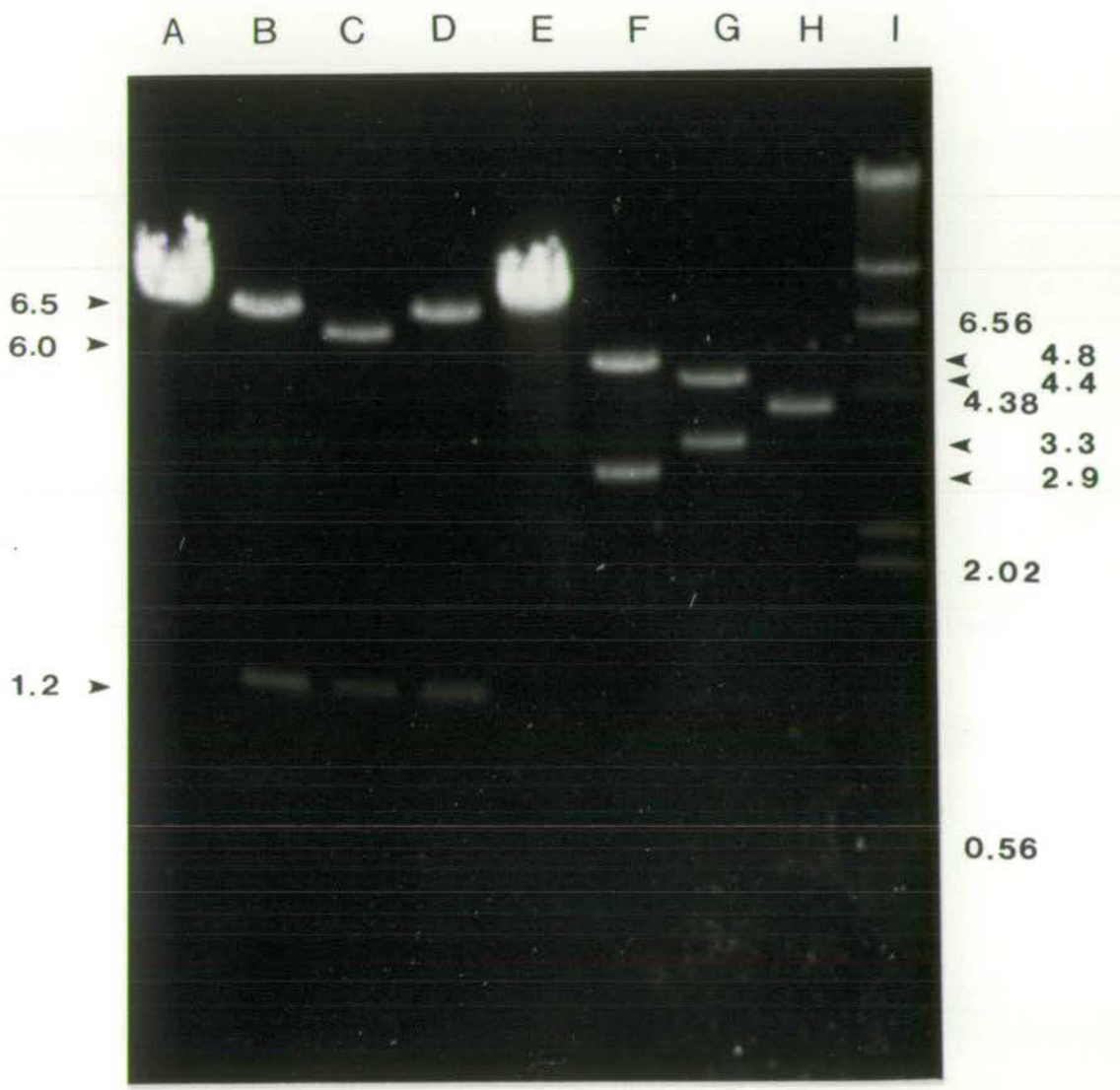

FIGURE A.8

recovered. The recombinant carrying the 1.18 kb BamHI fragment in the same orientation as transcription from P_L was designated pDK60 and the recombinant with the insert in the opposite orientation was named pDK61. Both recombinants yield the 6.5 kb vector and the 1.2 kb insert on BamHI digestion, and this insert has the same mobility as that of pDK20, from which it was derived. PstI digestion of pDK60 yields fragments closely corresponding in size to the predicted values of 2910 and 4770 bp. PstI digestion of pDK61 yields fragments consistent with the predicted values of 3320 and 4360 bp. In addition, a SalI digestion of pDK60 further confirmed the orientation of the insert (results not shown).

The 2.3 kb EcoRI fragment was cloned into pHUB2 in a similar fashion except that there was no selection for insertions as there was with the BamHI cloning. Recombinants were screened for insertion by restriction analysis of miniprep DNA, but, despite repeated attempts, only a few clones with 2.3 kb EcoRI insertions were obtained, and each of these fragments had the insert oriented in the same direction as P_L (designated pDK70, results not shown). This construction duplicated that of pNS23 by Neil Sullivan in our lab (Neil Sullivan, PhD thesis), and his clone was used in the gene product experiment described in chapter 6. Vicky Derbyshire (personal communication) constructed a KpnI deletion on the 2.3 kb EcoRI insert of pNS23 to show that expression of the 2 unique gene products by pNS23 was destroyed by an internal deletion from the insert (see chapter 6).

A.11 Cloning the 1.2 kb BamHI fragment upstream of the 2.2 kb BamHI-EcoRI insert in pNS28

Neil Sullivan constructed pNS28, a pKO6 recombinant carrying the 2.2 kb BamHI-EcoRI fragment (Robinson et al.,

1984). pNS28 has a single BamHI site near the N-terminus of ftsQ, and does not complement ftsQ. In an effort to clone into a high copy vector a fragment carrying both ftsQ and its promoter (see chapter 7 for a discussion of why this may be difficult), the 1.18 kb BamHI fragment was inserted into the BamHI site of pNS28. This was done by ligating BamHI digested pNS28 and pDK20 DNA, transforming the ligation mix into C600K$^-$, and plating the cells onto MacConkey-gal-Ap plates. Some red and many white colonies were recovered. Red colonies were patched onto NB-Ap-Cm plates to screen against ligation with the pBR325 vector of pDK20. About half of the recombinants were Ap^rCm^s, and these were screened for BamHI insertion by restriction analysis of miniprep DNA. Out of 78 Ap^rCm^s recombinants screened, only 1 was found to carry the 1.18 kb BamHI insert. This recombinant was designated pDK81, and found to carry the insert in the opposite orientation from galK (and thus from ftsQ and ftsA). Orientation was confirmed by PstI and PstI-HindIII double digests, both which gave fragments consistent with the predicted values (results not shown). See chapter 7 for further information about this construction.

JOURNAL OF BACTERIOLOGY, Nov. 1984, p. 546–555
0021-9193/84/110546-10$02.00/0

DNA Sequence and Transcriptional Organization of Essential Cell Division Genes *ftsQ* and *ftsA* of *Escherichia coli*: Evidence for Overlapping Transcriptional Units

ARTHUR C. ROBINSON,* DANIEL J. KENAN,† GRAHAM F. HATFULL,‡ NEIL F. SULLIVAN,§ RENATE SPIEGELBERG, AND WILLIAM D. DONACHIE

Department of Molecular Biology, University of Edinburgh, Edinburgh EH9 3JR, Scotland

Received 26 April 1984/Accepted 3 August 1984

The DNA sequence of a cloned segment of the *Escherichia coli* chromosome containing *ftsQ*, *ftsA*, and part of the *ftsZ* gene was determined and interpreted for genetic complementation and promoter fusion data for the region. The contiguous genes *ftsQ*, *ftsA*, and *ftsZ* were transcribed in the same direction (clockwise on the genetic map) and each had at least one associated promoter which allowed it to be transcribed independently of neighboring genes. *ftsA* and *ftsZ* possessed promoters within the coding sequences of the juxtaposed upstream structural genes, and a promoter element for *ftsA* was surrounded by a region of twofold symmetry which corresponded closely to a symmetrical element in the region of a putative *ftsZ* promoter. The structural gene of *ftsQ* consisted of 838 nucleotides, encoding a 276-residue amino acid polypeptide of molecular weight 31,400; the structural gene of *ftsA* consisted of 1,260 nucleotides, encoding a 420-residue amino acid polypeptide of molecular weight 45,400. The observation that the termination codon of *ftsQ* overlaps with a potential initiation codon for *ftsA* suggested that these two genes may be translationally coupled when transcription is initiated upstream of the *ftsQ* coding sequence.

Little is known about the molecular events which constitute or control cell division in *Escherichia coli*. A genetic analysis of division mutants has resulted in the identification of genes specifically involved in the division process, and these studies have been aided, in recent years, by the introduction of in vitro recombination methodologies and the ability to transform cells with novel genetic constructions.

Many genes that are involved in the morphogenesis and function of the *E. coli* cell envelope (13) are located in two clusters: one at 2 minutes and one at 14 minutes on the genetic map (1). The arrangement of genes in the 2-minute region is as follows: (*mraA mraB*) *pbpB murE murF murG murC ddl ftsQ ftsA ftsZ envA secA azi*. A number of temperature-sensitive, filament-forming mutants (designated *fts*) have been isolated, and the mutations in many instances were found to map within this cluster (K. J. Begg, unpublished data). Such *fts* cells continue to grow but are unable to divide at the restrictive temperature. The essential cell division genes which are considered in this communication are *ftsQ*, *ftsA*, and *ftsZ* (4, 25). Temperature-sensitive mutants of *ftsQ*, *ftsA*, and *ftsZ* form multinucleated filaments at restrictive temperatures, but there are differences in their phenotypes. Mutations in *ftsA* result in filaments with indentations along their length (presumably partially completed septa), whereas mutations in *ftsQ* and *ftsZ* result in the formation of filamentous cells with no such constrictions.

Earlier work in this laboratory identified the product of the *ftsA* gene as a protein with a molecular weight of 50,000 as measured by sodium dodecyl sulfate-polyacrylamide gel electrophoresis (24). It was demonstrated that if cell division is to occur, synthesis of the *ftsA* protein is required durin the 10- to 15-min period before the cells divide (12). It is nc known whether the synthesis of *ftsA* protein occurs throug out the cell cycle or only during the period immediatel before division. There is some evidence (K. J. Begg, perso al communication) that synthesis of the *ftsQ* protein als may be required during this critical period, which prompt speculation as to whether the expression of these two gene may be coordinately regulated.

Lutkenhaus (23) has recently shown that *sulB* is an allel of *ftsZ* and that the product of the *ftsZ* gene (which i required for an essential early step in division) is itself target for an inhibitor of cell division. This inhibitor i believed to be the product of the *sulA*(*sfiA*) gene (18) and i produced as part of the SOS response (22) in cells whic have suffered damage to their DNA. Lutkenhaus and W (26) reported that an element required for full *ftsZ* expres sion appears to be located within the *ftsA* structural gene and Sullivan and Donachie (46) have shown that the *fts* gene is preceded by at least two promoters. At least one c these was reported to lie within the coding sequence of *ftsA* The DNA sequence reported in the present work permits u to identify putative promoters for *ftsQ*, *ftsA*, and *ftsZ* and t confirm that the element required for full *ftsZ* expression lie within the *ftsA* structural gene. We also conclude that promoter or promoters for *ftsA* must lie within the structura gene of *ftsQ*.

MATERIALS AND METHODS

Bacterial strains. *E. coli* strains ED8654 (8) and NFS6 (46 were used as hosts for plasmid constructions. *E. coli* JM10 (28) was employed for growth of M13 phage and its recombi nants. Unless otherwise stated, cultures were routinel grown in L broth, which consists of Difco tryptone (10 g liter, Difco yeast extract (5 g/liter), and NaCl (5 g/liter).

Enzymes and biochemicals. Restriction enzymes, with th exception of *Bam*HI and *Eco*RI, were purchased fror Bethesda Research Laboratories. Deoxyribonucleotide an

* Corresponding author.
† Present address: Duke University Medical College, Durham, NC 27710.
‡ Present address: Department of Molecular Biophysics and Biochemistry, Yale University, New Haven, CT 06510.
§ Present address: Department of Molecular Genetics, Research and Development, Smith, Kline and French Laboratories, Philadelphia, PA 19101.

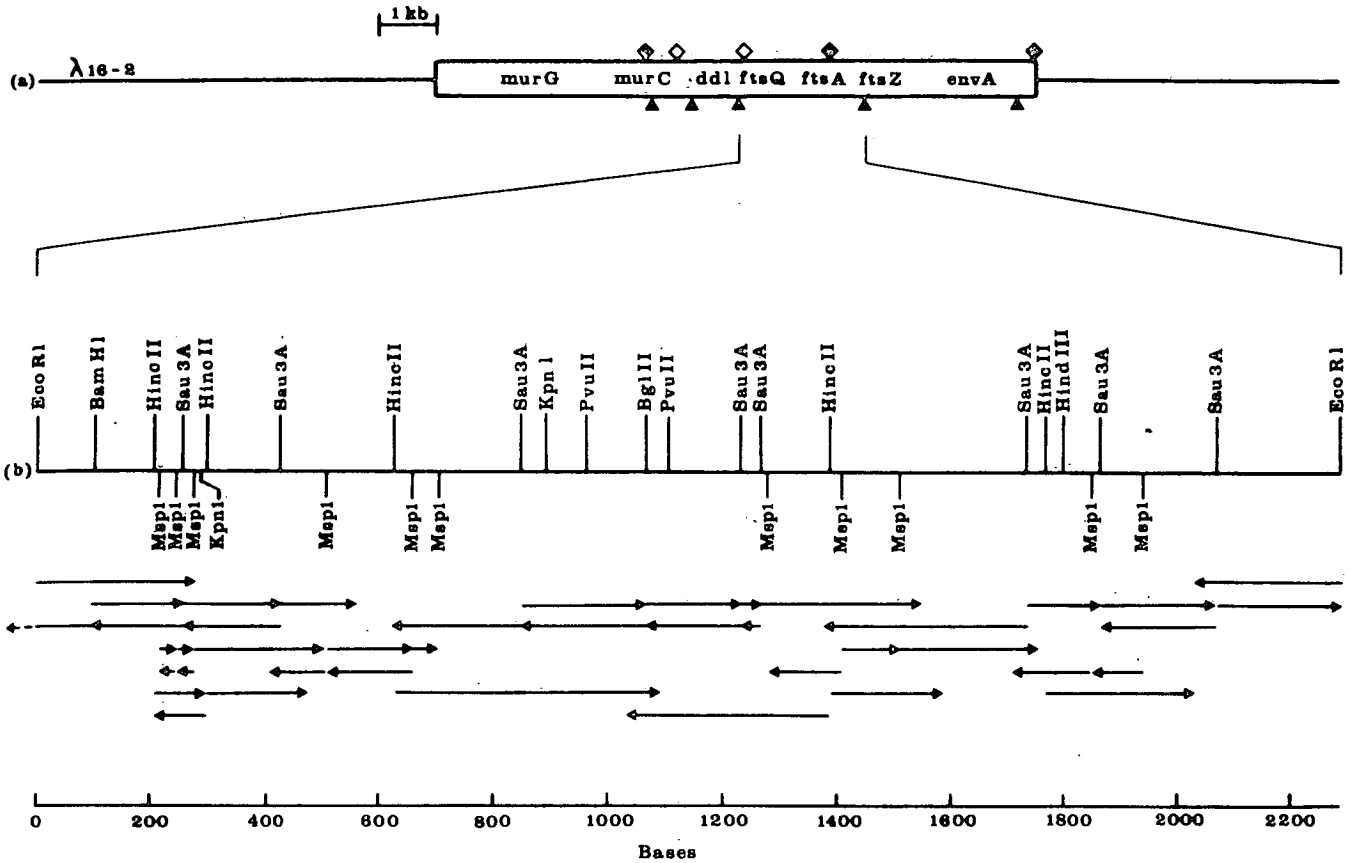

FIG. 1. Restriction enzyme cleavage sites and strategy for determining the sequence of the *ftsQ ftsA* region. (a) Genetic map of λ16-2 (25) showing cleavage sites for *Eco*RI (▲), *Hin*dIII (◆), and *Bam*HI (◇). (b) Restriction map of the 2.3-kb *Eco*RI fragment from the *ftsQ ftsA* region cloned into pBR325 (7). Restriction enzyme sites were determined as described in the text and verified by the established nucleotide sequence. The arrows beneath the map show the direction of sequencing and the length of the sequence determined. The broken arrow extending leftwards from the left-hand *Eco*RI site indicates sequence that was determined from an adjacent, overlapping *Bam*HI fragment. The numbering of bases corresponds to that described in the legend to Fig. 4.

dideoxyribonucleotide triphosphates, DNA polymerase I (Klenow enzyme and Kornberg polymerase), calf intestinal phosphatase, polynucleotide kinase, and restriction endonucleases *Bam*HI and *Eco*RI were supplied by Boehringer Corp., Ltd. T4 DNA ligase was obtained from New England Biolabs. The [α-^{32}P]dCTP, [α-^{32}P]dTTP, [α-^{35}S]dATP (specific activities, >400 Ci/mmol), and [γ-^{32}P]ATP (specific activity, >5,000 Ci/mmol) were purchased from Amersham International.

DNA isolation and ligation. Covalently closed circular plasmid DNA was isolated from cleared lysates (21) and subsequently purified by two consecutive centrifugations in ethidium bromide-cesium chloride density gradients (9). Specific DNA restriction fragments were isolated by separation on 1% agarose gels in Tris-acetate buffer (5 mM sodium acetate, 1 mM EDTA, 40 mM Tris [pH 7.5], followed by electroelution into a solution of 5 mM Tris–2.5 mM sodium acetate. After dialysis against a low-salt buffer (0.2 M NaCl, 1 mM EDTA, 20 mM Tris-hydrochloride [pH 7.4]), the DNA was concentrated by binding to an Elutip-d column (Schleicher and Schuell), eluted in high-salt buffer (1.0 M NaCl, 1 mM EDTA, 20 mM Tris-hydrochloride [pH 7.4]), and ethanol precipitated. Ligations were carried out in buffer conditions recommended by the manufacturer at 14°C overnight for fragments with protruding 5′ or 3′ ends and at 20°C overnight for fragments with blunt ends. Transformations were performed by conventional calcium heat shock procedure.

Construction of plasmids carrying cloned chromosomal fragments. A 2.3-kilobase (kb)-pair *Eco*RI restriction fragment derived from phage λ16-2 (25) was cloned into vector pBR325 (7). This plasmid was designated pGH4. This same 2.3-kb fragment was inserted into the *Eco*RI cloning site of the pBR322 derivative pKO-6 (27) to give pNS27. pNS27 has the fragment oriented such that transcription initiated within it would also transcribe the *galK* gene of the pKO-6 vector (see Fig. 2). pNS27 was in turn used to construct pNS28 (by deletion of a *Bam*HI fragment), pNS29 (by deletion of a *Bam*HI-*Bgl*II fragment from pNS27), and pNS30 (by deletion of a *Hin*dIII fragment from pNS27). pNS54 was obtained by deleting a *Hin*dIII-*Eco*RI fragment from pNS29. Both pGH300 and pDK302 carry the same 2.3-kb *Eco*RI fragment as does pNS27, but in these cases inserted into the *Eco*RI cloning site of pKO-1 (27). pDK302 carries this chromosomal insert in the same orientation as pNS27 does, but pGH300 carries it in the reverse orientation (see Fig. 2). pGH300 was used to construct pNS45 (by deletion of a *Hin*dIII fragment). pDK302 was used to produce pNS36 and pNS37 (by *Pvu*II and *Sma*I digestion) and pDK340 (by *Hin*dIII digestion). pGH301, which contains the same chromosomal insert as pDK302 does, was used to construct pGH305 (by *Bam*HI and *Bgl*II digestion), pGH360 (by *Kpn*I

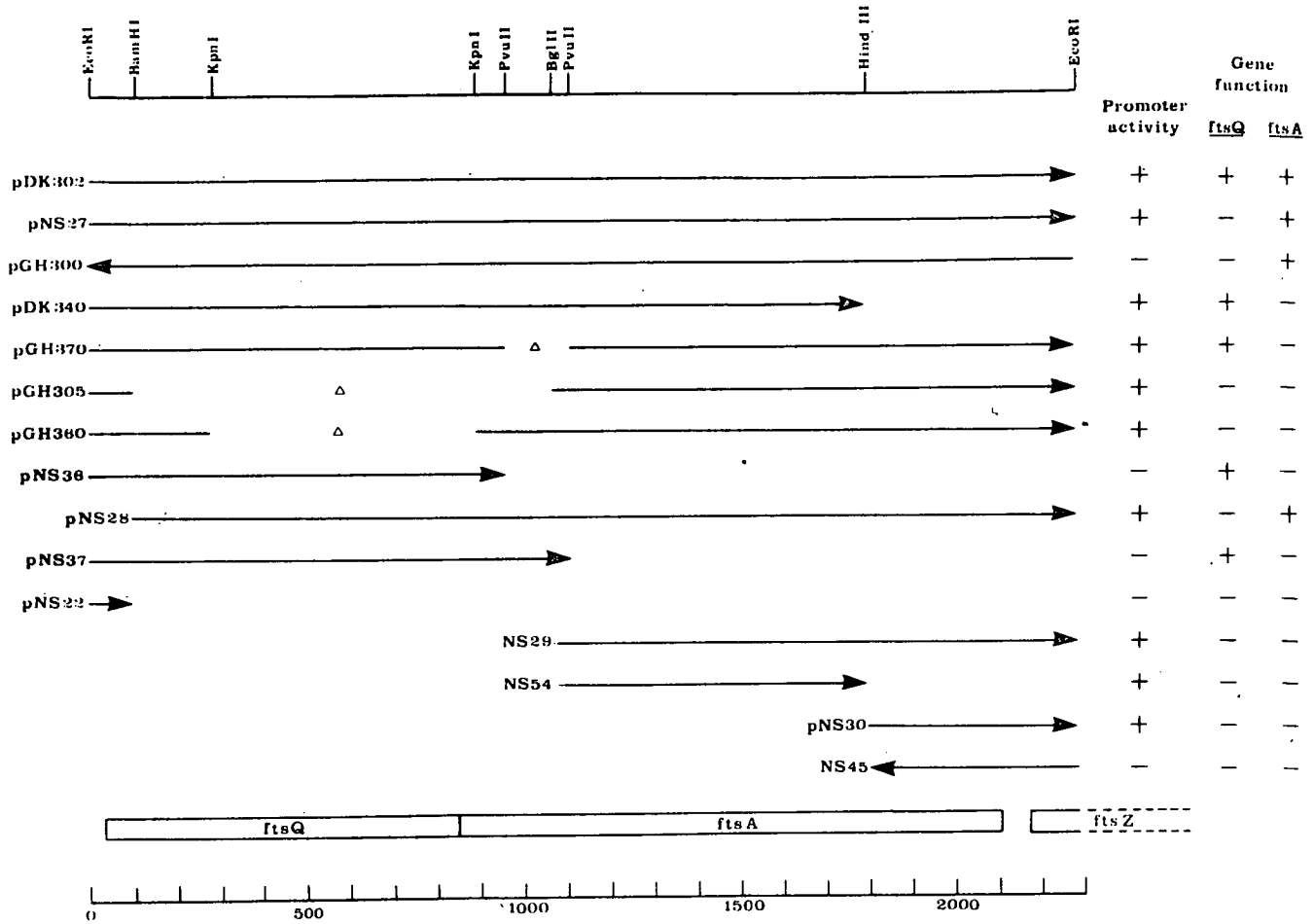

FIG. 2. Location of coding sequences and promoters within the *ftsQ ftsA ftsZ* region. Top, locations of restriction sites used for plasmid constructions. Horizontal lines beneath the map denote fragments cloned into pKO vectors upstream of *galK*. At one end of each insert is an arrowhead which shows the orientation of the fragment relative to the *galK* coding sequence in the complete plasmid (see the text for construction details). The columns to the right of the figure show the results of the tests for promoter activity (column 1) and gene function (columns 2 and 3). Column 1, *galK*$^-$ cells carrying the plasmid which form red (+) or white (−) colonies on galactose indicator plates; columns 2 and 3, positive or negative plasmid complementation of temperature-sensitive mutants of the gene. Normal gene function is defined as both the ability to form colonies on plates at the restrictive temperature and to allow normal growth and morphology of the cells at this temperature. Bottom, locations of the coding sequences of the genes as determined from this data and the nucleotide sequence of the region (see the legend to Fig. 4).

digestion), and pGH370 (by *Pvu*II digestion). pNS20 (data not shown) again carries the same 2.3-kb *Eco*RI fragment as pNS27 does, but cloned into the *Eco*RI site of pKO-4 (27). pNS20 was used to construct pNS22 (by *Bam*HI digestion).

Restriction mapping and DNA sequencing. The restriction enzyme map of pGH4 was determined by the use of partial restriction enzyme digests of singly 5′ ^{32}P-labeled DNA fragments (40). Restriction fragments from the 2.3-kb *Eco*RI fragment and an overlapping upstream 1.2-kb *Bam*HI fragment, derived from phage λ16-2, were subcloned into phage vectors M13mp7, M13mp8, and M13mp9 (28, 29). Radioactive probes were prepared by DNA nick translation in the presence of [α-^{32}P]dCTP by the method of Rigby et al. (34), and phage plaques were screened after blotting onto nitrocellulose filters (5). The recombinants were sequenced by the dideoxy chain termination method of Sanger et al. (36, 37). Initially, all sequencing reactions were carried out with ^{32}P-labeled deoxynucleotide triphosphates. Subsequently, [α-^{35}S]dATP was employed for all reactions (6). Reverse sequencing was carried out by the method of Hong (16). Computer analysis of DNA sequence data employed programs developed by Staden (41–43) and Devereux et al. (11).

Genetic tests for gene expression. Plasmids to be tested were introduced by transformation into either TOE-*ftsQ*(Ts) (4) or TOE-13 *ftsA13*(Ts) (K. J. Begg, unpublished data). Transformants were selected for ampicillin resistance at 30°C (27). Individual colonies were streaked for purification and then checked for the presence of plasmid DNA of the expected size and restriction pattern. Single colonies were then either inoculated into Oxoid nutrient broth and grown to an optical density at 540 nm of 0.2 at 30°C before shifting to 42°C or patched onto solid medium and incubated at either 30 or 42°C. Expression of cloned wild-type alleles was judged by the growth of cells of normal rod shape after 2 to 3 generations at 42°C in liquid medium and by the formation of colonies on solid medium after overnight growth at 42°C. In the absence of wild-type gene expression from the cloned DNA, the *fts* mutant strains at 42°C formed populations of long filamentous cells (4, 12). None of the mutant strains formed colonies on plates at 42°C.

Tests for the presence of promoters on cloned DNA fragments. Assay for the presence of transcriptional promoters

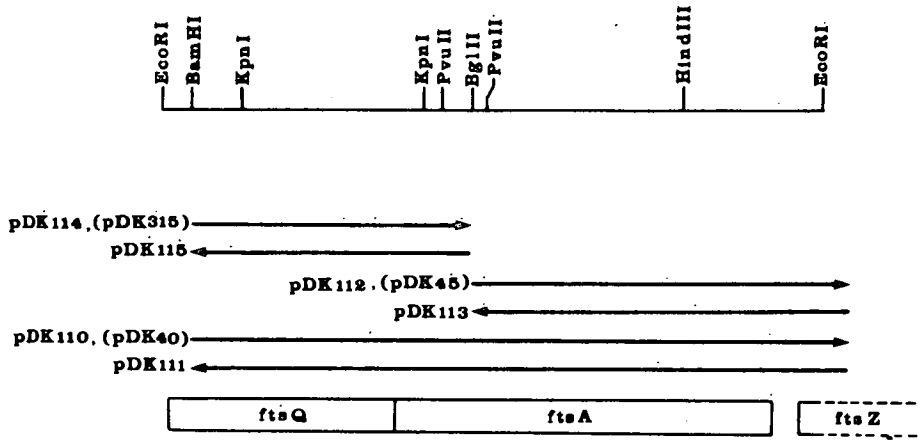

FIG. 3. Chromosomal segments cloned between P*gal* and *galK* to test for the presence of transcriptional terminators. Top, restriction site in the chromosomal DNA as described in the legend to Fig. 2; bottom, location of coding sequences. The horizontal lines beneath the ma show the extent of cloned inserts, and the arrowheads show their orientation relative to the *galK* coding sequence. The plasmid designation are shown on the left; those designations shown in parentheses refer to the same chromosomal segment cloned into pKO-4. The shor rightward extension beyond the right-hand *Eco*RI site is the ca. 100-base-pair *Eco*RI-*Bam*HI chromosomal segment covering the start of *ftsQ* See the text for details of these constructions.

on chromosomal fragments cloned into pKO vectors was carried out as described in the procedures of McKenny et al. (27). The vectors constructed by these authors and employed in the present work (pKO-1, pKO-4, and pKO-6) each contain three unique restriction sites for cloning. These sites vary in different pKO plasmids, but they are located at the same relative positions: *Eco*RI, *Hin*dIII, and *Sma*I in pKO-1; *Eco*RI, *Hin*dIII, and *Bam*HI in pKO-4; *Bam*HI, *Hin*dIII, and *Eco*RI in pKO-6. The cloning sites are located in the plasmid such that transcription originating within DNA which has been cloned in the correct orientation in one of these locations will also transcribe a *galK* coding sequence in the plasmid. To prevent possible translational coupling between transcripts originating in cloned DNA and *galK*, translational stop codons have been inserted upstream of *galK* in all three reading frames, and polar effects on the translation of *galK* have been minimized by the inclusion of a 150-base-pair leader sequence which contains a ribosome binding site (38, 45). The presence of a correctly oriented promoter in a cloned segment gives rise to the Gal^+ phenotype (red colonies on McConkey agar-galactose indicator plates) after transformation of *E. coli* C600 $galK^-$ (46), whereas Gal^- colonies are white. Galactokinase activities were also measured directly for all constructs by the methods of McKenney et al. (27). Those constructs which gave rise to red colonies were found to have consistently higher galactokinase activities compared with controls (data not shown).

Tests for the presence of terminators on cloned DNA fragments. Plasmid pHR9 (30) is a derivative of pKO-4 which carries the *Eco*RI-(*gal* promoter)-*Hin*dIII fragment from the terminator-monitoring plasmid pKG1800 (27). Expression of *galK* in pHR9 is therefore dependent on transcription initiated at the *gal* promoter (P*gal*). Insertion of fragments bearing transcriptional terminators between this promoter and the *galK* gene results in a reduction of *galK* expression and permits a quantitative estimate to be made of the extent of transcriptional readthrough. A search for the presence of transcriptional terminators within the *ftsQ ftsA ftsZ* region was made by performing the following constructions (see Fig. 3). The 2.3-kb *Eco*RI fragment was first purified, ligated to form a circle, and then cut with *Bam*HI. The resulting fragment with *Bam*HI cohesive termini was inserted int pHR9 at the *Bam* site between P*gal* and *galK*. Two clone (pDK110 and pDK111) were selected with this insert in th two possible orientations. pDK111 was digested wit *Bam*HI and *Bgl*II and religated to give pDK112, pDK113 pDK114, and pDK115. A complication in these construc tions is that fragments from the *ftsQ-ftsZ* region themselve carry promoters which are capable of expressing *galK* (se Fig. 2). An estimate of the extent of readthrough from P*ga* therefore requires a quantitative measurement of galactokin ase activities in pairs of plasmids containing the sam chromosomal fragments, in the same position relative t *galK*, but with only one of the pair possessing an upstrean P*gal*. This was achieved by cloning the equivalent restrictio fragment into pKO-4 (from which pHR9 is derived). Th pairs of plasmids constructed are as follows (the pHR derivative is given first, and the pKO-4 derivative is give second): pDK110 and pDK40, pDK114 and pDK315, an pDK112 and pDK45. Galactokinase activities were mea sured in *E. coli* C600 $galK^-$ cells (46) and expressed as percentage of the activity determined for pHR9-carryin cells. The relative amount of transcriptional readthrough i each cloned fragment was calculated as the difference be tween the galactokinase activities found in cells carrying th fragment in the same orientation in pHR9 and pKO-4 vec tors.

RESULTS

Restriction mapping, genetic complementation tests, an identification of DNA fragments bearing transcriptional pro moters. A physical map of the 2.3-kb *Eco*RI fragment wa constructed for the enzymes *Bam*HI, *Bgl*II, *Hin*cII, *Hin*dIII *Kpn*I, *Msp*I, *Pvu*II, and *Sau*3AI (Fig. 1). Figure 2 shows th locations and extents of the sequences subcloned from th 2.3-kb fragment into pKO vector plasmids. The ability c specific restriction fragments to complement mutations at chromosomal locus was tested by introducing each plasmi into host cells carrying a temperature-sensitive allele of th appropriate gene on the chromosome and by determinin whether these cells were normal sized and able to forn colonies at the restrictive temperature of 42°C. Mutant cell

carrying a particular plasmid showed either the typical mutant phenotype at 42°C or apparently normal cell growth and division (Fig. 2).

The coding sequence for *ftsQ* can be assigned to lie within the *Eco*RI-*Pvu*II segment carried by pNS36 (position 0 to position 970), but its expression depends upon the orientation of the cloned segment in the plasmid (compare pDK302 with pGH300). *ftsQ*(Ts) cells carrying pDK302 exhibited a wild-type phenotype at 42°C, and such cells carrying pGH300 exhibited the typical *ftsQ*(Ts) mutant phenotype. These results suggested that *ftsQ* was probably being transcribed (from left to right [Fig. 2]) by readthrough transcription from the P4 promoter of the pKO vector (27). To investigate this possibility, the plasmid pNS27 was constructed in which the 2.3-kb fragment was cloned into the *Eco*RI site of pKO-6 rather than the *Eco*RI site of pKO-1, as in pDK302 and pGH300. The difference between the two kinds of constructions lies in the location of a weak terminator sequence (27) relative to the cloned *Eco*RI fragment. In pDK302 and pGH300, this terminator lies between the cloned segment and *galK* and therefore does not affect readthrough transcription from the plasmid P4 promoter into the cloned segment. In pNS27, this terminator lies upstream of the cloned insert, i.e., between the *ftsQ* coding sequence and the P4 promoter. pNS27 does not show expression of *ftsQ*, thereby showing that the *ftsQ* sequence on the 2.3-kb fragment was being expressed from this plasmid promoter.

The maximum size of the *ftsA* functional unit defined by deletion derivatives was shown to be the 2.2-kb *Bam*HI-*Eco*RI sequence carried by pNS28, and the minimum size must be greater than 900 base pairs (including the sequence between the *Kpn*I site at position 900 and the *Hin*dIII site at position 1800). Since neither the orientation of the 2.3-kb fragment, as in pDK302 and pGH300, nor the presence of an upstream terminator, as in pNS27, has any effect on *ftsA* expression, we concluded that this segment includes a promoter capable of expressing *ftsA*. This finding is consistent with the ability of phage λJFL41 (26), which carries the 2.3-kb *Eco*RI fragment, to complement mutations in *ftsA*.

The plasmids shown in Fig. 2 were also used to locate promoter sites and to determine the directions of transcription originating at these sites. The genetic evidence discussed above clearly demonstrates the existence of a promoter capable of expressing *ftsA* which must lie within the 2.2-kb *Bam*HI-*Eco*RI fragment (pNS28). In addition, the reported molecular weight of the *ftsA* protein of 50,000 (24) requires that promoter activity lie either within the 800-base-pair *Bam*HI-*Kpn*I fragment (position 100 to position 900) and transcribe from left to right or within the 500-base-pair *Hin*dIII-*Eco*RI fragment (position 1800 to position 2300) and transcribe from right to left. The analysis of the nucleotide sequence reported below shows that *ftsA* is transcribed from left to right; hence, the promoter which is responsible for *ftsA* expression should be carried by pNS36. A very low level of transcription attributable to this region has been reported previously (46). Although this level is not sufficient to give Gal$^+$ phenotype on indicator plates, it is evidently sufficient to complement an *ftsA* mutation (Fig. 2). The fact that we were unable to detect this clearly by *galK* expression may be attributed to the limited sensitivity of that method of detection.

The identification of promoter activity upstream of the *ftsZ* coding sequence (pNS29, pNS30, and pNS54) has been reported elsewhere (46), but these results are included in Fig. 2, for completeness. Promoter activity is associated with the 720-base-pair *Bgl*II-*Hin*dIII fragment (pNS54) and the 500-base-pair *Hin*dIII-*Eco*RI fragment (pNS30). Transcription is from left to right in both cases (Fig. 2).

TABLE 1. Transcription from P*gal* through cloned segments of the *ftsQ* to *ftsZ* region[a]

Plasmid	Vector	Activity (%) of:	
		Galactokinase (relative to pHR9)	Readthrough transcription
pKO1		7	
pHR9		100	100
pDK315	pKO4	3	48
pDK114	pHR9	51	
pDK115	pHR9	0	0
pDK45	pKO4	32	
pDK112	pHR9	59	27
pDK113	pHR9	0	0
pDK40	pKO4	35	ND
pDK110	pHR9	ND	ND
pDK111	pHR9	0	0

[a] Restriction fragments (Fig. 3) were cloned into pKO-4 in the correct orientation to transcribe the *galK* gene in the plasmid, and the same fragments were also inserted, in both orientations, into the *Bam*HI site of pHR9. See the text and legend to Fig. 3 for details of constructions and for calculation of percentage of readthrough transcription. ND, Not determined.

Transcriptional termination. A search was carried out for the presence of transcriptional terminators by cloning restriction fragments into the *Bam*HI site of pHR9 and pKO-4 (Fig. 3). The results (Table 1) show that the extent of readthrough transcription from the *Bam*HI site to the *Bgl*II site (clones pDK114) and pDK315) was 48%, and from the *Bgl*II site to the *Bam*HI site (clones pDK112 and pDK45) was 27%, when the fragments were oriented such that any internal promoters would initiate transcription towards *galK*. When these same fragments or the entire 2.3-kb fragment were inserted in the opposite orientation, as in pDK115, pDK113, and pDK111, no expression of *galK* was detectable. No role for transcriptional termination in the anti-clockwise sense was evident, since all downstream promoters (in the *ftsZ envA secA* region) have been found to initiate transcription in the clockwise sense (31; Sullivan and Donachie, submitted for publication).

It was impossible to test for the extent of transcriptional readthrough in the clockwise sense for the whole 2.3-kb fragment (covering the *ftsQ-ftsZ'* sequence) because cells carrying this fragment cloned downstream of P*gal* grew very poorly when the chromosomal fragment was oriented such that P*gal* would transcribe the coding sequences within it (as in pDK110; Fig. 3). Since the *ftsQ* coding sequence was interrupted by the rearrangement necessary to insert the 2.3-kb fragment into pHR9, and since neither pDK112 nor pDK114 (which do not carry an intact *ftsA* coding sequence) had deleterious effects on cell growth, the effect with pDK110 might be attributable to overexpression of *ftsA* by P*gal*. In contrast, pDK111 (which carries the same 2.3-kb fragment as pDK110 does, but in the opposite orientation) had no effect on cell growth but was capable of complementing a chromosomal *ftsA*.ts mutation. Opposing transcription initiated at P*gal* does not, therefore, prevent expression of *ftsA* from its own promoter (internal to *ftsQ*), despite the apparently low levels of transcription from this promoter (see above).

DNA nucleotide sequence and assignment of open reading frames. The strategy used for sequencing the 2.3-kb *Eco*RI fragment (and part of the overlapping upstream 1.2-kb *Bam*HI fragment) is shown in Fig. 1. With the exception of

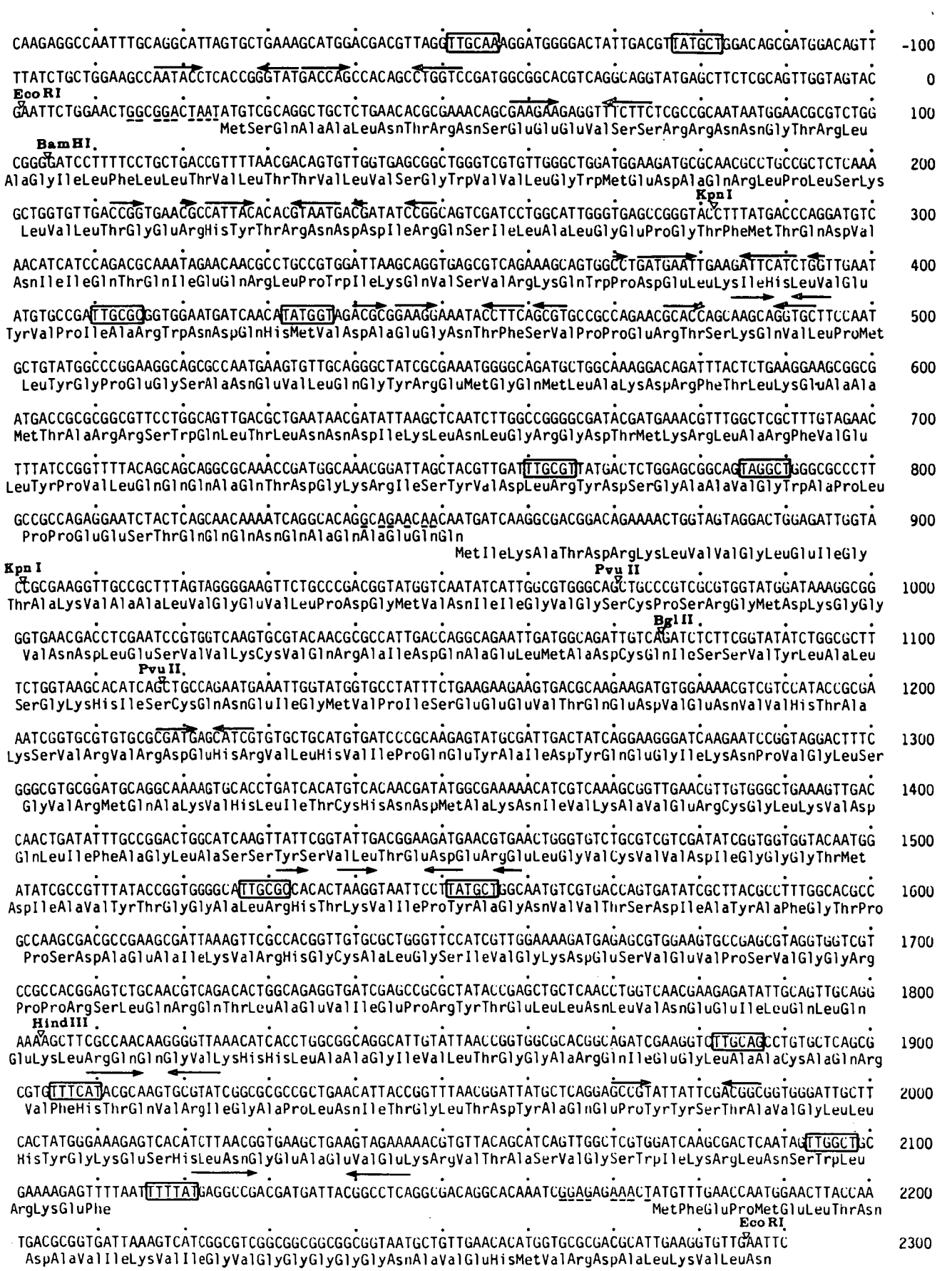

FIG. 4. DNA nucleotide sequence of the noncoding strand of the *fisQ fisA fisZ* region. The amino acid sequences deduced for the products of *fisQ* (nucleotides 25 to 852), *fisA* (nucleotides 852 to 2111), and *fisZ* (nucleotide 2175 onwards) are shown beneath the sequence. Bases are numbered arbitrarily from the left-hand *Eco*RI site of the 2.3-kb *Eco*RI fragment (see Fig. 1). Putative promoter sequences are shown in boxes (see Table 2), and inverted repeat sequences are overlined with arrows. Bases upstream of ATG codons which match the consensus for ribosome binding are underlined. The cutting sites for the restriction enzymes shown in Fig. 2 and 3 are also depicted.

the 200 bases immediately upstream of the left-hand *Eco*RI site, the sequence of the entire region was determined in both orientations from recombinant M13 phage generated by random cloning of restriction fragments and forced cloning of specific restriction fragments where necessary.

The nucleotide sequence of 2,490 base pairs thus determined was numbered arbitrarily from the left-hand *Eco*RI site (Fig. 4). Analysis of this sequence for potential polypeptide coding regions showed that it contains two large open translational reading frames, both of which are in the left-to-right sense (clockwise on the *E. coli* genetic map). The first possible initiation codons for these large open reading frames were at nucleotides 25 to 27 and 852 to 854. The first frame, which from the genetic complementation data must correspond to the structural gene of *ftsQ*, coded for a protein of 276 amino acid residues with a calculated molecular weight of 31,400 and was terminated by the nonsense triplet TGA (nucleotides 853 to 855). The first potential translational initiation codon of the second large open reading frame was found to overlap with the termination codon of the upstream *ftsQ* reading frame. The second frame coded for a 420-residue amino acid protein with a calculated molecular weight of 45,400 and was terminated by the nonsense triplet TAA at nucleotides 2112 to 2114. This must correspond to the structural gene of *ftsA*. The ATG codon at position 25 is immediately preceded by a sequence showing strong homology to a ribosome binding site (38, 45). We concluded that this was the probable start site for *ftsQ* translation since this was the only ATG codon within the proposed *ftsQ* structural gene which showed such homology. There was no close adherence to the consensus of preferred bases for ribosome binding upstream of the ATG codon at position 852, although this was not surprising, given the constraints imposed upon this sequence by its being within the upstream structural gene. An inspection of the sequences immediately preceding the other seven ATG codons within this open reading frame revealed less homology to the consensus than that found upstream of position 852. We concluded that this was the probable start site for *ftsA* translation. The 10% discrepancy between the calculated molecular weight of the *ftsA* product (see Table 4), determined from the deduced amino acid sequence, and the molecular weight determined by gel electrophoresis (24) might be due to anomalous migration (2) of this protein on sodium dodecyl sulfate-polyacrylamide gels.

Ward and Lutkenhaus (47) reported the isolation of an in-frame *lacZ-ftsZ* gene fusion and showed that the *ftsZ* coding sequence begins within the 2.3-kb *Eco*RI fragment. An inspection of the DNA sequence downstream of the termination codon TAA (nucleotides 2112 to 2114) of the proposed *ftsA* structural gene revealed only one open reading frame which extends to the *Eco*RI site. Since the ATG codon at position 2175 was preceded by a sequence showing a strong resemblance to a ribosome binding site, we concluded that this was the probable translational start site for the *ftsZ* structural gene.

Identification of potential transcriptional regulatory sequences. The nucleotide sequence was analyzed for sequences known to be involved in interactions with RNA polymerase and which are well conserved in promoters of *E. coli* genes (15, 35). A total of six possible promoters were identified from consensus considerations and their respective −10 and −35 are shown in Table 2. Their locations and orientation (all in the clockwise sense) were in full agreement with genetic complementation and promoter fusion data, and in all cases the separation of the −35 and −10 regions was within the range of 15 to 21 base pairs observed for other *E. coli* promoters (15).

TABLE 2. Comparison of −35 and −10 regions of putative promoters for *ftsQ*, *ftsA*, and *ftsZ* with consensus sequences for *E. coli* promoter[a]

Promoter	Sequence		Separation (base pairs)
	−35	−10	
ftsQ p_1	TTGCAA	$TATGCT^{-118}$	20
ftsA p_1	TTGCGT	$TAGGCT^{790}$	19
ftsA p_2	TTGCGC	$TATGGT^{437}$	16
ftsZ p_1	TTGGCT	$TTTTAT^{2121}$	17
ftsZ p_2	TTGCAG	$TTTCAT^{1910}$	17
ftsZ p_3	TTGCGC	$TATGCT^{1556}$	18
Consensus	TTGACA	TATRAT	17

[a] The separation of these two regions is also shown, since this is known to influence promoter efficiency (44). The position of the conserved T of the −10 sequence is given as a superscript. R, Purine.

A potential promoter was identified upstream of the presumed start site for translation of *ftsQ* and was designated *ftsQ* P_1. Since the genetic evidence described above demonstrated that *ftsA* was able to be expressed independently of neighboring genes in this cluster, a search was made for promoter-like elements upstream of *ftsA* (i.e., within the *ftsQ* structural gene). Two potential promoters were identified and designated *ftsA*p_1 and *ftsA*p_2. The *ftsA* P_2 promoter sequence was of particular interest since it was surrounded by extensive regions of twofold symmetry and followed by a decanucleotide sequence, TGCCGCCAGA (nucleotides 464 to 473), which was repeated 10 nucleotides downstream from the −10 region of *ftsA*p_1 (nucleotides 800 to 809).

Lutkenhaus et al. (25) and Lutkenhaus and Wu (26) previously located the *ftsZ* gene between *ftsA* and *envA* and inferred its direction of transcription to be in the same sense as that of *ftsA* (i.e., clockwise on the *E. coli* genetic map). They found that expression of the *ftsZ* gene product from a phage that carried only a 3.5-kb *Hin*dIII fragment (λ *envA*$^+$) was weak. This is the region downstream from the *Hin*dIII site (nucleotides 1803 to 1808) within the structural gene of *ftsA*. Furthermore, the addition of bacterial DNA upstream of the *Hin*dIII site was found to restore expression to normal levels, which suggests that some element required for full *ftsZ* expression might be located within the *ftsA* structural gene. Since both the 487-base-pair *Hin*dIII-*Eco*RI fragment (nucleotides 1804 to 2290) and the 727-base-pair *Bgl*II-*Hin*dIII fragment (nucleotides 1076 to 1803) showed promoter activity in the left-to-right sense (46), a search was made for consensus promoter sequences in these fragments. Three putative promoters (designated *ftsZ*p_1, *ftsZ*p_2, and *ftsZ*p_3) were identified, all of which were located within the proposed *ftsA* coding sequence. This designation supercedes that given previously (46). Both *ftsZ*p_1 and *ftsZ*p_2 were associated with twofold symmetry, and an unusual 17-base sequence of alternating purine-pyrimidine residues, which encompassed a region of twofold symmetry, overlapped the −10 sequence of *ftsZ*p_2. A region of twofold symmetry was again found to be coincident with the only promoter-like element, which is upstream of the *Hin*dIII site, within the structural gene of *ftsA*. This putative promoter is designated *ftsZ*p_3. A comparison of the inverted repeat sequences within the regions of *ftsA*p_2 and *ftsZ*p_3 revealed a strong degree of correspondence: of the 13 base pairs that surround the centers of symmetry, 11 were identical. There are no

TABLE 3. Codon usage in *ftsQ* and *ftsA*

Amino acid	Codon	Codon usage in		Amino acid	Codon	Codon usage in	
		ftsQ	*ftsA*			*ftsQ*	*ftsA*
Gly	GGG	2	7	Trp	UGG	7	2
Gly	GGA	3	5	End	UGA	0	0
Gly	GGU	3	18	Cys	UGU	0	5
Gly	GGC	9	10	Cys	UGC	0	4
Glu	GAG	3	11	End	UAG	1	0
Glu	GAA	16	22	End	UAA	0	1
Asp	GAU	9	11	Tyr	UAU	5	11
Asp	GAC	4	7	Tyr	UAC	2	1
Val	GUG	9	19	Leu	UUG	10	6
Val	GUA	3	11	Leu	UUA	2	3
Val	GUU	5	10	Phe	UUU	3	4
Val	GUC	3	10	Phe	UUC	2	0
Ala	GCG	10	12	Ser	UCG	2	7
Ala	GCA	5	10	Ser	UCA	1	3
Ala	GCU	3	6	Ser	UCU	4	3
Ala	GCC	1	7	Ser	UCC	1	2
Arg	AGG	0	0	Arg	CGG	5	3
Arg	AGA	2	1	Arg	CGA	1	2
Ser	AGU	0	4	Arg	CGU	5	9
Ser	AGC	7	5	Arg	CGC	8	7
Lys	AAG	8	8	Gln	CAG	16	11
Lys	AAA	2	13	Gln	CAA	9	8
Asn	AAU	9	5	His	CAU	3	6
Asn	AAC	4	8	His	CAC	0	7
Met	AUG	9	8	Leu	CUG	13	18
Ile	AUA	1	2	Leu	CUA	0	0
Ile	AUU	5	10	Leu	CUU	4	6
Ile	AUC	5	16	Leu	CUC	2	3
Thr	ACG	6	7	Pro	CCG	8	9
Thr	ACA	2	4	Pro	CCA	3	2
Thr	ACU	2	1	Pro	CCU	1	2
Thr	ACC	8	7	Pro	CCC	1	1

recognizable transcriptional terminators (33) in the entire region of the sequence (Fig. 4).

Codon usage and amino acid composition of *ftsQ* and *ftsA* proteins. Codon usage in *ftsQ* and *ftsA* is shown in Table 3. The following codons, corresponding to weakly interacting or minor tRNAs (19; reviewed by Grosjean and Fiers [14]), occurred very infrequently or not at all in both *ftsQ* and *ftsA*: CUA for leucine, AUA for isoleucine, and CGA/AGA/AGG for arginine. In accordance with the general trend for efficiently expressed genes of *E. coli*, the following codons were found to predominate: CUG for leucine, GGPy (Py is pyrimidine) for glycine, AUPy for isoleucine, CCG for proline, GCG for alanine, GAA for glutamine, and CGPy for arginine. Exceptions to the trend were found in *ftsQ* (use of AAG for lysine rather than AAA, and AAU for asparagine rather than AAC). Both *ftsQ* and *ftsA* showed a predominant use of the UAU codon for tyrosine, whereas the trend for highly expressed genes was to favor UAC, and both genes utilized the CGG codon for arginine (which corresponds to a minor tRNA species).

The amino acid composition of the predicted *ftsQ* and *ftsA* proteins is shown in Table 4, together with the calculated average composition of *E. coli* proteins (10). No significant differences are apparent in either case.

DISCUSSION

The results reported here identify the coding sequences for the essential cell division genes *ftsQ* and *ftsA*, together with part of the *ftsZ* gene. All of the DNA sequence shown in Fig. 4, with the exception of the 200 bases immediately upstream of the *Eco*RI site at position 1, was determined in both orientations from overlapping clones to avoid potential errors. Owing to technical difficulties, such as stacking of DNA fragments on gels, it is important to apply several criteria in judging the validity of lengthy nucleotide sequences. If portions of a DNA sequence are translated in an incorrect frame, then regions with many uncommon amino acids are found, even if no nonsense codon is encountered. The open reading frames assigned to *ftsQ*, *ftsA*, and *ftsZ* contain no detectable regions of this sort. Termination codons are found to be distributed uniformly throughout the alternative reading frames (data not shown). Furthermore, an analysis of codon usage in *ftsQ*, *ftsA*, and the N-terminal part of the *ftsZ* gene shows a codon preference associated with efficient gene expression in *E. coli* (14). The amino-terminal sequences of the *ftsQ*, *ftsA*, and *ftsZ* proteins, and hence the positions of translational starts, are unknown. However, an analysis of the genetic data (Fig. 2) and DNA sequence (Fig. 4) permits the identification of structural genes and potential ribosome binding sites associated with translational start codons.

The observation that the termination codon TGA of *ftsQ* overlaps with a potential initiation codon for the *ftsA* gene suggests that these two genes may be translationally coupled. Translational coupling in *E. coli* has previously been

TABLE 4. Amino acid composition of polypeptides encoded by *ftsQ* and *ftsA*

Amino acid	Protein				
	ftsQ		*ftsA*		*E. coli* (% of total)[a]
	No. of residues	% Of total	No. of residues	% Of total	
Alanine	19	6.9	35	8.3	8.6
Arginine	21	7.6	22	5.2	4.9
Aspartic acid	13	4.7	18	4.3	5.5
Asparagine	13	4.7	13	3.1	4.3
Cysteine	0	0.0	9	2.1	2.9
Glutamic acid	19	6.9	33	7.9	6.0
Glutamine	25	9.1	19	4.5	3.9
Glycine	17	6.2	40	9.5	8.4
Histidine	3	1.1	13	3.1	2.0
Isoleucine	11	4.0	28	6.7	4.5
Leucine	31	11.2	36	8.6	7.4
Lysine	10	3.6	21	5.0	6.6
Methionine	9	3.3	8	1.9	1.7
Phenylalanine	5	1.8	4	1.0	3.6
Proline	13	4.7	14	3.3	5.2
Serine	15	5.4	24	5.7	7.0
Threonine	18	6.5	19	4.5	6.1
Tryptophan	7	2.5	2	0.5	1.3
Tyrosine	7	2.5	12	2.9	3.4
Valine	20	7.3	50	11.9	6.6
% Nonpolar	42		42		39
% Polar, uncharged	34		26		36
% Polar, charged	24		32		24
Calculated molecular weight	31,434		45,416		

[a] Data from Dayhoff et al. (10).

reported in the tryptophan operon (32), galactose operon (39), and ribosomal protein operons (3, 48). Although the mechanisms of translational coupling of two adjacent genes are poorly understood at present, it is thought that the close proximity or overlapping of translational termination and initiation codons ensures the coordinated expression of genes of related function. The significance of this finding in relation to *ftsQ* and *ftsA* is unclear at present, since *ftsA*(Ts) mutant cells which carry a cloned fragment of the wild-type *ftsA* gene, without a juxtaposed, intact, upstream *ftsQ* structural gene, appear to grow and divide normally (clone pNS28).

The designation of the ATG codon at position 2175 as the proposed start site for translation of *ftsZ* is consistent with the conclusion of Ward and Lutkenhaus (47) that the *ftsZ* coding sequence begins no more than 300 bases upstream of the *Eco*RI site in *ftsZ*. The DNA sequence presented here offers no alternative start site for this gene.

Although a precise identification of the various components of promoters (i.e., polymerase binding sites and regulatory sites) is uncertain in the absence of additional data, the locations of the putative promoters that we have identified are entirely consistent with the genetic and promoter fusion results presented here. The identification of the putative promoter $ftsQp_1$ is consistent with the detection of promoter activity within the overlapping, upstream 900-base-pair *Eco*RI-*Bam*HI fragment which does not complement mutations in the upstream *ddl* gene (D. Kenan, unpublished data). We are able to conclude that *ftsQ*, *ftsA*, and *ftsZ* are each preceded by at least one promoter, such that they may be expressed from this promoter in the absence of expression of any upstream or downstream neighboring genes. The DNA sequence reveals that the promoter(s) of *ftsA* must lie within the coding sequence of *ftsQ*; this therefore represents a second overlapping transcriptional unit within the gene cluster, similar to the case of *ftsZ* in which an element required for full *ftsZ* expression lies within the coding sequence for *ftsA* (46). Indeed, the three putative *ftsZ* promoters identified here are all found to overlap or lie within the *ftsA* structural gene.

Since *ftsQ*, *ftsA*, and *ftsZ* are all transcribed in the same direction, it is conceivable that the majority of the transcription of this region originates upstream of this cluster, and we are currently investigating this possibility. Further work, currently in progress, will also permit the precise transcriptional start sites to be determined. The existence of overlapping transcriptional units such as those we have identified here implies that there can be no strong transcriptional terminators, and our results bear this out. Transcription from an exogenous promoter (P*gal*) is not blocked by the insertion downstream of fragments from the *ftsQ-ftsZ'* region. The possibility exists that the dissection of the region with *Bam*HI, *Eco*RI, and *Bgl*II may have destroyed termination signals, and we cannot rule this out at present. Some reduction in downstream *galK* expression results from insertion of these fragments (Table 1), but this may be due to polarity effects rather than partial termination signals. Such transcriptional polarity would provide an explanation for the existence of the internal promoters within the cluster. The occurrence of promoters and regulatory sequences within bacterial structural genes is unusual but not unprecedented. The *trpD* gene of *E. coli* has been shown to contain an internal promoter which may confer a bypass function that is advantageous to the cell under conditions of severe nutritional deprivation (17), and an internal operator has been identified within the *galE* gene (20).

It is intriguing that there should be such a strong correspondence between the inverted repeat sequences surrounding $ftsAp_2$ and $ftsZp_3$. The correspondence is especially remarkable when considered in the context of the constraints imposed upon these sequences by their being located within structural genes. These and other regions of twofold symmetry identified here may be binding sites for proteins which regulate the transcription of *ftsA* and *ftsZ*. Alternatively, they may reflect secondary structure in the mRNA and be involved in posttranscriptional regulation.

An interesting point to come out of this work is that apparently normal cell growth and division take place even when essential genes from this cluster are being expressed from internal promoters in cloned fragments, either in multicopy plasmids as described here or in single copy in chromosomally inserted λ vectors (24–26). Coordinate transcription of the cluster is not, therefore, essential for biologically effective function of the genes under normal laboratory conditions.

In conclusion, the analysis presented here forms the basis of our current investigation into the organisation of the *ftsQ ftsA ftsZ* region. The observation that transcriptional units within this cluster overlap is most interesting and potentially important in understanding the expression of these genes. Further experiments in progress should reveal how the expression of this region is related to the complex process of cell division.

ACKNOWLEDGMENTS

We are indebted to our colleague, Richard Hayward, for many helpful discussions.

This study was supported in part by a Training Fellowship Award (to R.S.) from the European Molecular Biology Organization.

LITERATURE CITED

1. **Bachmann, B. J.** 1983. Linkage map of *Escherichia coli* K-12, edition 7. Microbiol. Rev. **47**:180–230.
2. **Banker, G. A., and C. W. Cotman.** 1972. Measurement of free electrophoretic mobility and retardation coefficient of protein-sodium dodecyl sulphate complexes by gel electrophoresis. J. Biol. Chem. **247**:5856–5861.
3. **Baughman, G., and M. Nomura.** 1983. Localisation of the target site for translational regulation of the L11 operon and direct evidence for translational coupling in *Escherichia coli*. Cell **34**:979–988.
4. **Begg, K. J., G. F. Hatfull, and W. D. Donachie.** 1980. Identification of new genes in a cell envelope-cell division gene cluster of *Escherichia coli*: cell division gene *ftsQ*. J. Bacteriol. **144**:435–437.
5. **Benton, W. D., and R. W. Davis.** 1977. Screening λgt recombinant clones by hybridisation to single plaques *in situ*. Science **196**:180–182.
6. **Biggin, M. D., T. J. Gibson, and G. F. Hong.** 1983. Buffer gradient gels and ^{35}S label as an aid to rapid DNA sequence determination. Proc. Natl. Acad. Sci. U.S.A. **80**:3963–3965.
7. **Bolivar, F.** 1978. Construction and characterisation of new cloning vehicles. III. Derivatives of plasmid pBR 322 carrying unique *Eco*RI sites for selection of *Eco*RI generated recombinant DNA molecules. Gene **4**:121–136.
8. **Borck, K., J. D. Beggs, W. J. Brammar, A. S. Hopkins, and N. E. Murray.** 1976. The construction *in vitro* of transducing derivatives of phage lambda. Mol. Gen. Genet. **146**:199–207.
9. **Clewell, D. B., and D. R. Helinski.** 1969. Supercoiled circular DNA-protein complex in *Escherichia coli*: purification and induced conversion to an open circular DNA form. Proc. Natl. Acad. Sci. U.S.A. **62**:1159–1166.
10. **Dayhoff, M. (ed.).** 1978. Atlas of protein sequences and structure, vol. 5, suppl. 3.
11. **Devereux, J., P. Haeberli, and O. Smithies.** 1984. A comprehensive set of sequence analysis programs for the VAX. Nucleic Acids Res. **12**:387–395.
12. **Donachie, W. D., K. J. Begg, J. F. Lutkenhaus, G. P. C. Salmond, E. Martinez-Salas, and M. Vicente.** 1979. Role of the *ftsA*

gene product in control of *Escherichia coli* cell division. J. Bacteriol. **140**:388–394.
13. **Donachie, W. D., K. J. Begg, and N. F. Sullivan.** 1984. The morphogenes of *Escherichia coli*. *In* J. Losick and L. Shapiro (ed.), Microbial Development. Cold Spring Harbor Laboratories, Cold Spring Harbor, N.Y.
14. **Grosjean, H., and W. Fiers.** 1982. Preferential codon usage in prokaryotic genes: the optimal codon-anticodon interaction energy and the selective codon usage in efficiently expressed genes. Gene **18**:199–209.
15. **Hawley, D. K., and W. R. McClure.** 1983. Compilation and analysis of *Escherichia coli* promoter sequences. Nucleic Acids Res. **11**:2237–2255.
16. **Hong, G. F.** 1981. A method for sequencing single stranded cloned DNA in both directions. Biosci. Rep. **1**:243–252.
17. **Horowitz, H., and T. Platt.** 1982. Identification of *trp-p2*, an internal promoter in the tryptophan operon of *Escherichia coli*. J. Mol. Biol. **156**:257–267.
18. **Huisman, O. R., R. D'Ari, and G. George.** 1980. Inducible *sfiA* division inhibition in *Escherichia coli*. Mol. Gen. Genet. **177**:629–636.
19. **Ikemura, T.** 1981. Correlation between abundance of *Escherichia coli* transfer RNAs and occurrence of the respective codons in its protein genes: a proposal for synonymous codon choice that is optimal for the *E. coli* translational system. J. Mol. Biol. **151**:389–409.
20. **Irani, M. H., L. Orosz, and S. Adhya.** 1983. A control element within a structural gene: the *gal* operon of *Escherichia coli*. Cell **32**:783–788.
21. **Katz, L., D. T. Kingsbury, and D. R. Helinski.** 1973. Stimulation by cyclic adenosine monophosphate of plasmid deoxyribonucleic acid replication and catabolite repression of the plasmid deoxyribonucleic acid-protein relaxation complex. J. Bacteriol. **114**:577–591.
22. **Little, J., and D. W. Mount.** 1982. The SOS regulatory system of *Escherichia coli*. Cell **29**:11–22.
23. **Lutkenhaus, J. F.** 1983. Coupling of DNA replication and cell division: *sulB* is an allele of *ftsZ*. J. Bacteriol. **154**:1339–1346.
24. **Lutkenhaus, J. F., and W. D. Donachie.** 1979. Identification of the *ftsA* gene product. J. Bacteriol. **137**:1088–1094.
25. **Lutkenhaus, J. F., H. Wolf-Watz, and W. D. Donachie.** 1980. Organization of genes in the *ftsA-envA* region of the *Escherichia coli* genetic map and identification of a new *fts* locus (*ftsZ*). J. Bacteriol. **142**:615–620.
26. **Lutkenhaus, J. F., and H. C. Wu.** 1980. Determination of transcriptional units and gene products from the *ftsA* region of *Escherichia coli*. J. Bacteriol. **143**:1281–1288.
27. **McKenny, K., H. Shimatake, D. Court, U. Schmeissner, C. Brady, and M. Rosenberg.** 1981. A system to study promoter and terminator signals recognised by *Escherichia coli* RNA polymerase, p. 383–415. In J. G. Chirikjiam and T. S. Papas (ed.) Gene amplification and analysis, vol. 2. Analysis of nucleic acids by enzymatic methods. Elsevier/North-Holland Publishing Co., New York.
28. **Messing, J., R. Crea, and P. H. Seeberg.** 1981. A system for shotgun DNA sequencing. Nucleic Acids Res. **9**:309–321.
29. **Messing, J., and J. Vieira.** 1982. A new pair of M13 vectors for selecting either DNA strand of double digest restriction fragments. Gene **19**:269–276.
30. **Newman, A. J., J.-C. Ma, K. M. Howe, I. Garner, and R. S. Hayward.** 1982. Evidence that rifampicin can stimulate readthrough of transcriptional terminators in *Escherichia coli*, including the attenuator of the *rpo*BC operon. Nucleic Acids Res. **10**:7409–7424.
31. **Oliver, D. B., and J. Beckwith.** 1982. Identification of a new gene (*secA*) and gene product involved in the secretion of envelope proteins in *Escherichia coli*. J. Bacteriol. **150**:686–691.
32. **Oppenheim, D. F., and C. Yanofsky.** 1980. Translational coupling during expression of the tryptophan operon of *Escherichia coli*. Genetics **95**:785–795.
33. **Platt, T., and T. G. Bear.** 1984. Role of RNA polymerase, ρ factor, and ribosomes in transcription termination. *In* J. Beckwith, J. Davies, and J. Gallant (ed.), Gene function in prokaryotes. Cold Spring Harbor Laboratories, Cold Spring Harbor, N.Y.
34. **Rigby, P. J. W., M. Dieckmann, C. Rhodes, and P. Berg.** 1977. Labelling deoxyribonucleic acid to high specific activity *in vitro* by nick translation with DNA polymerase I. J. Mol. Biol. **113**:237–251.
35. **Rosenberg, M., and D. Court.** 1979. Regulatory sequences involved in the promotion and termination of RNA transcription. Annu. Rev. Genet. **13**:319–353.
36. **Sanger, F., A. R. Coulson, B. G. Barrell, A. J. H. Smith, and B. A. Roe.** 1980. Cloning in single-stranded bacteriophage as an aid to rapid DNA sequencing. J. Mol. Biol. **143**:161–178.
37. **Sanger, F., S. Nicklen, and A. R. Coulson.** 1977. DNA sequencing with chain terminating inhibitors. Proc. Natl. Acad. Sci. U.S.A. **74**:5463–5467.
38. **Scherer, G. E. F., M. D. Walkinshaw, S. Arnott, and D. J. Morré.** 1980. The ribosomal binding sites recognised by *E. coli* ribosomes have regions with signal character in both the leader and protein coding segments. Nucleic Acids Res. **8**:3895–3907.
39. **Schümperli, D., K. McKenny, D. A. Sobieski, and M. Rosenberg.** 1982. Translational coupling at an intercistronic boundary of the *Escherichia coli* galactose operon. Cell **30**:865–871.
40. **Smith, H. O., and M. L. Birnstiel.** 1976. A simple method for DNA restriction site mapping. Nucleic Acids Res. **3**:2387–2398.
41. **Staden, R.** 1977. Sequence data handling by computer. Nucleic Acids Res. **4**:4037–4051.
42. **Staden, R.** 1978. Further procedures for sequence analysis by computer. Nucleic Acids Res. **5**:1013–1015.
43. **Staden, R.** 1979. A strategy of DNA sequencing employing computer programs. Nucleic Acids Res. **6**:2601–2610.
44. **Stefano, J. E., and J. D. Gralla.** 1982. Spacer mutations in the *lacp*^{s} promoter. Proc. Natl. Acad. Sci. U.S.A. **79**:1069–1072.
45. **Stormo, G. D., T. D. Schneider, and L. M. Gold.** 1982. Characterisation of translational initiation sites in *E. coli*. Nucleic Acids Res. **10**:2971–2996.
46. **Sullivan, N. F., and W. D. Donachie.** 1984. Overlapping functional units in a cell division gene cluster in *Escherichia coli*. J. Bacteriol. **158**:1198–1201.
47. **Ward, J. E., Jr., and J. F. Lutkenhaus.** 1984. A *lacZ-ftsZ* gene fusion is an analog of the cell division inhibitor *sulA*. J. Bacteriol. **157**:815–820.
48. **Yates, J. L., and M. Nomura.** 1981. Feedback regulation of ribosomal protein synthesis in *Escherichia coli*: localisation of the mRNA target sites for repressor action of ribosomal protein L1. Cell **24**:243–249.

Adler, H., Fisher, W., Cohen, A., and Hardigree, A. (1967). Miniature Escherichia coli cells deficient in DNA. Proc. Nat. Acad. Sci. USA 57:321-326.

Allen, J.J., Filip, C.C., Gustafson, R.A., Allen, R.G. and Walker, J.R. (1974). Regulation of bacterial cell division: genetic and phenotypic analysis of temperature-sensitive, multinucleate, filament-forming mutants of Escherichia coli. J. Bacteriol. 117:978-986.

Bachman, B.J. (1983). Linkage map of Escherichia coli K-12, edition 7. Microbiol. Rev. 47:180-230.

Banker, G. & Cotman, C. (1972). Measurement of free electrophoretic mobility and retardation coefficient of protein-sodium dodecyl sulphate complexes by gel electrophoresis. J. Biol. Chem. 247:5856- 5861.

Barnickel, G., Naumann, D., Bradaczek, H., Labischinski, H., and Giesbrecht, P. (1983). Computer aided molecular modelling of the three-dimensional structure of bacterial peptidoglycan. In: R. Hakenbeck, J.-V. Holtje, H. Labischinski, The target of penicillin. Proc. Int. FEMS Symp. Berlin March 13-18. Walter de Gruyter, Berlin.

Baughman, G. & Nomura, M. (1983). Localization of the target site for translational regulation of the L11 operon and direct evidence for translational coupling in Escherichia coli. Cell 34:979-988.

Bayer, M.E. (1974). Ultrastructure and organization of the bacterial envelope. Ann. N.Y. Acad. Sci. 235:6-28.

Begg, K.J. and Donachie, W.D. (1984). Concentration of a

major outer membrane protein at the cell poles in Escherichia coli. J. Gen. Microbiol. 130:2339-2346.

Begg, K.J., Hatfull, G.F., & Donachie, W.D. (1980). Identification of new genes in a cell envelope-cell division gene cluster of Escherichia coli: cell division gene ftsQ. J. Bacteriol. 144:435-437.

Bernard, H.-U., Remaut, E., Hershfield, M., Das, H., Helinski, D., Yanofsky, C., & Franklin, N. (1979). Construction of plasmid cloning vehicles that promote gene expression from the bacteriophage lambda P_L promoter. Gene 5: 59-76.

Blobel, G. and Dobberstein, B. (1975). Transfer of proteins across membranes. I. Presence of proteolytically processed and nonprocessed nascent immunoglobulin light chains on membrane-bound ribosomes of murine myeloma. J. Cell Biol. 67:835-851.

Bolivar, F. (1978). Construction and characterization of new cloning vehicles. III. Derivatives of plasmid pBR322 carrying unique EcoRI sites for selection of EcoRI generated recombinant DNA molecules. Gene 4:121-136.

Botta, G.A. and Park, J.T. (1981). Evidence for involvement of penicillin-binding protein 3 in murein synthesis during septation but not during cell elongation. J. Bacteriol. 145:333-340.

Boyd, A. and Holland, I.B. (1979). Regulation of the synthesis of surface protein in the cell cycle of E. coli B/r. Cell 18:287-296.

Brahms, J.G., Dargouge, O., Brahms, S., Ohara, Y. and Vagner, V. (1985). Activation and inhibition of

transcription by supercoiling. J. Mol. Biol. 181:455-465.

Broome-Smith, J.K., Hedge, P.J. and Spratt, B.G. (1985). Production of thiol-penicillin-binding protein 3 of Escherichia coli using a two primer method of site-directed mutagenesis. EMBO J. 4:231-235.

Buchanan, C.E. (1981). Topographical distribution of penicillin-binding proteins in the Escherichia coli membrane. J. Bacteriol. 145:1293-1298.

Burdett, I.D.J. and Murray, R.G.E. (1974). Septum formation in Escherichia coli: characterization of septal structure and the effects of antibiotics on cell division. J. Bacteriol. 119:303-324.

Burge, R.E., Adams, R., Balyuzi, H.H., Reaveley, D.A. (1977). Structure of the peptidoglycan of bacterial cell walls II. J. Mol. Biol. 117:955-974.

Burman, L.G. and Park, J.T. (1983). Changes in the composition of Escherichia coli murein as it ages during exponential growth. J. Bacteriol. 155:447-453.

Burman, L.G. and Park, J.T. (1984). Molecular model for elongation of the murein sacculus of Escherichia coli. Proc. Natl. Acad. Sci. U.S.A. 81:1844-1848.

Burman, L.G., Reichler, J., and Park, J.T. (1983). Evidence for multisite growth of Escherichia coli murein involving concommitant endopeptidase and transpeptidase activities. J. Bacteriol. 156:386-392.

Burton, P. and Holland, I.B. (1983). Two pathways of division inhibition in uv-irradiated E. coli. Mol.

Gen. Genet. 109:309-314.

Campbell, A.M. (1957). Synchronization of cell division. Bacteriol. Rev. 21:263.

Capaldo, F.N. and Barbour, S.D. (1975). DNA content, synthesis, and integrity in dividing and non-dividing cells of Rec$^-$ strains of Escherichia coli K-12. J. Mol. Biol. 91:53-66.

Clarke, L. and Carbon, J. (1975). Biochemical construction and selection of hybrid plasmids containing specific segments of the Escherichia coli genome. Proc. Natl. Acad. Sci. USA 72:4361-4265.

Clarke, L. and Carbon, J. (1976). A colony bank containing synthetic ColE1 hybrid plasmids representative of the entire E. coli genome. Cell 9:91-99.

Close, T.J. and Rodriguez, R.L. (1982). Construction and characterization of the chloramphenicol-resistance gene cartridge: A new approach to the transcriptional mapping of extrachromosomal elements. Gene 20:305-316.

Cooper, S. and Helmstetter, C.E. (1968). Chromosome replication and the division cycle of Escherichia coli B/r. J. Mol. Biol. 31:519-540.

Cronan, J.E. Jr. (1978). Molecular biology of bacterial membrane lipids. Ann. Rev. Biochem. 47:163.

Daneo-Moore, L. & Shockman, G.D. (1977). The bacterial cell surface in growth and division; p. 597-715, in; Cell Surface Reviews, vol. 4. eds. Poste, G. & Nicolson, G. (Elsevier/North Holland Publishing Co., Amsterdam).

de Boer, H.A. (1984). A versatile plasmid system for the study of prokaryotic transcription signals in Escherichia coli. Gene 30:251-255.

DePedro, M.A. and Schwarz, U. (1981). Heterogeneity of newly inserted and preexisting murein in the sacculus of Escherichia coli. Proc. Natl. Acad. Sci. USA 78:5856-5860.

Donachie, W.D. (1968). Relationship between cell size and time of initiation of DNA replication. Nature (London) 219:1077-1979.

Donachie, W.D. (1981). The cell cycle of Escherichia coli. In; The cell cycle. Ed. P.C.L. John, Cambridge University Press.

Donachie, W.D., Begg, K.J., Lutkenhaus, J.F., Salmond, G., Martinez-Salas, E., & Vicente, M. (1979). Role of the ftsA gene product in control of Escherichia coli cell division. J. Bacteriol. 140:388-394.

Donachie, W.D., Begg, K.J., & Sullivan, N. (1984). The morphogenes of Escherichia coli. In J. Losick and L. Shapiro (ed.), Microbial Development. Cold Spring Harbor Laboratories, Cold Spring Harbor, N.Y.

Donachie, W.D., Begg, K.J., & Vicente, M. (1976). Cell length, cell growth, and cell division. Nature 264:328-333.

Donachie, W.D. and Masters, M. (1969). Temporal control of gene expression in bacteria. In The cell cycle (ed. G.M. Padilla et al) p. 37-76. Academic Press, New York.

Donachie, W.D., Sullivan, N.F., Kenan, D.J., Derbyshire, V., Begg, K.J., Kagan-Zur, V. (1983). Genes and cell division in Escherichia coli. In Progress in cell cycle controls (ed. J. Chaloupka et al.) p. 28. Czechoslovak Academy of Science, Prague.

Endermann, R., Kramer, C., and Henning, U. (1978). Major outer membrane proteins of Escherichia coli K-12: evidence for protein II being a transmembrane protein. FEBS Lett. 86:21-24.

Essig, P., Martin, H.H., and Gmeiner, J. (1982). Murein and lipopolysaccharide biosynthesis in synchronized cells of Escherichia coli K-12 and the effect of penicillin G, mecillinam and nalidixic acid. Arch. Microbiol. 132:245-250.

Fairweather, N.F., Orr, E. and Holland, I.B. (1980). Inhibition of deoxyribonucleic acid gyrase: effects on nucleic acid synthesis and cell division in Escherichia coli K-12. J. Bacteriol. 142:153-161.

Fletcher, G., Irwin, C.A., Henson, J.M., Fillingim, C., Malone, M.M., and Walker, J.R. (1978). Identification of the Escherichia coli cell division gene sep and organization of the cell division-cell envelope genes in the sep-mur-ftsA-envA cluster as determined with specialized transducing lambda bacteriophages. J. Bacteriol. 133:91-100.

Frazer, A.C. and Curtiss, R. III, (1975). Production, properties and utility of bacterial minicells. Curr. Top. Microbiol. Immunol. 69:1.

Fung, J., MacAlister, T.J., Rothfield, L.I. (1978). Role of murein lipoprotein in morphogenesis of the bacterial

division septum: phenotypic similarity of lkyD and lpo mutants. J. Bacteriol. 133:1467-1471.

George, J., Castellazzi, M., & Buttin, G. (1975). Prophage induction and cell division in E. coli. III. Mutations sfiA and sfiB restore division in tif and lon strains and permit the expression of mutator properties of tif. Mol. Gen. Genet. 140:309-332.

Germino, J., and Bastia, D. (1984). Rapid purification of a cloned gene product by genetic fusion and site-specific proteolysis. Proc. Natl. Acad. Sci. USA 81:4692-4696.

Ghuysen, J. & Shockman, G. (1973). Biosynthesis of peptidoglycan. p. 37-130. In: Bacterial Membranes and Walls. L. Leive (ed). M. Dekker Inc., New York.

Hatfull, G.F. (1981). PhD thesis; University of Edinburgh.

Hawley, D. & McClure, W. (1983). Compilation and analysis of Escherichia coli promoter sequences. Nucleic Acids Res. 11:2237- 2255.

Helmstetter, C.E., Cooper, S., Pierucci, O. and Revelas, E. (1968). The bacterial life sequence. Cold Spring Harbor Symp. Quant. Biol. 33:809-822.

Helmstetter, C.E., Pierucci, O., Weinberger, M., Holmes, M., and Tang, M.-S. (1979). Control of cell division in Escherichia coli. In "The Bacteria" vol. 7,517-579. Ed. J.R. Sokatch and L.N. Ornston. Academic Press, New York.

Henning, U. (1975). Determination of cell shape in bacteria. Ann. Rev. Microbiol. 29:45-60.

Herrero, E., Fairweather, N.F. and Holland, I.B. (1982). Envelope protein synthesis and inhibition of cell division in Escherichia coli during inactivation of the B subunit of DNA gyrase. J. Gen. Microbiol. 128:361-369.

Hirota, Y., Jacob, F., Ryter, A., Buttin, G., & Nakai, T. (1968). On the process of cellular division in Escherichia coli. I. Asymmetrical cell division and production of deoxyribonucleic acid-less bacteria. J. Mol. Biol. 35:175-192.

Hirota, Y., Suzuki, H., Nishimura, Y., et al. (1977). On the process of cellular division in Escherichia coli: a mutant of E. coli lacking a murein-lipoprotein. Proc. Natl. Acad. Sci. USA 74:1417-1420.

Holland, I.B. and Darby, V. (1976). Genetical and physiological studies on a thermosensitive mutant of Escherichia coli defective in cell division. J. Gen. Microbiol. 92:156.

Horowitz, H. & Platt, T. (1982). Identification of trp-p2, an internal promoter in the Tryptophan operon of Escherichia coli. J. Mol. Biol. 156: 257-267.

Howe, W.E. and Mount, D.W. (1975). Production of cells without deoxyribonucleic acid during thymidine starvation of lexA$^-$ cultures of Escherichia coli K-12. J. Bacteriol. 124:1113-1121.

Huisman, O. D'Ari, R., & George, J. (1980). Inducible sfi dependent division inhibition in Escherichia coli. Molec. Gen. Genet. 177:629-636.

Huisman, O., Jacques, M., D'Ari, R., and Caro, L. (1983).

Role of the sfiA-dependent cell division regulation system in Escherichia coli. J. Bacteriol. 153:1072-1074.

Ingraham, J.L., Maaloe, O., and Neidhardt, F.C. (1983). Growth of the bacterial cell. Sinauer Associates, Inc., Sunderland, Mass.

Inouye, M. (1969). Unlinking of cell division from deoxyribonucleic acid replication in a temperature-sensitive deoxyribonucleic acid synthesis mutant of Escherichia coli. J. Bacteriol. 99:842-850.

Inouye, M. (1971). Pleiotropic effect of the recA gene of E. coli: Uncoupling of cell division from DNA replication. J. Bacteriol. 106:539.

Inouye, M. and Halegova, S. (1980). Secretion and membrane localization of proteins in Escherichia coli. CRC Crit. Rev. Biochem. p. 39.

Irani, M., Orosz, L., & Adhya, S. (1983). A control element within a structural gene: the gal operon of Eschericia coli. Cell 32: 783-788.

Jones, C.A. and Holland, I.B. (1984). Inactivation of essential division genes, ftsA, ftsZ, suppresses mutations at sfiB, a locus mediating division inhibition during the SOS response in E. coli. EMBO J. 3:1181-1186.

Jones, N.C. and Donachie, W.D. (1973). Chromosome replication, transcription and control of cell division in Escherichia coli. Nature (London) New Biol. 243:100-103.

Kastelein, R.A., Berkhout, B., Overbeek, G.P. and Van Duin, J. (1983). Effects of the sequences upstream from the ribosome binding site on the yield of protein from the cloned gene for phage MS2 coat protein. Gene 23:245-254.

Koch, A.L. and Burdett, I.D.J. (1984). The variable T model for Gram-negative morphology. J. Gen. Microbiol. 130:2325-2338.

Kornberg, A. (1982). 1982 Supplement to DNA replication. W.F. Freeman and Company, New York.

Kornberg, A. (1980). DNA replication. W.F. Freeman and Company, New York.

Leduc, M., Frehel, C. and van Heijenoort, J. (1985). Correlation between degradation and ultrastructure of peptidoglycan during autolysis of Escherichia coli. J. Bacteriol. 161:627-635.

Leduc, M., Kasra, R. and van Heijenoort, J. (1982). Induction and control of the autolytic system of Escherichia coli. J. Bacteriol. 152:26-34.

Leduc, M. & van Heijenoort, J. (1980). Autolysis of Eschericia coli. J. Bacteriol. 142:52-59.

Leibowitz, P.J. and Schaecter, M. (1975). The attachment of the bacterial chromosome to the cell membrane. Int. Rev. Cytol. 41:1-28.

Little, J.W. & Mount, D.W. (1982). The SOS regulatory system of Escherichia coli. Cell 29:11-22.

Lugtenberg, E.J.J. & van Schijndel-van Dam, A. (1972a).

Temperature-sensitive mutants of Escherichia coli K-12 with low activities of the L-alanine adding enzyme and the D-alanyl-D-alanine adding enzyme. J. Bacteriol. 110:35-40.

Lugtenberg, E.J.J. & van Schijndel-van Dam, A. (1972b). Temperature-sensitive mutants of Escherichia coli K-12 with low activity of the diaminopimelic acid adding enzyme. J. Bacteriol. 110:41-46.

Lugtenberg, E. & van Schijndel-van Dam, A. (1973). Temperature-sensitive mutant of Escherichia coli K-12 with an impaired D-alanine:D-alanine ligase. J. Bacteriol. 113:96-104.

Lutkenhaus, J.F. (1983). Coupling of DNA replication and cell division: sulB is an allele of ftsZ. J. Bacteriol. 154:1339-1346.

Lutkenhaus, J.F. & Donachie, W.D. (1979). Identification of the ftsA gene product. J. Bacteriol. 137:1088-1094.

Lutkenhaus, J.F., Moore, B.A., Masters, M., & Donachie, W.D. (1979). Individual proteins are synthesized continuously throughout the Eschericia coli cell cycle. J. Bacteriol. 138:352-360.

Lutkenhaus, J.F., Wolf-Watz, H., & Donachie, W.D. (1980). Organization of genes in the ftsA-envA region of the Escherichia coli genetic map and identification of a new fts locus (ftsZ). J. Bacteriol. 142:615-620.

Lutkenhaus, J.F. & Wu, H.C. (1980). Determination of transcriptional units and gene products from the ftsA region of Escherichia coli. J. Bacteriol. 143:1281-1288.

Markiewicz, Z., Broome-Smith, J.K., Schwarz, U., and Spratt, B.G. (1982). Spherical E. coli due to elevated levels of D-alanine carboxypeptidase. Nature 297:702-704.

Marr, A.G., Harvey, R.J., & Trentini, W.C. (1966). Growth and division of Escherichia coli. J. Bacteriol. 91:2388-2389.

Matsuhashi, M., Nakagawa, J., Tomioka, S., Ishino, F., & Tamaki, S. (1982). Mechanism of peptidoglycan synthesis by penicillin-binding proteins in bacteria and effect of antibiotics. p. 1-14. In Microbial Drug Resistance, Vol. 3. S. Mitsuhashi & M. Inoue, eds. Japan Scientific Societies Press (Tokyo).

Matsuhashi, M., Ishino, F., Nakagawa, J., Mitsui, K., Nakajima-Iijima, S., & Tamaki, S. (1981). Enzymatic activities of penicillin-binding proteins of Escherichia coli and their sensitivities to Beta-lactam antibiotics. In: Beta-Lactam Antibiotics--Mode of Action, New Developments, and Future Prospects. Eds. M. Salton and G. Shockman. Academic Press (New York).

Matsuzawa, H., Matsuhashi, M. Oka, A. and Sugino, Y. (1969). Genetic and biochemical studies on cell wall peptidoglycan synthesis in Escherichia coli K-12. Biochem. Biophys. Res. Commun. 36:682-689.

McKenney, K., Shimatake, H., Court, D., Schmeissner, U., Brady, C., & Rosenberg, M. (1981). A system to study promoter and terminator signals recognized by Escherichia coli RNA polymerase. In Gene Amplification and Analysis Vol. 2: Analysis of Nucleic Acids by Enzymatic Methods. Eds. J. Chirikjian and T. Papas. Elsevier-North Holland Publishing Co., New

York.

Mendelson, N.H. (1982). Bacterial growth and division: genes, structures, forces, and clocks. Microbiol. Rev. 46:341-375.

Mengin-Lecreulx, D., Flouret, B. and van Heijenoort, J. (1982). Cytoplasmic steps of peptidoglycan synthesis in Escherichia coli. J. Bacteriol. 151:1109-1117.

Mirelman, D., Yashouv-Gan, Y. Nuchamovitz, Y., Rozenhak, S. and Ron, E.Z. (1978). Murein biosynthesis during a synchronous cell cycle of Escherichia coli B. J. Bacteriol. 134:458-461.

Mirelman, D., Yashouv-Gan, Y., Schwarz, U. (1977). Regulation of murein biosynthesis and septum formation in filamentous cells of Escherichia coli PAT84. J. Bacteriol. 129:1593-1600.

Mitchell, P. and Moyle, J. (1956). Osmotic function and structure in bacteria. Symp. Soc. Gen. Microbiol. 6:150.

Miyakawa, T., Matsuzawa, H., Matsuhashi, M., & Sugino, Y. (1972). Cell wall peptidoglycan mutants of Escherichia coli K-12: existence of two clusters of genes, mra & mrb, for cell wall peptidoglycan biosynthesis. J. Bacteriol. 112:950-958.

Mizusawa, S. and Gottesman, S. (1983). Protein degradation in E. coli: the lon gene controls the stability of sulA protein. Proc. Natl. Acad. Sci. USA 80:358

Morita, M. and Oka, A. (1979). The structure of a transcriptional unit on colicin E1 plasmid. Eur. J.

Biochem. 97:435-443.

Murray, N.E. (1977). Expression of bacterial genes in phage lambda vectors, p. 123-135. In R.F. Beers, Jr. and E.G. Basset (ed.), Recombinant molecules: impact in science and society. Raven Press, New York.

Murray, N.E. (1983). Phage lambda and molecular cloning. In R. Hendrix, J. Roberts, F. Stahl, and R. Weisberg (eds.). Lambda II. Cold Spring Harbor Laboratory, New York.

Nakamura, M., Maruyama, I.N., Soma, M., Kato, J., Suzuki, H., & Hirota, Y. (1983). On the process of cellular division in Escherichia coli: nucleotide sequence of the gene for penicillin binding protein 3. Mol. Gen. Genet. 191:1-9.

Neidhardt, F., Vaughn, V., Phillips, T.A., Block, P.L. (1983). Gene protein index of Escherichia coli K-12. Microbiol. Rev. 47:231-284.

Newman, A.J., Ma, J.-C., Howe, K., Garner, I., & Hayward, R. (1982). Evidence that rifampicin can stimulate readthrough of transcriptional terminators in Escherichia coli, including the attenuator of the rpoBC operon. Nucleic Acids Res. 10:7409-7424.

Nikaido, H. and Vaara, M. (1985). Molecular basis of bacterial outer membrane permeability. Microbiol. Rev. 49:1-32.

Nishimura, Y., Takeda, Y., Nishimura, A., Suzuki, H., Inouye, M. and Hirota, Y. (1977). Synthetic ColE1 plasmids carrying genes for cell division in Escherichia coli. Plasmid 1:67-77.

Normark, S., Bowman, H., and Matsson, E. (1969). Mutant of Escherichia coli with anomalous cell division and ability to decrease episomally and chromosomally mediated resistance to ampicillin and several other antibiotics. J. Bacteriol. 97:1334.

Normark, S., Norlander, L., Grundstrom, T., Bloom, G., Bouquet, P., and Frelat, G. (1976). Septum formation defective mutant of E. coli. J. Bacteriol. 128:401.

Oliver, D.B. and Beckwith, J. (1981). Escherichia coli mutant pleiotropically defective in the export of secreted proteins. Cell 25:765-772.

Oliver, D.B. and Beckwith, J. (1982). Identification of a new gene (secA) and gene product involved in the secretion of envelope proteins in Eschericia coli. J. Bacteriol. 150:686-691.

Orr, E., Fairweather, N.F., Holland, I.B., & Pritchard, R.H. (1979). Isolation and characterisation of a strain carrying a conditional lethal mutation in the cou gene of Escherichia coli K12. Mol. Gen. Genet. 177:103-112.

Osborn, M.J. and Wu, H.C.P. (1980). Proteins of the outer membrane of Gram-negative bacteria. Ann. Rev. Microbiol. 34:369.

Palva, E.T. (1979). Protein interactions in the outer membrane of Escherichia coli. Eur. J. Biochem. 93:495-503.

Pettijohn, D.E. (1982). Structure and properties of the bacterial nucleoid. Cell 30:667-669.

Platt, T. & Bear, T. (1984). Role of RNA polymerase, rho

factor, and ribosomes in transcription termination. In J. Beckwith, J. Davies, and J. Gallant (ed.), Gene function in prokaryotes. Cold Spring Harbor Laboratories, Cold Spring Harbor. N.Y.

Randall, L.L. and Hardy, S.J.S. (1984). Export of protein in bacteria. Microbiol. Rev. 48:290-298.

Ricard, M. and Hirota, Y. (1973). Process of cellular division in Escherichia coli: physiological study on thermosensitive mutants defective in cell division. J. Bacteriol. 116:314-322.

Robinson, A.C., Kenan, D.J., Hatfull, G.F., Sullivan, N.F., Spiegelberg, R., Donachie, W.D. (1984). DNA sequence and transcriptional organization of essential cell division genes ftsQ and ftsA of Escherichia coli: Evidence for overlapping transcriptional units. J. Bacteriol. 160:546-555.

Rodriguez-Tebar, A., Baras, J.A. and Vazquez, D. (1985). Location of some proteins involved in peptidoglycan synthesis in the inner and outer membranes of Escherichia coli. J. Bacteriol. 161:243-248.

Rosenberg, M., McKenney, K., and Schumperli, D. (1981). Use of the Escherichia coli galactokinase gene to study procaryotic and eucaryotic regulatory signals, p.387-406. In B. L. Rodriguez and M. J. Chamberlin (ed.), Promoters, structure and function. Praeger Scientific Publishers, East Sussex, England.

Rosenberger, R.F., Grover, N.B. Zaritsky, A. and Woldringh, L.L. (1978). Surface growth in rod-shaped bacteria. J. Theor. Biol. 73:711-721.

Salmond, G.P.C., Lutkenhaus, J.F., and Donachie, W.D. (1980). Identification of new genes in a cell envelope-cell division gene cluster of Escherichia coli: cell envelope gene murG. J. Bacteriol. 144:438-440.

Salmond, G.P.C. and Plakidou, S. (1984). Genetic analysis of essential genes in the ftsE region of the Escherichia coli genetic map and identification of a new cell division gene, ftsS. Mol. Gen. Genet. 197:304-308.

Santos, D. and de Almeida, D.F. (1975). Isolation and characterization of a new temperature-sensitive cell division mutant of Escherichia coli K-12. J. Bacteriol. 124:502.

Schaumberg, T.H. and Kuempel, P.J. (1983). Genetic mapping of the minB locus in Escherichia coli K-12. J. Bacteriol. 153:1063.

Schoemaker, J.M., Henderson, G.W., and Markovitz, A. (1982). Escherichia coli polypeptide controlled by the lon (capR) ATP hydrolysis-dependent protease and possibly involved in cell division. J. Bacteriol. 152:919-923.

Schumperli, D., Mckenny, K., Sobieski, D., & Rosenberg, M. (1982). Translational coupling at an intercistronic boundary of the Escherichia coli galactose operon. Cell 30:865-871.

Silhavy, T.J., Berman, M.L., and Enquist, L.W. (1984). Experiments with gene fusions. Cold Spring Harbor Laboratory.

Singer, S.J. and Nicholson, G.L. (1972). The fluid mosaic model of the structure of cell membranes. Science

175:720-731.

Smith, C.L. (1983). recF-dependent induction of recA synthesis by coumermycin, a specific inhibitor of the B subunit of DNA gyrase. Proc. Natl. Acad. Sci. U.S.A. 80:2510-2513.

Smith, H. & Birnstiel, M. (1976). A simple method for DNA restriction site mapping. Nuc. Acids Res. 3:2387-2399.

Sonntag, I., Schwarz, H., Hirota, Y., and Henning, U. (1978). Cell envelope and shape of Escherichia coli: multiple mutants missing the outer membrane lipoprotein and other major outer membrane proteins. J. Bacteriol. 136:280-281.

Southern, E.M. (1979). Measurement of DNA length by gel electrophoresis. Analyt. Biochem. 100:319-323.

Spratt, B.G. (1977a). Penicillin-binding proteins of Escherichia coli: general properities and characterization of mutants, p. 182-190. In D. Schessinger (ed.), Microbiology-1977. American Society for Microbiology, Washington, D.C.

Spratt, B.G. (1977b). Temperature-sensitive cell division mutants of Escherichia coli with thermolabile penicillin-binding proteins. J. Bacteriol. 131:293-305.

Steck, T.R. and Drlica, K. (1984). Bacterial chromosome segregation: evidence for DNA gyrase involvement in decatenation. Cell 36:1081-1088.

Stoker, N.G., Broome-Smith, J.K., Edelman, & Spratt, B. (1983). Organization and subcloning of the dacA-rodA,

pbpA cluster of cell shape genes in E. coli. J. Bacteriol. 155:847-853.

Stoker, N.G., Fairweather, N., & Spratt, B. (1982). Versatile low-copy-number plasmid vectors for cloning in Escherichia coli. Gene 18:335-341.

Stoker, N.G., Pratt, J.M., & Spratt, B.G. (1983). Identification of the rodA gene product of E. coli. J. Bacteriol. 155:854-859.

Sullivan, N. & Donachie, W. (1984a). Overlapping functional units in a cell division gene cluster in Escherichia coli. J. Bacteriol. 158:1198-1201.

Sullivan, N. & Donachie, W. (1984b). Transcriptional organization within an Escherichia coli cell division gene cluster: direction of transcription of the cell separation gene envA. J. Bacteriol. 160:724-732.

Tamaki, S., Nakajima, S., and Matsuhashi, M. (1977). Thermosensitive mutation in Escherichia coli simultaneously causing defects in penicillin-binding protein-1Bs and in enzyme activity for peptidoglycan synthesis in vitro. Proc. Natl. Acad. Sci. USA 74:5472-5476.

Teather, R.M., Collins, J.F. and Donachie, W.D. (1974). Quantal behavior of a diffusible factor which initiates septum formation at potential division sites in Escherichia coli. J. Bacteriol. 118:407-413.

Tipper, D.J. and Wright, A. (1979). The structure and biosynthesis of bacterial cell walls. In: J.R. Sokatch and L.N. Ornston (eds.) The bacteria, vol. VII. Academic Press, New York.

Tormo, A., Fernandez-Cabrera, C. and Vicente, M. (1985). The ftsA gene product: a possible connection between DNA replication and septation in Escherichia coli. J. Gen. Microbiol. 131:239-244.

Tormo, A., Martinez-Salas, E., and Vicente, M. (1980). Involvement of the ftsA gene product in late stages of the Escherichia coli cell cycle. J. Bacteriol. 141:806-813.

Tormo, A. and Vicente, M. (1984). The ftsA gene product participates in formation of the Escherichia coli septum structure. J. Bacteriol. 157:779-784.

Torti, S. and Park, J.T. (1980). Genetic characterization of a filament-forming, lipoprotein-deficient mutant of Escherichia coli. J. Bacteriol. 143:1289-1294.

Treuba, F.J. and Woldringh, C.L. (1980). Changes in cell diameter during the division cycle of Escherichia coli. J. Bacteriol. 142:869-878.

Utsumi, R., Kawamukai, M., Obata, K., Morita, J., Himeno, M. and Komano, T. (1983). Identification of a membrane protein induced concurrently with cell filamentation by cyclic AMP in an Escherichia coli K-12 fic mutant. J. Bacteriol. 155:398-401.

Utsumi, R., Nakamoto, Y., Kawamutai, M. Himeno, M. and Komano, T. (1982). Involvement of cyclic AMP and its receptor protein in filamentation of an Escherichia coli fic mutant. J. Bacteriol. 151:807-812.

van Heijenoort, J., Parquet, C., Flouret, B., and van Heijenoort, Y. (1975). Envelope-bound

N-acetyl-muramyl-L-alanine amidase of Escherichia coli K-12. Purification and properties of the enzyme. Eur. J. Biochem. 58:611-619.

Verwer, R.W.H., Beachley, E.H., Keck, W., Stoub, A.M. and Poldermans, J.E. (1980). Oriented fragmentation of Escherichia coli sacculi by sonication. J. Bacteriol. 141:327-332.

Verwer, R.W.H. and Nanninga, N. (1980). Patterns of meso-DL-2,6 diaminopimelic acid incorporation during the division cycle of Escherichia coli. J. Bacteriol. 144:327-336.

Verwer, R., Nanninga, N., Keck, W., and Schwarz, U. (1978). Arrangement of glycan chains in the sacculus of Escherichia coli. J. Bacteriol. 136:723-729.

Wahle, E., Mueller, K. and Orr, E. (1984). Gene expression in a temperature-sensitive gyrB mutant of Escherichia coli. EMBO J. 3:315-320.

Walker, G.C. (1984). Mutagenesis and inducible responses to deoxyribonucleic acid damage in Escherichia coli. Microbiol. Rev. 48:60-93.

Walker, J., Kovarik, A., Allen, J., and Gustafson, R. (1975). Regulation of bacterial cell division: temperature sensitive mutants of Escherichia coli that are defective in septum formation. J. Bacteriol. 123:693-703.

Ward, J. & Lutkenhaus, J. (1984). A lacZ-ftsZ gene fusion is an analog of the cell division inhibitor sulA. J. Bacteriol. 157:815-820.

Ward, D.F. and Murray, N.E. (1979). Convergent transcription in bacteriophage lambda: interference with gene expression. J. Mol. Biol. 133:249-266.

Waxman, D.J. and Strominger, J.L. (1983). Penicillin-binding proteins and the mechanism of action of Beta-lactam antibiotics. Ann. Rev. Biochem. 52:825-869.

Wickner, W. (1979). The assembly of proteins into biological membranes: the membrane trigger hypothesis. Annu. Rev. Biochem. 48:23-45.

Wilson, G. & Murray, N. (1979). Molecular cloning of the DNA ligase gene from bacteriophage T4. I. Characterization of the recombinants. J. Mol. Biol. 132:471-491.

Wijsman, H.J.W. (1972). A genetic map of several mutations affecting the mucopeptide layer of Escherichia coli. Genet. Res. 20:65-74.

Wolf-Watz, H., & Normark, S. (1976). Evidence for a role of N-acetylmuramyl-L-alanine amidase in septum separation in Escherichia coli. J. Bacteriol. 128:580-586.

Worcel, A. and Burgi, E. (1974). Properties of a membrane-attached form of the folded chromosome of Escherichia coli. J. Mol. Biol. 82:91-105.

Wright, A. and Tipper, D.J. (1979). The outer membrane of Gram-negative bacteria. In J.R. Sokatch and L.N. Ornston (eds). The bacteria, vol. VII. Acacemic Press, New York.

Wu, H.C., Hou, C., Lin, J.J., et al. (1977). Biochemical characterization of a mutant lipoprotein of Escherichia coli. Proc. Natl. Acad. Sci. USA

74:1388-1392.

Yamada, H. and Mizushima, S. (1978). Reconstitution of an ordered structure from major outer membrane constituents and the lipoprotein- bearing peptidoglycan sacculus of Escherichia coli. J. Bacteriol. 135:1024-1031.

Yura, T. and Wada, C. (1968). Phenethyl alcohol resistance in Escherichia coli. I. Resistance of strain C600 and its relation to azide resistance. Genetic. 59:177-190.

Zaritsky, A. (1975). On dimensional determination of rod-shaped bacteria. J. Theoret. Biol. 54:243-248.

Zehnbauer, B.A., Foley, E.C., Henderson, G.W. and Markovitz, A. (1981). Identification and purification of the lon$^+$ (capR$^+$) gene product, a DNA-binding protein. Proc. Natl. Acad. Sci. USA 78:2043-2047.

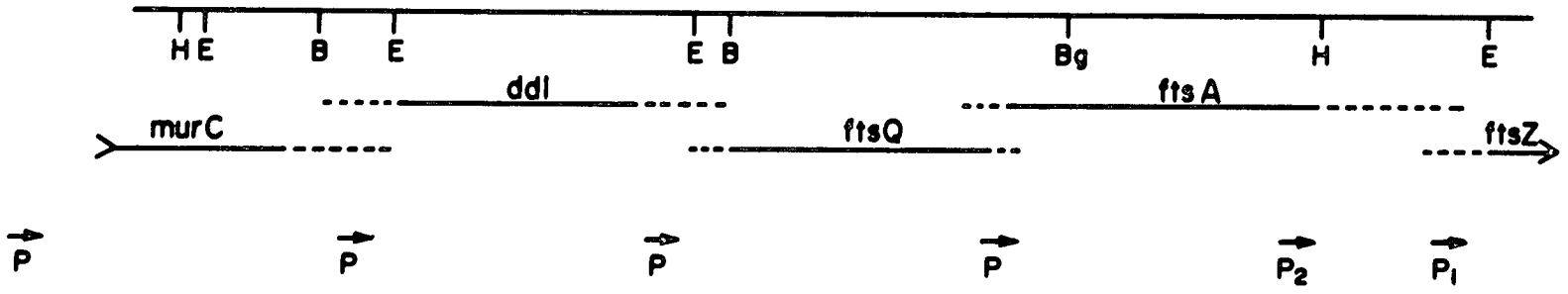

Figure 8.1

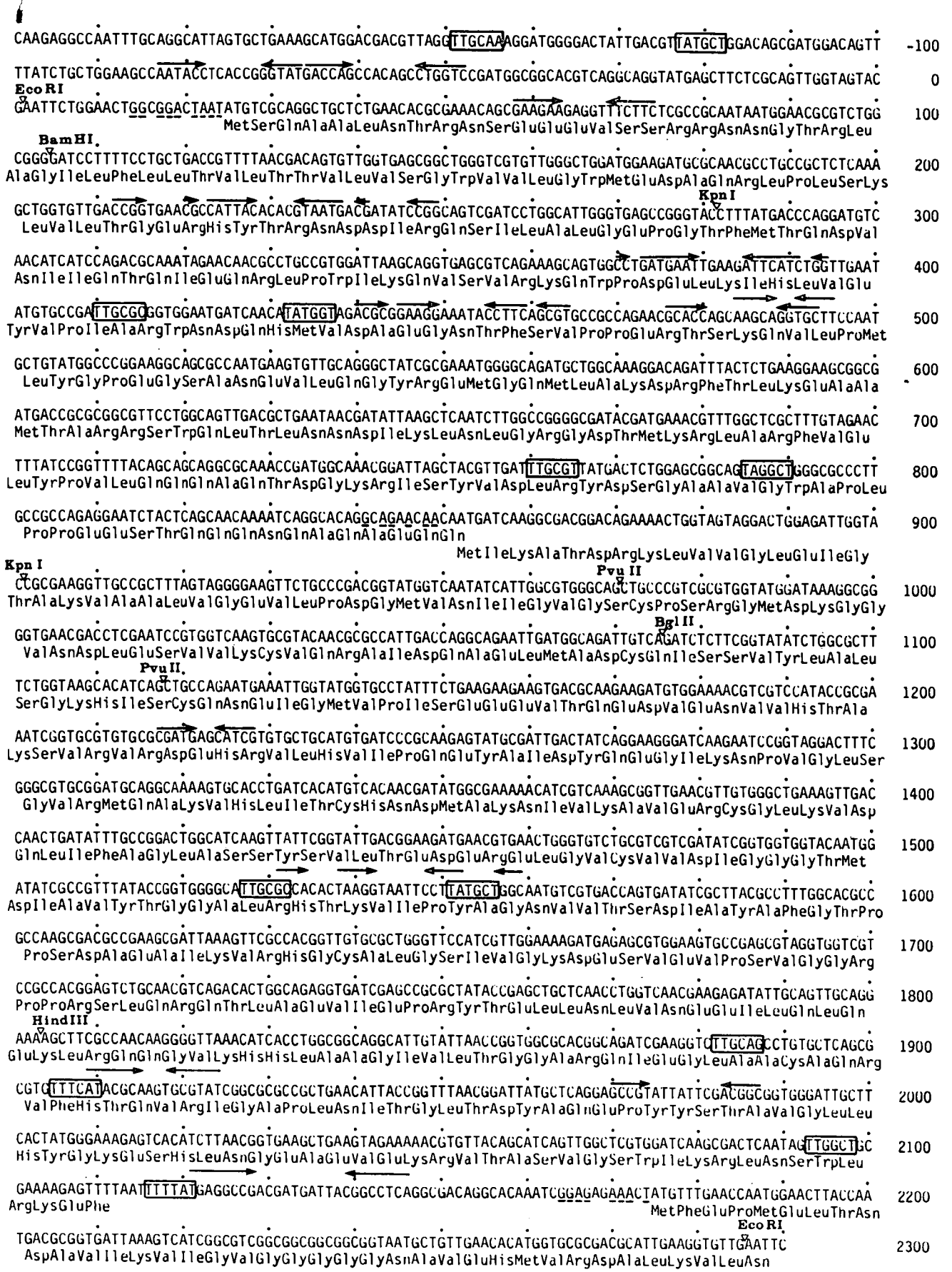

FIG. 4. DNA nucleotide sequence of the noncoding strand of the *ftsQ ftsA ftsZ* region. The amino acid sequences deduced for the products of *ftsQ* (nucleotides 25 to 852), *ftsA* (nucleotides 852 to 2111), and *ftsZ* (nucleotide 2175 onwards) are shown beneath the sequence. Bases are numbered arbitrarily from the left-hand *Eco*RI site of the 2.3-kb *Eco*RI fragment (see Fig. 1). Putative promoter sequences are shown in boxes (see Table 2), and inverted repeat sequences are overlined with arrows. Bases upstream of ATG codons which match the consensus for ribosome binding are underlined. The cutting sites for the restriction enzymes shown in Fig. 2 and 3 are also depicted.

UNIVERSITY OF EDINBURGH

ABSTRACT OF THESIS (Regulation 7.9)

Name of Candidate DANIEL J. KENAN

Address .....

Degree M. Phil. *Date* 8/85

Title of Thesis Organization of gene expression within the 2-minute morphogenetic cluster of Escherichia coli

No. of words in the main text of Thesis Approximately 30,000

The 2-minute region of the Escherichia coli chromosome contains a remarkable cluster of genes involved in cell division, cell envelope growth, and morphogenesis (Donachie et al., 1984). The absence of biochemical assays for most morphogenetic factors has hindered their characterization, however molecular genetic approaches are being used successfully to reveal the organization of morphogenetic pathways. A segment of the 2-minute cluster, spanning the genes murG, murC, ddl, ftsQ, ftsA, ftsZ, and envA, has been incorporated into a lambda transducing phage and was used in the preliminary characterization of this region (Lutkenhaus and Wu, 1980). I expanded upon their work by using subcloning techniques and deletion analysis to map the genetic boundaries of ddl, ftsQ, ftsA, and ftsZ. Moreover, functional promoter and terminator sequences were mapped through use of a gal-operon fusion system, and the gene products of ddl, ftsQ, and ftsA were identified by expression of cloned fragments from a P_L vector in a minicell system. My results complement the preliminary molecular genetic analysis by Lutkenhaus and Wu (1980) and the sequence data of Robinson et al. (1984). All loci between murC and ftsZ are transcribed in a clockwise sense; these loci are tightly linked without large intervening sequences; each of these loci has at least one independent promoter; a second promoter for ftsZ lies within the coding sequence of the adjacent locus, ftsA; no strong transcriptional terminators are found between murC and ftsZ; and expression of several adjacent loci within this cluster may be coordinated. The ddl product is identified as a 32,000 dalton protein, the ftsQ protein is 35,000 daltons, and the ftsA protein is 46,000 daltons. Over-expression of ftsQ and ftsA together is deleterious to the cell, and inactivation of ftsA reverses this effect. Transcription of ftsA in the absence of ftsQ translation disturbs cellular morphology, and ftsQ may be deleterious in high copy number unless its promoter is removed in the cloning process. A fortuitous galE-ftsQ fusion produces a hybrid protein that retains FtsQ function and is not deleterious in spite of high levels of transcription. These findings are correlated with the sequence data, and possibilities for future investigations are discussed.